

Design and synthesis of (Glyco) polymers and peptidoglycan complex with new bacterial killing mechanism

Xu, Yuan

2019

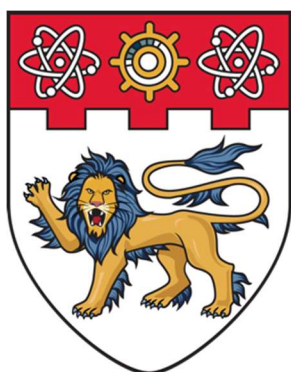
Xu, Y. (2019). Design and synthesis of (Glyco) polymers and peptidoglycan complex with new bacterial killing mechanism. Doctoral thesis, Nanyang Technological University, Singapore.

<https://hdl.handle.net/10356/85300>

<https://doi.org/10.32657/10220/48211>

This work is licensed under a Creative Commons Attribution-NonCommercial 4.0 International License (CC BY-NC 4.0).

Downloaded on 13 Mar 2024 18:49:56 SGT



**NANYANG
TECHNOLOGICAL
UNIVERSITY**

SINGAPORE

**DESIGN AND SYNTHESIS OF (GLYCO)POLYMERS
AND PEPTIDOGLYCAN COMPLEX
WITH NEW BACTERIAL KILLING MECHANISM**

XU YUAN

SCHOOL OF PHYSICAL AND MATHEMATICAL SCIENCES

2019

**DESIGN AND SYNTHESIS OF (GLYCO)POLYMERS
AND PEPTIDOGLYCAN COMPLEX
WITH NEW BACTERIAL KILLING MECHANISM**

XU YUAN

SCHOOL OF PHYSICAL AND MATHEMATICAL SCIENCES

A thesis submitted to the Nanyang Technological University
in partial fulfilment of the requirement for the degree of
Doctor of Philosophy

2019

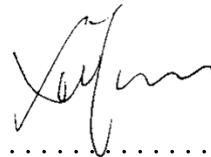
Statement of Originality

I hereby certify that the work embodied in this thesis is the result of original research done by me except where otherwise stated in this thesis. The thesis work has not been submitted for a degree or professional qualification to any other university or institution. I declare that this thesis is written by myself and is free of plagiarism and of sufficient grammatical clarity to be examined. I confirm that the investigations were conducted in accord with the ethics policies and integrity standards of Nanyang Technological University and that the research data are presented honestly and without prejudice.

2nd JAN, 2019

.....

Date



.....

XU YUAN

Supervisor Declaration Statement

I have reviewed the content and presentation style of this thesis and declare it of sufficient grammatical clarity to be examined. To the best of my knowledge, the thesis is free of plagiarism and the research and writing are those of the candidate's except as acknowledged in the Author Attribution Statement. I confirm that the investigations were conducted in accord with the ethics policies and integrity standards of Nanyang Technological University and that the research data are presented honestly and without prejudice.

7th JAN, 2019

.....
Date



.....
LIU XUE-WEI

Authorship Attribution Statement

This thesis contains material from 2 papers published in the following peer-reviewed journals where I was the first author.

Chapter 2 is published as Y. Xu, K. Zhang, S. Reghu, Y. Lin, M. B. Chan-Park, and X.-W. Liu, Synthesis of antibacterial glycosylated polycaprolactones bearing imidazoliums with reduced hemolytic activity. *Biomacromolecules* **20**, 949-958 (2019). DOI: 10.1021/acs.biomac.8b01577.

The contributions of the co-authors are as follows:

- A/Prof Liu provided the initial project direction, guidance on the collaboration and edited the manuscript drafts.
- Prof Chan-Park provided suggestions on the biological tests and the manuscript drafts.
- I prepared the manuscript drafts. The manuscript was revised together with Ms. K. Zhang.
- I co-designed the study with A/Prof Liu and performed the most laboratory work at the School of Physical and Mathematical Sciences.
- All the synthesis and characterization, including sample preparation, was conducted by me in the Division of Chemistry & Biological Chemistry at the School of Physical and Mathematical Sciences.
- The hemolysis testing was performed by Ms. K. Zhang.
- Ms. S. Reghu conducted the MIC and MTT assays.
- Dr. Y. Lin assisted in the collection of GPC data.

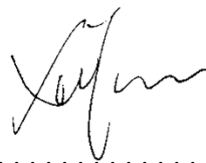
Chapter 3 is published as A. Mallick,[‡] Y. Xu,[‡] Y. Lin,[‡] J. He, M. B. Chan-Park and X.-W. Liu, Oxadiazabicyclooctenone as a versatile monomer for the construction of pH sensitive functional polymers via ROMP. *Polymer Chemistry* **9**, 372-377 (2018). DOI: 10.1039/c7py01413a. ([‡] co-first author)

The contributions of the co-authors are as follows:

- A/Prof Liu provided the initial project direction and edited the manuscript drafts.
- Prof Chan-Park provided suggestions on preparation of the manuscript drafts.
- I prepared the manuscript drafts together with Dr. A. Mallick. The manuscript was revised together with Mr. J. He.
- All the synthesis and characterization, including sample preparation, was performed by Dr. A. Mallick and me in the Division of Chemistry & Biological Chemistry at the School of Physical and Mathematical Sciences.
- Dr Y. Lin assisted in analyzing the GPC data and conducted the TGA analysis.

2nd JAN, 2019

.....
Date



.....
XU YUAN

Abstract

Human has been facing microbial infections for centuries until the discovery of antibiotics. Unfortunately, negligible use of conventional antibiotics has stimulated the emerging of multi-drug-resistant microbes which is considered as one of the greatest threats to the global society. In this context, antimicrobial polymers which mimic antimicrobial peptides (AMPs) in the host defense systems have attracted great attention in past decades. However, most synthetic antimicrobial polymers consist of non-degradable carbon-based backbones, limiting their potential in clinical applications. In this sense, synthesis of antimicrobial polymers with degradable structures are of great interest to scientists.

Chapter 1 serves as a general introduction for the field of antimicrobial polymeric materials. Briefly, an overview of conventional antibiotics and drug resistance has been presented. Besides, polymeric materials with antimicrobial activity have been introduced with a focus on the development of synthetic materials.

In chapter 2, we have described the successful synthesis of degradable antibacterial polycaprolactones bearing imidazolium groups. A series of glycosylated polycaprolactones have been prepared by combination of ring-opening polymerization and CuAAC reaction. To systematically study the structure-activity relationship, various carbohydrates and imidazoliums were incorporated by grafting onto the backbone in one-pot. The antibacterial activity and toxicity of resultant polymers were examined, and promising candidate has been identified. Moreover, degradation study has revealed that the polymers are hydrolytically degradable in physiochemical conditions and antibacterial action is much faster than degradation.

A series of ROMP polymers with acid and base sensitivity have been presented in chapter 3. Homopolymers from urea-based bicyclic olefins have been demonstrated to be degradable in acidic and basic conditions. In addition, this degradability has been successfully introduced into copolymers with functional norbornenes. Through systematically varying the composition, the critical ratio responsible for the vulnerability has been identified. Preliminary results suggest that the scaffold is possible to be applied in developing antimicrobial polymers although some remained issues need to be addressed.

Alternative strategy to combat bacterial infections has been described in chapter 4. Specifically, inspired by the extensive applications of immunotherapy in cancer treatment, remarkable efforts have been spent on developing agents to induce immune responses for combatting pathogens. Amongst them, molecules labeling bacterial surface by metabolic process appears to be more promising in terms of efficiency, however, no effective agent has been reported to be active towards both Gram-positive and Gram-negative strains. We successfully synthesized lipid II analogues with more efficient approach, which could target both strains, proving the feasibility of developing antibody recruiting molecules with broader spectrum of activity.

Acknowledgements

In the 4 years of PhD study, there are many great moments worth memorizing. I could not finish this work without the help and support from many people.

Firstly, I would like to give my sincere thanks to my supervisor Prof. Liu Xuewei for providing this opportunity to pursue higher degree in his group. Also, I would like to give my deep gratitude to Prof Liu for his patient guidance, encouragement and support on my research during the past several years. He is knowledgeable, generous and full of energy, his enthusiasm inspired me to keep going at the frustrated moments. Moreover, I have learned a lot from his philosophical thinking of science especially on the interdisciplinary ideas, and his strictness on science is significantly beneficial to my growing as a scientist which will be a great fortune in the future.

Besides, I want to take this opportunity to thank my co-supervisor Prof. Mary Chan for her kind help in solving the problem of my biological tests in her group. I would not finish this study without her help and support both in science and finance. Meanwhile, I am grateful to my committee members, Prof. Zhang Qichun and Dr. Mihaiela Stuparu, for their advisory in my study.

I am also thankful to the faculties in Division of Chemistry and Biological Chemistry, especially NMR and MS managers, Ms Goh Ee Ling, Mr Keith Leung for their kind help in the NMR and Ms Zhu Wenwei for her support in the MS facilities.

In addition, I would like to express my great appreciation for my seniors who took care of me both in and outside the lab, scientific and personal levels, especially when I was confused in the early days: Dr. Leow Min Li, Dr Le Mai Hoang Kim, Dr. Asadulla Mallick, Dr. Ronny William, Dr. Chai Hua, Dr. Tan Yu Jia, Dr. Liao Hongze, Dr. Leng Wei Lin, Dr.

Yao Hui and Dr. Vu Minh Duy. I am much obliged to, Dr. Asadulla Mallick for his valuable advice and help in the synthesis, Dr Lin Yichao for his advice in GPC, Ms Sheethal Reghu, Ms Zhang Kaixi and Ms Ruan Lin for their help in biological experiments. Furthermore, I also want to extend my thankfulness to my labmates who gave me a wonderful environment to learn and do the research in NTU and Singapore: He Jingxi, Das Mrinmoy, Kho Shu Hui, Guo Aoxin, Lin Jun Jie Desmond, Zhang Shasha, Dr. Lu Zhiqiang, Dr. Huang Nianyu, Dr. Zhang Qi, Dr. Guo Zhong, Dr. Kumar Bhaskar Pal, Li Sha, Song Shihao and Wang Yi.

Finally, I would like to express profound gratitude to my family. I am very grateful to have them in my life. This work could not be finished without their continuous understanding, support and encouragement.

Table of Contents

Abstract	1
Acknowledgements	3
Table of Contents	5
List of Abbreviations	7
Summary	9
Chapter 1 Introduction of Polymeric Materials in Antimicrobial Applications .	10
1.1 Microorganisms and Drug Resistance	11
1.1.1 Gram-positive and Gram-negative Bacteria	12
1.1.2 Conventional Antibiotics and their Targets in Bacterial Cells	13
1.1.3 Mechanism of Drug Resistance	15
1.1.4 Solutions to Drug Resistance	17
1.2 Polymeric Materials with Antimicrobial Activity	19
1.2.1 Amino Acid-based Antimicrobial Polymers	20
1.2.2 Non-Amino Acid-based Antimicrobial Polymeric Materials	28
1.3 Problems and Research Objectives	42
1.3.1 Problems and Challenges of Current Antimicrobial Polymers	42
1.3.2 Research Objectives	43
1.4 References	44
Chapter 2 Synthesis of Antibacterial Glycosylated Polycaprolactones with Reduced Toxicities	53
2.1 Introduction	54

2.2	Results and Discussion	58
2.3	Conclusion	83
2.4	Experimental Section	84
2.5	References	100

Chapter 3 Construction of pH Sensitive Functional Polymers via ROMP 103

3.1	Introduction	104
3.2	Results and Discussion	108
3.3	Conclusion	127
3.4	Experimental Section	128
3.5	References	144

Chapter 4 Design and Synthesis of Peptidoglycan-Based Antibody-Recruiting Molecules 146

4.1	Introduction	147
4.2	Results and Discussion	157
4.3	Conclusion	163
4.4	Experimental Section	164
4.5	References	179

Chapter 5 Summary and Perspectives 183

List of Abbreviations

δ	chemical shift	Glc	glucose
$^{\circ}\text{C}$	degree centigrade	GlcNAc	<i>N</i> -acetylglucosamine
Ac	acetyl	h	hour(s)
AcOH	acetic acid	Hex	hexane
Bn	benzyl	HMBC	heteronuclear multiple bond correlation
Boc	<i>tert</i> -butoxycarbonyl	HMQC	heteronuclear multiple-quantum correlation
brs	broad singlet	HRMS	high resolution mass spectroscopy
calcd	calculated	HSQC	heteronuclear single-quantum correlation
cat.	catalyst	IC ₅₀	50% inhibitory concentration
CDCl ₃	deuterated chloroform	<i>i</i> Pr	isopropyl
CHCl ₃	chloroform	kDa	kilodaltons
d	doublet	<i>m</i>	<i>meta</i>
DCM	dichloromethane	m	multiplet
dd	doublet of doublets	Man	mannose
DIEA	diisopropylethylamine	MBC	minimum bactericidal concentration
DMAP	4-dimethylaminopyridine	Me	methyl
DMF	<i>N,N</i> -dimethylformamide	MeOH	methanol
DMSO	dimethyl sulfoxide	MIC	minimum inhibitory concentration
equiv.	equivalent	min	minute(s)
ESI	electrospray ionization	mL	milliliter(s)
Et	ethyl	mmol	millimole(s)
Et ₂ O	diethyl ether	mol	mole(s)
Et ₃ N	triethylamine	MS	mass spectroscopy
EtOAc	ethyl acetate	<i>n</i> Bu	<i>n</i> -butyl

EtOH	ethanol	NMR	nuclear magnetic resonance
NOESY	nuclear overhauser effect spectroscopy	s	singlet
<i>o</i>	<i>ortho</i>	t	triplet
<i>p</i>	<i>para</i>	TBAF	<i>tert</i> -butylammonium fluoride
PBS	phosphate buffered saline	TBS	<i>tert</i> -butyldimethylsilyl
Pd/C	palladium on charcoal	<i>t</i> Bu	<i>tert</i> -butyl
PEG	polyethylene glycol	TIPS	triisopropylsilyl
Ph	phenyl	TFA	trifluoroacetic acid
ppm	parts per million	THF	tetrahydrofuran
Py	pyridine	TLC	thin-layer chromatography
q	quartet	TOFMS	time-of-flight mass spectroscopy
Rha	rhamnose	Ts	tosyl
rt	room temperature		

Summary

Chapter 1 serves as a general introduction for the field of antimicrobial polymeric materials. An overview of conventional antibiotics and drug resistance has been presented briefly. Besides, polymeric materials with antimicrobial activity has been introduced with a focus on the development of synthetic materials.

In chapter 2, we have described the successful synthesis of degradable antibacterial polycaprolactones bearing imidazolium groups. A series of glycosylated polycaprolactones have been prepared, and structure-activity relationship has been studied. A promising candidate has been identified with degradation study and killing kinetics.

In chapter 3, a series of ROMP polymers with acid and base sensitivity have been presented. Homopolymers have been demonstrated to be degradable in acidic and basic conditions. In addition, this degradability has been successfully introduced into copolymers. Preliminary results suggest that the scaffold is possible to be applied in developing antimicrobial polymers.

In chapter 4, an alternative strategy to combat bacterial infections has been described. We successfully synthesized lipid II analogues with more efficient approach, which could target both strains, proving the feasibility of developing antibody recruiting molecules with broader spectrum of activity.

Chapter 1

Introduction of Polymeric Materials in Antimicrobial Applications

1.1 Microorganisms and Drug Resistance

It is well known that microbes are ubiquitous in our daily life. Also, some microorganisms are beneficial while some are harmful to human beings. On the one hand, probiotics exhibit commensalism with animals and help to digest foods. Furthermore, microbes were employed in producing fermented foods and beverages long time ago. For example, yeasts were utilized to make wine and lactobacillus was used in yoghurt and cheese production.¹ Besides, substances from the metabolism of some microbes could be applied in treatment of microbial infections, which is the main source of antibiotics in the early time.²

However, on the other hand, infectious diseases caused by pathogenic microorganisms were the principal cause of death before antibiotics were introduced into medical care, for example, 30% of deaths in USA were caused by tuberculosis, diarrheal, and pneumonia in 1990, whereas in 1997, less than 3% of deaths were caused by the same reason.³ In fact, microbial infections are not unusual at present days, especially in developing nations. What's worse is that, the problem is re-emerging in developed countries which is triggered by the rising of antibiotic-resistant pathogens and limited new approved antibiotics.⁴ Recently, the World Health Organization (WHO) has suggested a list of most dangerous pathogens with the highest priority R&D needs for new antibiotics or antibacterial agents.⁵ Therefore, the multi-drug-resistant bacteria or superbugs is of great concern to the medical systems, research communities and government departments.⁶ Moreover, there are also other microbes such as viruses (*e.g.*, influenza) and fungi being increasingly developing resistance towards existed antimicrobial agents.⁷ New treatment and novel antimicrobial

agents especially the ones with novel mode of action are urgently demanded in clinics for the foreseeable future.⁸

1.1.1 Gram-positive and Gram-negative Bacteria

Fundamentally, life on the earth are based on two different types of cells, prokaryotic and eukaryotic, and bacteria are prokaryotic which could be further divided into Gram-positive and Gram-negative by the Gram staining microbiological technique.⁹ For the microorganisms, including bacteria, fungi, virus and protozoa, bacteria are unicellular and extremely small which have different biochemistry compared with other microbes, especially eukaryotic cells.

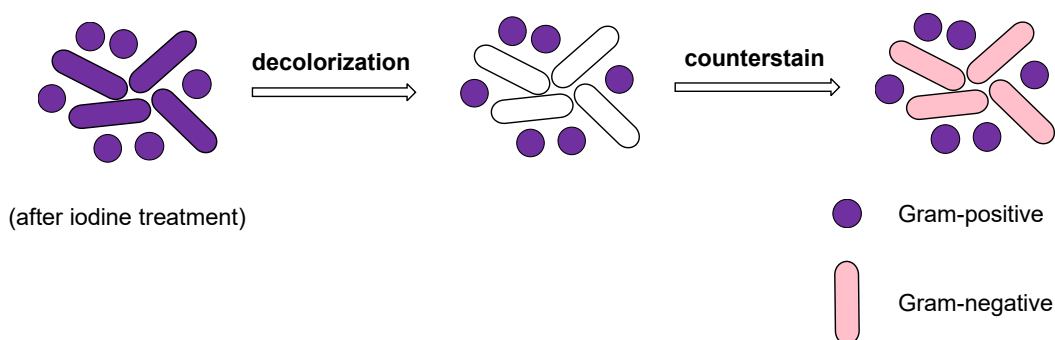


Figure 1.1⁹ Gram staining.

Experimentally, Gram-positive bacteria will retain the violet color whereas Gram-negative bacteria cannot retain the stain and obtain pink color by counter-stain (Figure 1.1).⁹

Actually, this is primarily because of the different structures of the two types of cells, in particular, Gram-positive strains possess thick cell walls with high content of

peptidoglycan whilst only thinner layer of peptidoglycan and an extra outer membrane could be found in Gram-negative cells (Figure 1.2).

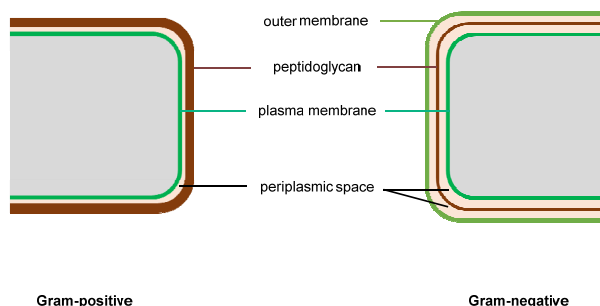


Figure 1.2 The primary difference of cell structures between Gram-positive and Gram-negative bacteria.

1.1.2 Conventional Antibiotics and their Targets in Bacterial Cells

In the early stage of antimicrobial practice, antibiotics are compounds generated from some microbial metabolites which are effective against other microbes. At this moment, a lot of antibiotics are manufactured by chemical synthesis owing to the rapid development of synthetic chemistry. Anyway, the conventional antibiotics can also be extended to the derivatives of early antibiotics or synthetic compounds with similar mode of actions.

The modern age of antimicrobial agents started with the organoarsenic compound Arsphenamine (also known as Salvarsan or compound 606) which was discovered by Paul Ehrlich and Sahachiro Hata, it was very successful antimicrobial drug for the treatment of syphilis until 1940s (Figure 1.3).¹⁰ However, it was the discovery of penicillin by Alexander Fleming that initiated the new era in infectious diseases treatment, which is considered as the first antibiotic (Figure 1.3). It is noteworthy that they were awarded the Noble Prize in 1945 for their great contribution to penicillin, and interestingly, it was also Sir Fleming

who warned that bacteria could develop resistance by the selection pressure from negligent use of penicillin.

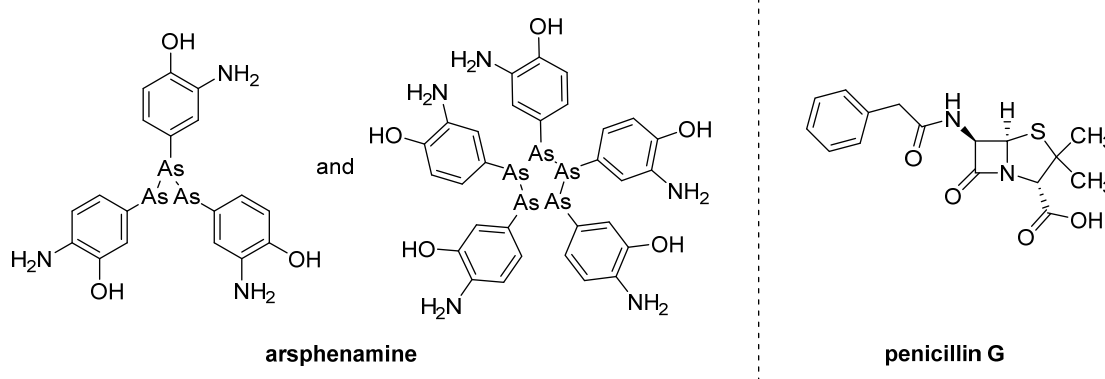


Figure 1.3 Structures of first modern antimicrobial agents.

As an ultimate goal, killing of pathogens or inhibition of their growth by antibacterial agents should not interfere with the host cells, *i.e.* selectivity. For the antibiotics inhibiting cell wall synthesis, the selectivity is very obvious as the mammalian cells have no cell walls inherently. But, in other cases, the situation is not clear and the basis for selectivity should be more subtle difference in the cells. Therefore, for the sake of developing antimicrobial agents with selective toxicity, extensive efforts have been made on the investigation of killing mechanism. Furthermore, the mode of actions is governed by the main targets of antibiotics in the bacterial cells, including protein, cell membrane, ribosome, peptidoglycan, etc.¹¹ For instance, the above mentioned penicillin exhibits its efficacy by targeting specific protein transpeptidase and inhibiting its catalytic ability in cross-linking of peptidoglycan which is a key reaction in bacterial cell wall synthesis.¹² Thus, design of new antimicrobial agents will be more effective by studying the targets and their possible mutation in bacterial cells. Most antibacterial agents kill bacteria by inhibiting the cellular

processes, and some selected groups of conventional antibiotics and their mode of action are listed in Table 1.1.¹²

Table 1.1 Examples of antibiotics and their modes of action.

Drug type	Example	Target	Mode of action
β -lactams	Penicillin	Penicillin-binding protein	Inhibit cell wall synthesis
Lipopeptides	Daptomycin	Cell membrane	Inhibit cell wall synthesis
Glycopeptides	Vancomycin	Peptidoglycan units	Inhibit cell wall synthesis
Rifamycins	Rifamycin	RNA polymerase	Inhibit RNA synthesis
Fluoroquinolones	Ciprofloxacin	Topoisomerase II and IV	Inhibit DNA synthesis
Macrolides	Erythromycin	50S ribosome	Inhibit protein synthesis
Tetracyclines	Tetracycline	30S ribosome	Inhibit protein synthesis
Aminoglycosides	Gentamicin	30S ribosome	Inhibit protein synthesis
Phenicols	Chloramphenicol	50S ribosome	Inhibit protein synthesis
Streptogramins	Pristinamycin	50S ribosome	Inhibit protein synthesis

1.1.3 Mechanisms of Drug Resistance

Although antibiotics had saved millions of lives since the first discovery, the golden age of conventional antibiotics is gradually going to the end as there are more and more resistant bacteria becoming headaches to the clinician.¹³ Even worse, there is very few newly approved antibiotics in the past decades and many programs in pharmaceutical companies have been terminated as they need to make a profit on more profitable drugs for chronic diseases.¹⁴ Therefore, to understand how the bacteria develop resistance, especially the multi-drug resistance, is quite crucial for developing new antibacterial agents with novel mode of actions.

Firstly, the drug resistance is stimulated by the selection pressure from exposing to antibiotics, which interestingly proved the theory of Darwin. Only mutated bacteria can

survive in the presence of antibiotics, the exchange of plasmid with mutated genetic information will significantly speed up the evolution of bacteria. Specifically, bacteria have the ability to transfer their resistant genetic information to the other independent bacterial cells by conjugation, transformation or transduction.¹⁵ Moreover, the bacteria that carry resistant genes could move faster and further than ever before since human travel has been becoming more frequent from continent to continent, rendering the problem a global threat.

Apart from these aspects, the bacteria could develop resistance by deactivating the drug, changing the permeability and pumping out drugs.¹⁶ For example, a lot of Gram-negative bacteria can hydrolyze the amine bond of β -lactams with β -lactamases, rendering the β -lactam antibiotics inactive.¹⁷ The opportunistic pathogen Gram-negative *Pseudomonas aeruginosa* (*P. aeruginosa*), could pump out the antibiotics by their strong efflux system, rendering very low concentration of antibiotics.¹⁸ The resistant mechanisms of some typical examples of antibiotics are depicted in Table 1.2.¹⁹

Table 1.2 Resistant mechanisms of selected antibiotics in current market.

Antibiotic	Target	Resistance mechanism
β -lactams	Transpeptidases or transglycosylases	β -lactamases, PBP mutants
Vancomycin	D-Ala-D-Ala termini of Lipid II	Altering to D-Ala-D-Lac or D-Ala-D-Ser
Fluoroquinolones	DNA gyrase	Gyrase mutations
Tetracyclines	Peptidyl transferase	Drug efflux
Aminoglycosides	Peptidyl transferase	Modifying drug structure

Moreover, some bacteria, for instance, Gram-positive *S. aureus* is able to resist multiple drugs, by its own mutation and adopting multiple-drug resistant genes, by which the strain conserves the power to escape from penicillin, gentamicin, methicillin, tetracycline, etc.²⁰ Typically, a superbug, MRSA (methicillin-resistant *Staphylococcus aureus*) caused more than 5000 deaths every year in Europe and is becoming the universal resistant pathogen all over the world.²¹ Currently, the MRSA strains are only susceptible to some glycopeptides such as vancomycin, but glycopeptides-resistant *S. aureus* strains are also isolated recently. Fortunately, some new antibiotics were developed against these strains, and more novel agents are under way.^{21a,22}

1.1.4 Solutions to Drug Resistance

At this moment, the whole world is facing the risk of virulent superbugs that cannot be eradicated by any antimicrobial agent if the drug development cannot catch up the pace of bacterial evolution. Accordingly, many nations as well as international organizations have taken necessary measures to control the usage of present antibiotics and surveil the spread of multi-drug resistant pathogens intensively.²³ Albeit antibiotic stewardship programs will slow down the situation, developing new antimicrobial agents is also suggested by the WHO. Therefore, the research community has tried all the possible strategies to revive the “golden age”, including the revitalization of conventional antibiotics.

1.1.4.1 Revitalization of Conventional Antibiotics

It is well-known that resistant strains will arise very soon after the marketing of a new antibiotic, therefore, limitless antibiotics should be produced in order to combat the endless mutation of bacterial strains, which seems to be infeasible. Thus, a cheaper and faster strategy that combining conventional antibiotics with few auxiliary compounds has been applied in developing new effective therapeutics for clinics.

Frequently, combination of antibiotic with a second antibiotic is used in clinical therapy because the second antibiotic can quell the strains which retain resistance to the primary antibiotic. Moreover, if infections caused by unknown bacteria is to be treated, combination of antibiotics will render a broader spectrum of activity.²⁴ In some cases, the antibiotics could enhance the efficacy of each other which is called synergy. For example, the synergistic combination of gentamicin and imipenem is used in the treatment of endocarditis.²⁵

Besides, combinations of antibiotic and non-antibiotic are also used in clinical practice, such as the above-mentioned combination for the treatment of β -lactam resistant infections. In particular, clavulanic acid has the ability to deactivate bacterial β -lactamase, resuscitating the killing efficacy of amoxicillin while clavulanic acid itself is ineffective.²⁶

1.1.4.2 New Antimicrobial Agents with Novel Mode of Action

Although revitalization of conventional antibiotics can lighten the financial burden and slow down the evolution of bacteria, resistance will eventually appear which is the historical experience. Indeed, mutated bacteria that could produce β -lactamases escaping

from the neutralization of clavulanic acid has emerged.²⁷ Therefore, antimicrobial agents with novel mode of action are urgently needed.

To address to this problem, a lot of scientists have exerted efforts on finding novel bacterial targets, for instance, carbonic anhydrases.²⁸ Carbonic anhydrases is metalloenzymes in omnipresent in both prokaryotic and eukaryotic cells, which is essential in bacterial physiology and life cycle.²⁹ Attention has been paid on the search of new antibiotics targeting these enzymes recently, and achieved results indicate that various compounds have inhibitory effects on carbonic anhydrases, such as sulfonamides, carboxylates, phenols.³⁰ Despite the fact that carbonic anhydrases have been proved to be an innovative target for developing new antibiotics, the results are still in pre-clinical phases, and there is still a long way to go.³¹

1.2 Polymeric Materials with Antimicrobial Activity

Besides, antimicrobial polymeric materials, especially polymers mimicking the antimicrobial peptides are very promising antimicrobial agents with novel mechanism of action. For example, PHMB (polyhexamethylene biguanide) has been well applied as disinfectant and commercialized (Figure 1.4).³²

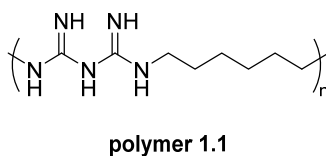


Figure 1.4 Structure of PHMB.

Generally, conventional antibiotics or low molecular weight antimicrobial agents have residual toxicity after treatment of infections, exerting great burden on the surrounding environment. In comparison, polymeric materials are long-standing and have immediate effects on contaminated materials or infected issues.³³ Moreover, polymeric materials have the potential to enhance the efficacy due to their polyvalent effects. The rapid development and versatility of polymer science and material science also provide great opportunity for the manufacture of antimicrobial polymers with various functions and applications.³⁴

1.2.1 Amino Acid-based Antimicrobial Polymers

Albeit the diversity of polymers, antimicrobial polymeric materials can be classified into different groups according to different criterion, natural and artificial, inherently active and active by attachment, soluble and insoluble, etc. Nonetheless, the story should be started with natural host-defense peptides.

1.2.1.1 Natural Host Defense Peptides

In the effort of searching new antibiotics, people found that peptides from the immune system or defense system of hosts could defeat the bacterial invasion without resistance observed.³⁵ It is the power of mother nature that oblige the multicellular organisms to develop this defense system by evolution although some antimicrobial peptides were isolated from microbes. A milestone in discovering host defense peptides is the report of cecropins by Boman in 1981 followed by the isolation and characterization of magainin by Zasloff in 1987.³⁶ Since that sprouting events on, the booming development of antimicrobial peptides has attracted enormous attentions from both clinical and academic

areas. Until now, more than 3000 antimicrobial peptides (including synthetic peptides) have been collected in the Antimicrobial Peptides Database wherein the number is still growing expeditiously.³⁷

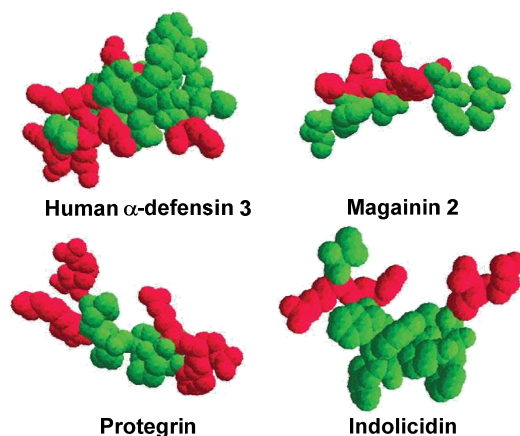


Figure 1.5³⁵ Amphiphilic features of typical antimicrobial peptides: Red, cationic; green, hydrophilic.

Host defense peptides are relatively short peptides consisting of 10-50 amino acid residues typically, which bear net positive charges and hydrophobic portions. Generally, the hydrophobic ends and cationic residues sequester on the opposite sides of the whole molecule, rendering the molecule amphiphilic (Figure 1.5).³⁵

Owing to this, antimicrobial peptides could adapt secondary structures in certain conditions, including α -helix, β -sheet, α,β -mixed and random coils (Figure 1.6).^{37a,38} For example, the very popular magainin from African frog displays secondary structure as α -helix especially in a non-polar environment. Moreover, antimicrobial peptides, like defensins, can also adapt β -sheet secondary structures due to the disulfide in these peptides.

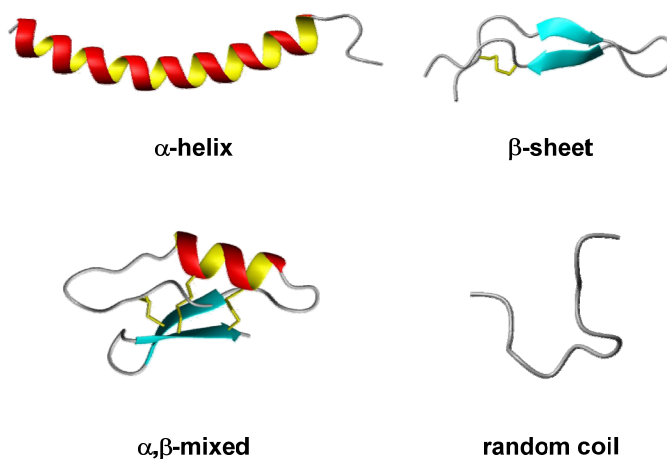


Figure 1.6^{37a} Secondary structures of typical antimicrobial peptides.

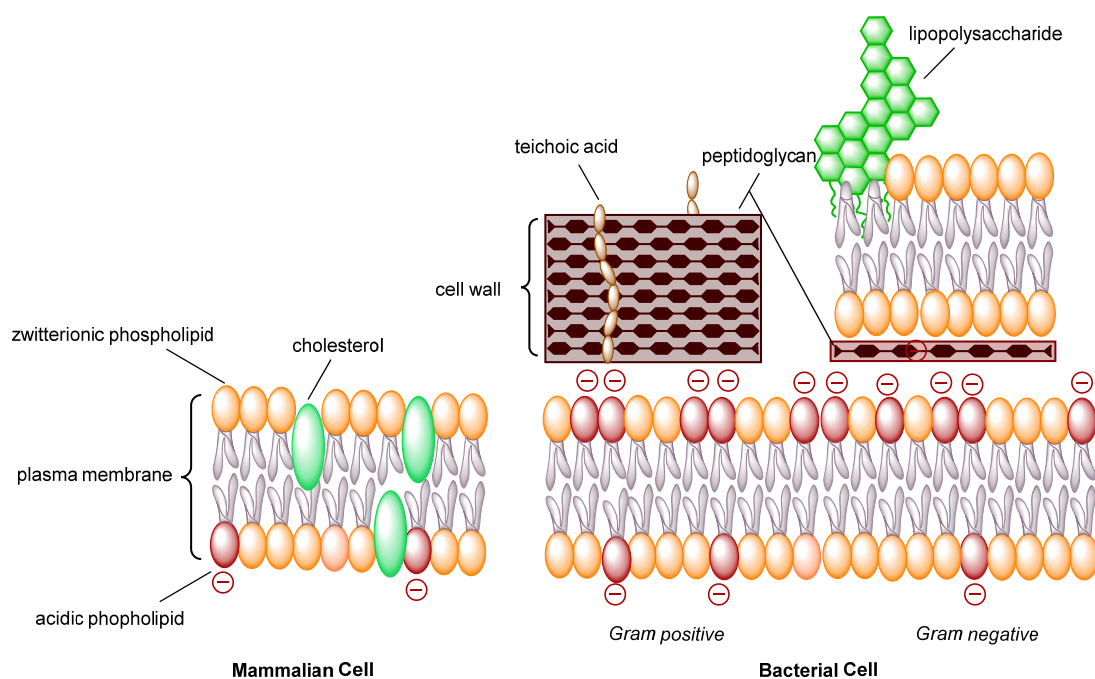


Figure 1.7 The major differences between mammalian cells and bacterial cells.

Besides, the mechanism of antimicrobial peptides killing bacteria is generally believed to be targeting bacterial membranes.³⁹ Specifically, the positively charged antimicrobial peptides selectively attach on the negatively charged bacterial membranes attributed to the electrostatic interactions, while negligible interaction with zwitterionic membranes of

mammalian cells gives rise to therapeutic selectivity. The basis of selectivity is principally because of the difference in the structures of two cell types. To be more specific, both mammalian cells and bacterial cells have cell membrane consisting of phospholipid bilayers, and almost same biomolecules constitute the membranes in both cases. However, the distribution of negative charges from the acidic phospholipids is different in bacterial and mammalian cells. More precisely, in mammalian cells, most negative charges are sequestered in the inner leaflets while the negatively charges are distributed in both sides of bacterial membranes (Figure 1.7).⁴⁰

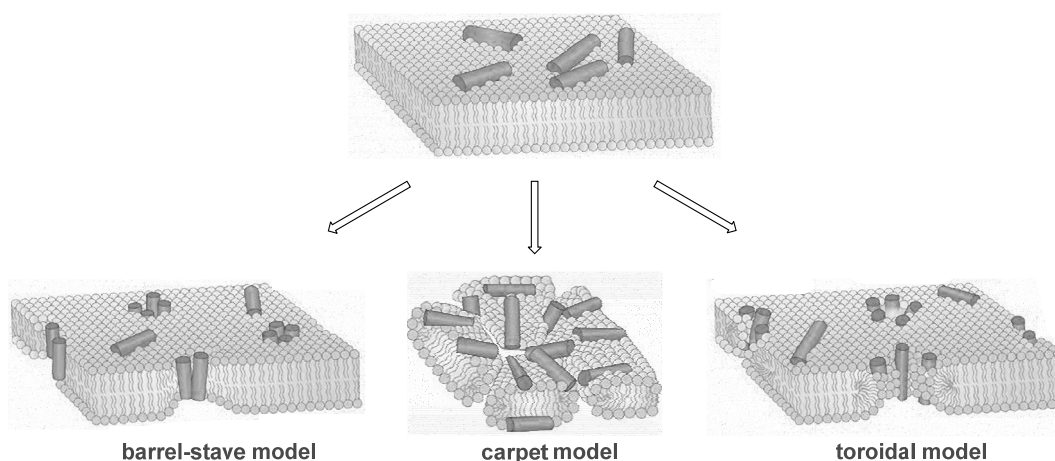


Figure 1.8³⁸ Three models of interaction between antimicrobial peptides and bacterial membranes.

Moreover, the killing effect of antibacterial activity is anticipated as disruption of cytoplasmic membrane and leakage of cytoplasmic contents even though there are also few peptides aiming at intracellular targets.⁴¹ This kind of nonspecific interactions result in less possibility for bacteria developing resistance towards antimicrobial peptides rendering antimicrobial peptides potential therapeutics in future market. And three major

models of membrane interaction were proposed which includes barrel-stave, toroidal and carpet model through which pores are formed on the surface of phospholipid bilayers or dissolve the membranes (Figure 1.8).³⁸

1.2.1.2 Synthetic Peptides

Due to the broad spectrum of antimicrobial activity and high selectivity, scientific community also spend continuous efforts on the design and synthesis of antimicrobial peptides. For example, fragments in the natural antimicrobial peptides are utilized in synthetic peptides, and by introducing lipids, carbohydrates and aromatic moieties, enhanced activities and reduced toxicities were achieved.^{40,42} The design of new sequence of antimicrobial peptides is a very tedious work owing to the difficulties in balancing the parameters that affect the activity and selectivity. Nevertheless, the natural peptides provide the key information of diverse structures for understanding and new design. Therefore, over the past years, many strategies have been developed to synthesize new antimicrobial peptides, especially the computer aided design which is a powerful tool to optimize the physicochemical properties. For instance, hydrophobicity is a crucial parameter to enhance the potency of peptides especially the ones with short sequences.⁴³ Meanwhile, introducing of hydrophilic segments such as PEG chains, improves the overall hydrophilicity of the peptides which will reduce the toxicity in most cases.⁴⁴

As a considerable drawback of natural peptides, the proteolysis is considered as one major problem to be addressed in the design of new antimicrobial peptides. To solve this, L-amino acids are replaced with D-amino acids, the N-terminus or C-terminus are protected as well as cyclization with the retainment of activity.⁴⁵

Additionally, with the help of computational design, more accurate prediction on the parameters can significantly reduce the time for rational design and molecular dynamic simulations could virtually determine the secondary structures which is also vital to antimicrobial activities. For example, ovispirin analogs has been successfully derivatized with higher activity and lower hemolysis with the help of computational design.⁴⁶

Overall, the antimicrobial peptides are great candidates for clinical therapy although there are still problems to be resolved. Indeed, there are already several peptide products have been approved, marketed and applied in clinics.⁴⁷ Moreover, numerous peptides have been studied by research community and many of them are in clinical trials with great possibility to be approved as therapeutic agents very soon.

1.2.1.3 Amino Acid-Based Peptidomimetics

Albeit the great progress achieved in antimicrobial peptides, as mentioned previously, there are still problems to be settled for the sake of more effective therapeutics. Amongst them, the cost of production in large quantity is a big problem for pharmaceutical manufacturing as well as the stability for storage. Therefore, considerable efforts have been made on the development of alternatives for antimicrobial peptides with the similarity in structures, in which peptidomimetics represent a very promising class of compounds, including oligomeric or polymeric synthetics.⁴⁸ Numerous and various functional groups could be introduced thanks to the versatility of chemistry tools, thus

plentiful antimicrobial peptidomimetics with reinforced stability and potency have been developed in the past decades, including β -peptides, peptoids, etc.⁴⁹

β -peptides are peptide analogs consisting of unnatural β -amino acid which has an extra carbon inserted between original α -carbon and carboxylic group, i.e. β -amino instead of α -amino group (Figure 1.9). This intrinsic feature attributes β -peptides unprecedented stability towards the proteases and more diversity in structures.⁵⁰

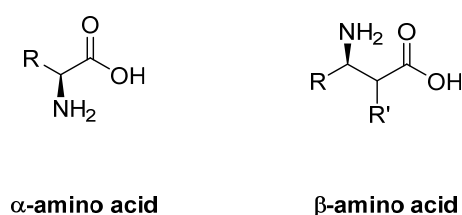


Figure 1.9 General structures of natural α -amino acid and unnatural β -amino acid.

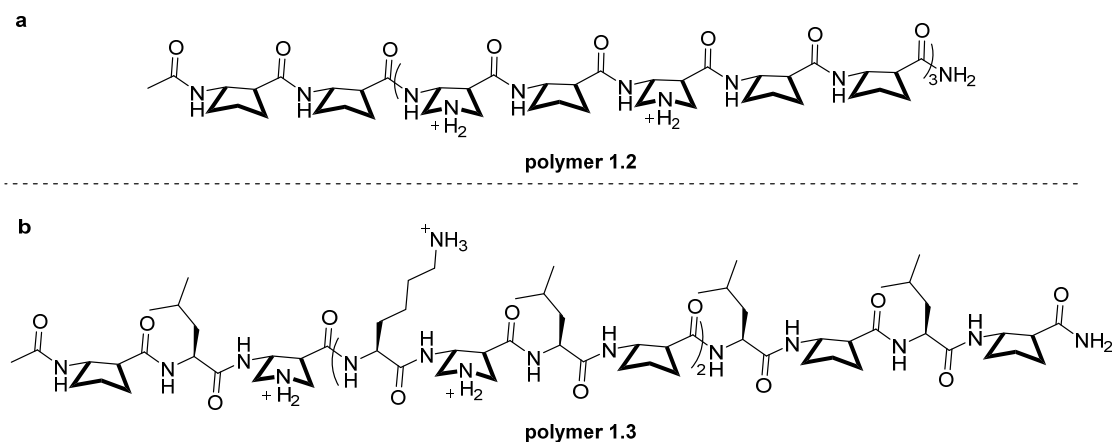


Figure 1.10 Nylon-3 copolymers reported by Gellman, *et al.* a) β -peptide; b) α,β -peptide

The initial design of antibacterial β -peptides was built on the amphiphilic and helical structures which was considered as the critical features for inhibiting bacteria and exhibiting high selectivity.⁵¹ Gellman and coworkers reported a series of random copolymers with β -amino acids, namely, Nylon-3 polymers (Figure 1.10).⁵²

The Nylon-3 polymers are reported to have high potency and broad spectrum of activity with low hemolytic toxicity. Commonly, as mentioned above, the hydrophobicity was believed to be responsible for the toxicity and the secondary structures, especially helical structures, are considered as the key factor in selectivity. Interestingly, after extensively studying the structure-activity relationship, Gellman and coworkers found that precise globally amphiphilic secondary structure is not really essential and the compounds will adopt an amphiphilic structure at the bacterial membrane surfaces.⁵³ Besides bacteria, the polymers also have efficacy in eradicating biofilm from drug resistant fungal pathogen and show synergistic effects with antifungal drugs.⁵⁴

Peptoids are oligomeric or polymeric N-substituted glycines which gained considerable attention in the past decades as promising antimicrobial peptoids have been reported in pharmaceutical discovery process (Figure 1.11).⁵⁵ Different from peptides, the substitutions on nitrogen atoms in amide bonds disable the hydrogen bonding in the backbone, rendering more flexible chains and diverse conformations. More importantly, the substituted nitrogens in peptoids bypass the recognition of proteases, making them tolerant towards degradation.⁵⁶ Nonetheless, amphiphilic peptoids were found to be active against *E. coli* and fungi with good selectivity, and rational design of amphiphilic peptoids could be realized by introducing side chains on the substituents on the amide nitrogens.⁵⁷

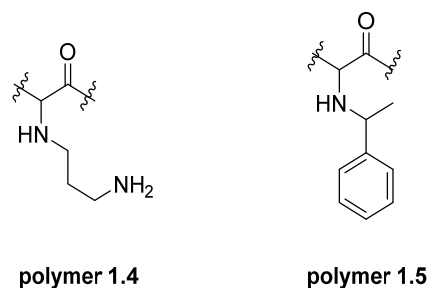


Figure 1.11 Representative structures of peptoids.

Likewise, in the searching of amphiphilic and helical peptoids, through systematic study of structure-activity relationship, Barron and coworkers found that helical structures are not necessary for the potency.⁵⁸

In addition, the integration of peptide and peptoids is a very interesting strategy to strengthen the potency of each compound. Indeed, it has been proved that hybrid peptoids possess great activity and low cytotoxicity.⁵⁹ For example, the hybrid of papiliocin and magainin displayed better activity than its individual origins and toxicity was reduced by the combination. These results demonstrate the great potential of peptoids in clinical applications.

1.2.2 Non-Amino Acid-based Antimicrobial Polymeric Materials

Besides the amino acid-based polymeric materials, there are plenty of polymeric materials from other natural sources or petroleum industry which can be developed into antimicrobial materials. Even if the stability problem of antimicrobial peptides has been addressed by peptidomimetics based on amino acids, and to some extent, the cost in synthesis of such compounds is lower than true antimicrobial peptides, the fact is that exploiting synthetic oligomers or polymers which is not based on amino acids is more

feasible in terms of cost, ease of synthesis and architecture control owing to the quick advancement of polymer science.

1.2.2.1 Modified Polymeric Matrices with Biocides

The development of antibiotic carrying polymeric materials was earlier than peptidomimetics.^{33,60} Therefore, polymeric materials which bearing antibiotics or biocides especially biocide-releasing materials have been well-studied and already applied in certain areas, such as water treatment. For instance, various polymers have been developed into water disinfectants. Quaternary ammonium salts functionalized polyolefin was demonstrated to be highly effective in removing various pathogens.⁶¹ N-halamine polymers reported by Worley could also be applied in water purification which has significant biocidal efficacy. More importantly, the material is very attractive owing their lower cost, ease of synthesis and especially rechargeability (Figure 1.12).⁶²

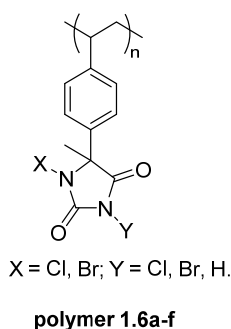


Figure 1.12 Structure of N-halamine polymers for water disinfection.

Despite their high efficacy, the continuous releasing of antimicrobial agents into surroundings will greatly raise up the chance for bacteria developing drug resistance which has already been a headache currently. Furthermore, the residual toxicity of

released antibiotics is another burden of our environment to be relieved. Therefore, immobilized antimicrobial compounds on surfaces without biocide leaching are probably more suitable and convenient for water purification and other applications. In this context, a variety of techniques have been developed to create immobilized antimicrobial materials.⁶³ As an example, quaternized poly-vinylpyridine was coated onto glass slides and displayed broad spectrum effects. Also, polymers bearing quaternary ammonium in mainchain was successfully coated onto surfaces and proved to be active (Figure 1.13).⁶⁴

On the other hand, even though antimicrobial surfaces or membranes are extensively studied and applied, they are usually for solid state purpose, such as food packing and water purification. Therefore, there are also high demands of antimicrobial agents used straightforwardly in solutions.

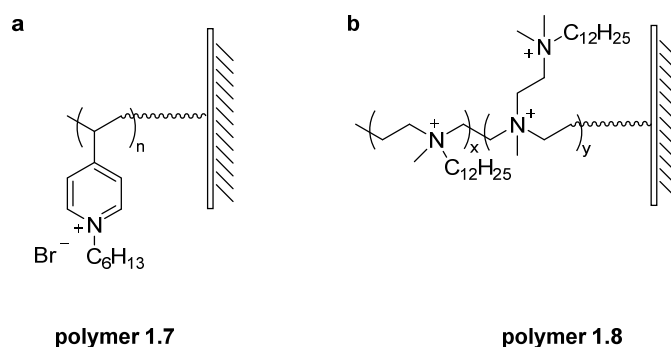


Figure 1.13 Antimicrobial surfaces preparation by coating quaternary ammonium polymers. a) Pendant active groups; b) Active groups in mainchain.

For example, as a well-known natural polysaccharide, chitosan derived from chitin has inherent antimicrobial activity. However, the relatively low efficacy has limited their further applications, which can be settled by modification with quaternary ammoniums

including pyridinium. Chitosan derivative bearing various quaternary ammoniums was reported by Sajomsang and coworkers (Figure 1.14).⁶⁵

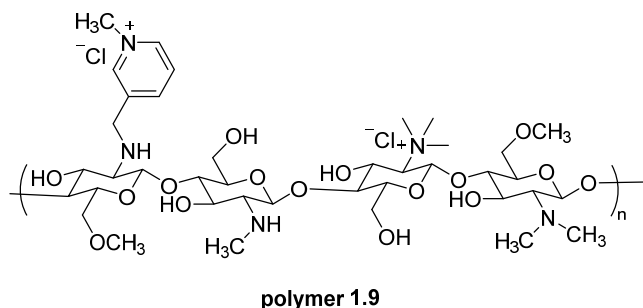


Figure 1.14 Water-soluble antimicrobial chitosan derivative prepared by quaternary ammoniums.

In brief, modification of polymeric matrices provides a wide range of antimicrobial polymeric substances for different areas including water treatment, food packaging, textiles and cosmetic consumables as well, regardless of natural or non-natural ones.⁶⁶ Moreover, the systematical exploration has furnished the world with better understanding of the relationship between structures and activities and shed light on the studies of synthetic antimicrobial polymers for biomedical purposes.

1.2.2.2 Synthetic Antimicrobial Materials with Programmed Amphiphilic

Structures

Although polymeric disinfectant materials have been widely studied and emerged independently almost the same time as the discovery of host defense peptides, the design and exploration of polymeric compounds with antimicrobial activity for biomedical applications are inspired by antimicrobial peptides.⁶⁷

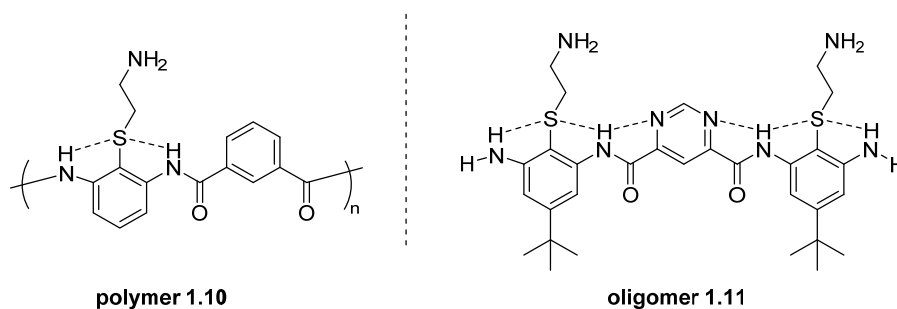


Figure 1.15 Arylamide oligomers with facial amphiphilicity restrained by hydrogen bonding.

Antimicrobial peptides are typically amphiphilic that form several secondary structures. Thus, in the early times of designing such compounds, researchers have concentrated more on the design of pre-programmed amphiphilic structures which were postulated to be unnecessary later, though. For example, the early design of arylamide oligomers reported by DeGrado and Tew groups are a class of compounds mimicking the facial amphiphilicity of antimicrobial peptides, which can also be considered as peptidomimetics. Facial amphiphilicity of the oligomers was obtained through the inflexible confirmation stabilized by hydrogen bonding (Figure 1.15).⁶⁸

The arylamides displayed good activity against a broad panel of bacteria and the issue of low selectivity in the initial design was addressed by systematically screening a series of compounds.⁶⁹ The authors concluded that the facial amphiphilicity designed in advance are responsible for the potency and selectivity as the more rigid structure has better performance.

In addition, oligomeric phenylene-ethynylene compounds were reported by Tew group, in which amide bonds are totally replaced with carbon-carbon bonds (Figure 1.16).⁷⁰ The phenylene-ethynylene oligomers are also facially amphiphilic and demonstrated superior

efficacy against a broad spectrum of bacteria including resistant strains with extraordinarily low toxicity. Also, the authors demonstrated the compounds could induce the leakage of dye in model phospholipid vesicles verifying the successful mimicking of antimicrobial peptides with emphasis on the amphiphilicity.^{70b,70c} Furthermore, the oligomers also exhibited high activity as anti-biofilm agent and anti-inflammatory agent *in vivo*.⁷¹

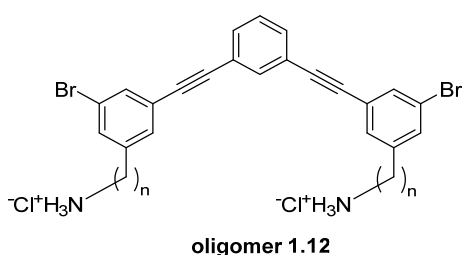


Figure 1.16 Oligomeric phenylene-ethynylenes with antimicrobial activity.

Albeit their low molecular weight comparable to that of small drugs, the non-amino acid building blocks in the arylamides and especially phenylene-ethynylenes sparked off the booming of antimicrobial polymeric materials.

Indeed, remarkable efforts have been focused on the development of antimicrobial polymers especially the amphiphilic structures mimicking antimicrobial peptides thereafter. Moreover, the great achievements in polymer science have facilitated the design and synthesis of polymers with better controllability, resulting in multitudes of antimicrobial peptide polymeric mimetics with powerful and selective activity and low toxicity.

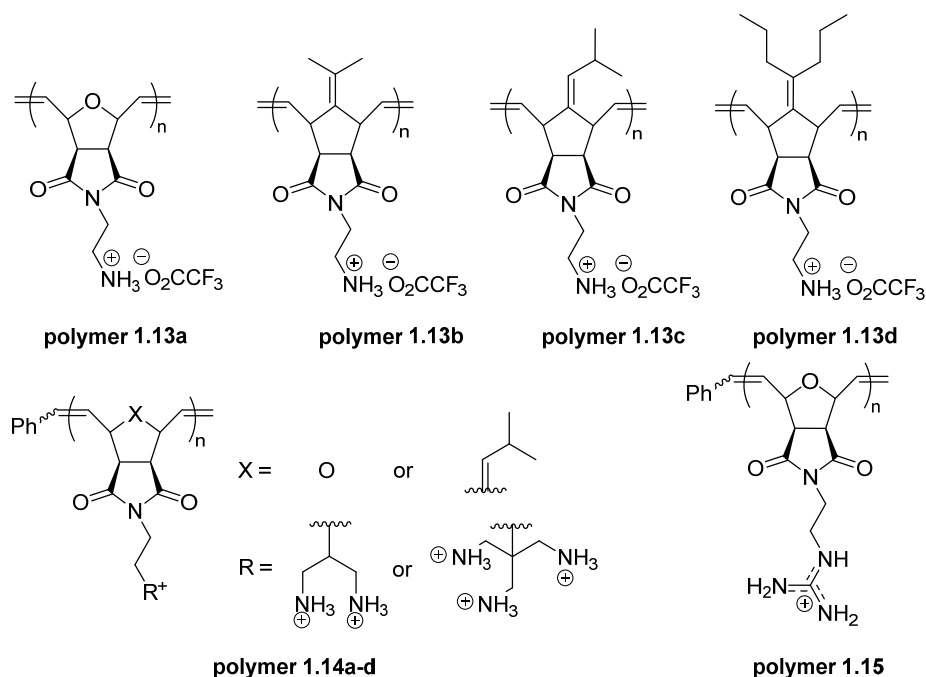


Figure 1.17 Antimicrobial homopolymers of poly(oxa)norbornenes with facial amphiphilicity.

Interestingly, it is also the Tew group who achieved a significant progress in the design and synthesis of antimicrobial polymers with facial amphiphilicity via ring opening metathesis polymerization technique. At their first attempts, homopolymers have been successfully achieved with facially amphiphilic monomers, which was believed to be critical for subsequent biological activities.⁷² The first series of homopolymers employed primary amine groups as the cationic moiety, which is frequently involved in antimicrobial peptides, and various aliphatic side groups to tune the hydrophobicity (Figure 1.17). The hydrophobic and amino groups are segregated at the opposite sides along the polymer chains, endowing facially amphiphilic structures. Besides, they also examined the effects of molecular weight and charge density on the biological activities of such polymers. Briefly, higher hydrophobicity in the polymer resulted in greater

hemolytic toxicity as well as better antibacterial activity whilst increased charge density significantly reduced hemolysis. Also, there was no observed relationship between activities and the molecular weight variation.

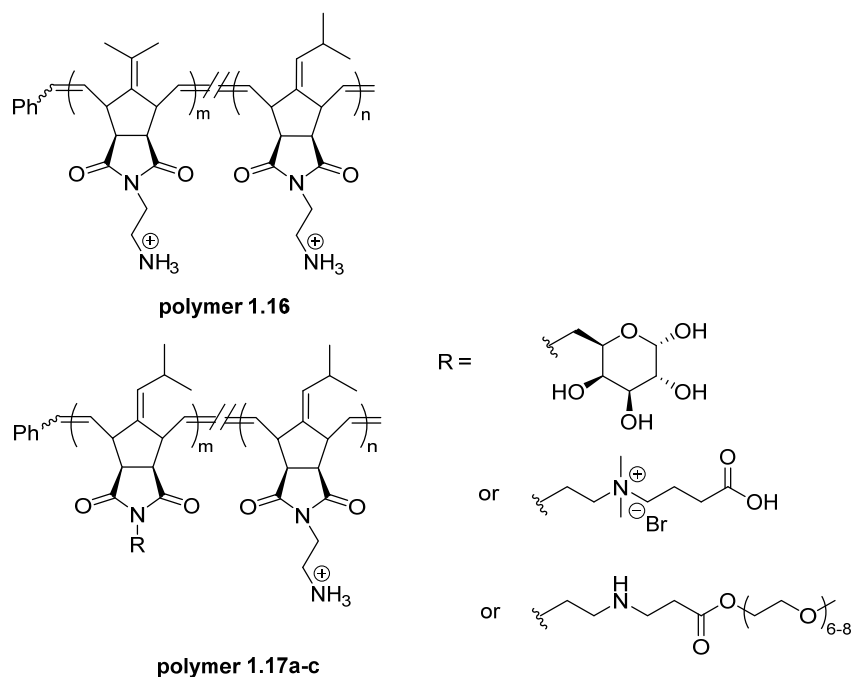


Figure 1.18 Antimicrobial copolymers of poly(oxa)norbornenes with facial amphiphilicity.

To further highlight the criticality of facial amphiphilicity and better understanding of such polymer system, copolymers were prepared over and above homopolymers (Figure 1.18).⁷³ With the monomers designed in the previous work, random copolymers were synthesized through varying the monomer ratios in the final products and the optimized polymer showed high selectivity of >100. On the other hand, more hydrophilic moieties were introduced as second constituent, however, moderately active copolymers have been

obtained which the authors ascribed to the lowered positive charges in the final compounds.⁷⁴

Rather than facially amphiphilic, Gellman among others believed that the globally amphiphilic structures of antimicrobial peptides are responsible for the biological activities including antimicrobial activity and toxicity.^{50,52b,75} Therefore, countless initial design of synthetic antimicrobial polymers especially peptides were programmed to adopt α -helix secondary structures wherein lipophilic and hydrophilic segments are dispersed on the opposite sides.⁷⁶

1.2.2.3 Synthetic Antimicrobial Polymeric Materials with Acquired Amphiphilic Structures

However, it is very interesting that Gellman and coworkers found that pre-organized amphiphilic structures are not really crucial for the target activity. Flexible structures bearing hydrophobic and cationic groups could automatically adapt global amphiphilicity at the surfaces of bacterial membrane bilayers, which is a great step forward in the knowledge of structure-activity relationship paving the way for further upsurge of antimicrobial polymers (Figure 1.19).⁵³

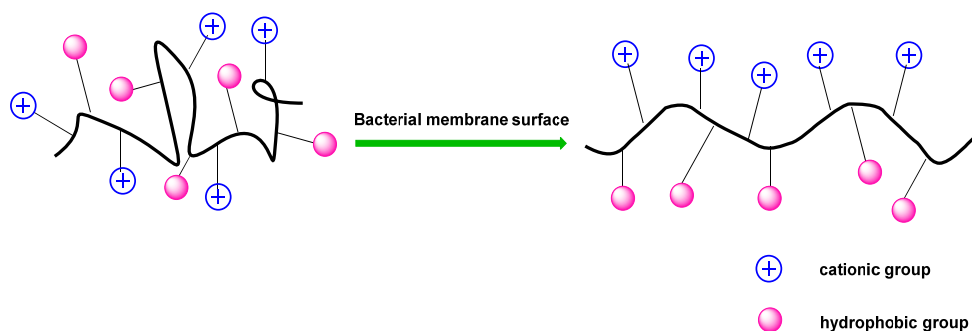


Figure 1.19 Induced amphiphilic structures of antimicrobial polymers.

Although to pre-program the amphiphilic monomers or polymers appeared to be unnecessary, amphiphilic feature of antimicrobial peptides is still considered as the golden rule in design new antimicrobial polymers. Thus, tremendous efforts have been paid on the development of amphiphilic polymeric materials mimicking antimicrobial peptides especially copolymers. Along with the exploration of new antimicrobial polymers, further understanding of structure-activity relationship has also been investigated.

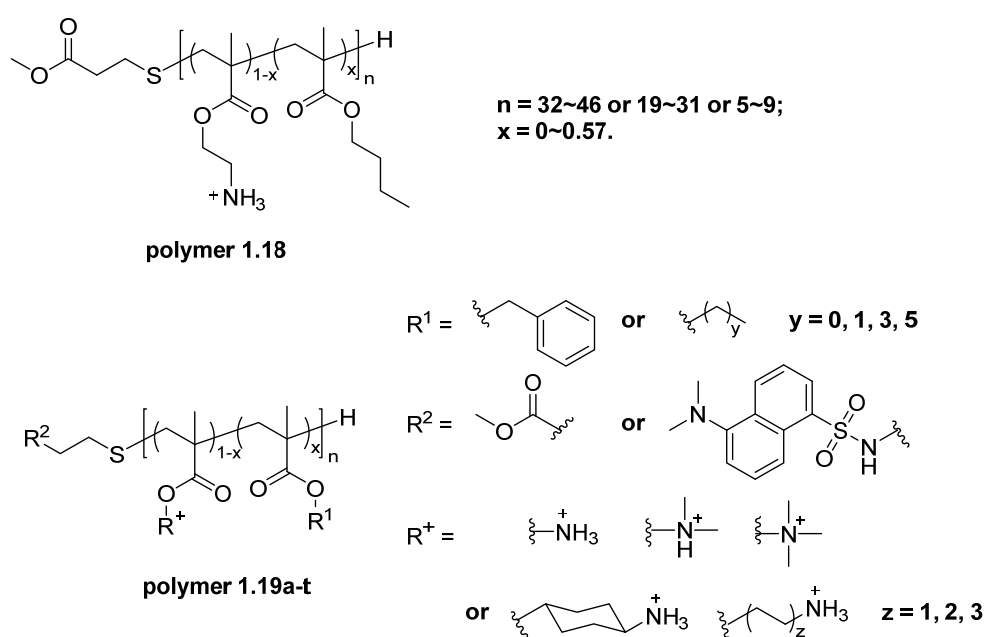


Figure 1.20 Developing the polymethacrylates into antimicrobial polymers with extensive screening.

Kuroda and others spent extensive efforts on poly(meth)acrylates platform to develop antimicrobial polymers.^{48c,77} Moreover, owing to the discovery of living radical polymerization techniques, tremendous polymers by ATRP, RAFT among others have been produced with high controllability of polymer microstructures and architectures.⁷⁸ Therefore, the first attempt in 2005 by Kuroda and DeGrado *et al.* has employed

methacrylate derivatized monomers bearing amino groups and tert-butyl groups in radical copolymerization, affording random copolymers with controlled polymer length and compositions (Figure 1.20).⁷⁹

The copolymers displayed good activity against *E. coli* and optimal selectivity has been found with low molecular weight copolymers consisting of 30% hydrophobic units. In particular, MIC values decreased with the increment of hydrophobic constituent until optimal ratio of 30% was reached, and no more enhancement afterwards. As expected, more hydrophobic contents involved resulted in higher hemolytic toxicity, and interestingly, higher molecular weight polymers exhibited higher toxicity compared to low molecular weight ones. Besides, further study of such effect was carried out by Kuroda and coworkers with every possible variation such hydrophobic monomers, distinct type of charge groups, as well as end groups.⁸⁰ Somehow, similar trend has been observed. These results suggested that it is very tough to obtain highly potent antimicrobial agents with no toxicity based on this molecular platform, but optimal candidates could be selected by systematically screening the amphiphilic balance, which is consistent with other polymer systems, to some extent. Nevertheless, much more work has been done by introducing guanidine groups as cationic groups, neutral polar molecules as hydrophilic components as well as ternary copolymers (Figure 1.21).⁸¹ Briefly, the incorporation of guanidine groups significantly enhanced the performance of polymers, with better activity and lower toxicity. Also, neutral hydrophilic groups such as PEG and sugars could reduce the toxicity impressively with slight sacrifice of activity.

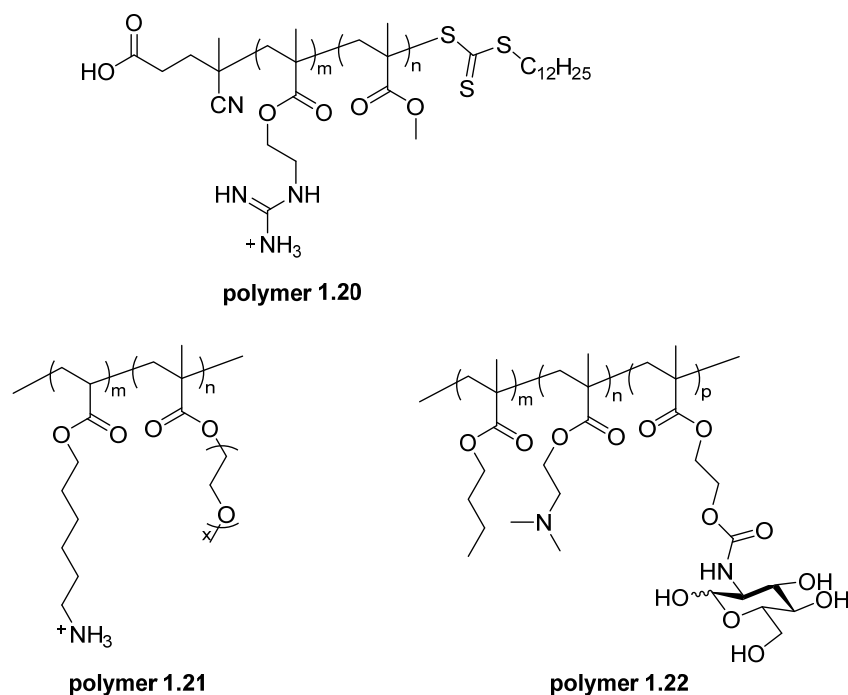


Figure 1.21 Optimizing the biological activities of poly(meth)acrylates by introducing different hydrophilic groups.

Besides, it is noteworthy to discuss the spatial distribution of cationic charges and hydrophobic tails which was directly compared in an early report by Sen and coworkers in a polymethacrylate-polystyrene-pyridinium system (Figure 1.22).⁸²

The results demonstrated that “different-centered” distribution has better activity than that of “same centered” cationic and hydrophobic groups while the “different-centered” polymers displayed higher toxicity which further explained the difficulty in optimizing random copolymers with “different-centered” groups. Therefore, more researchers designed copolymers with hydrophobic tails directly attached on the cationic centers and reasonable results have been achieved although this parameter is not the only thing to be taken into account (Figure 1.23).⁸³

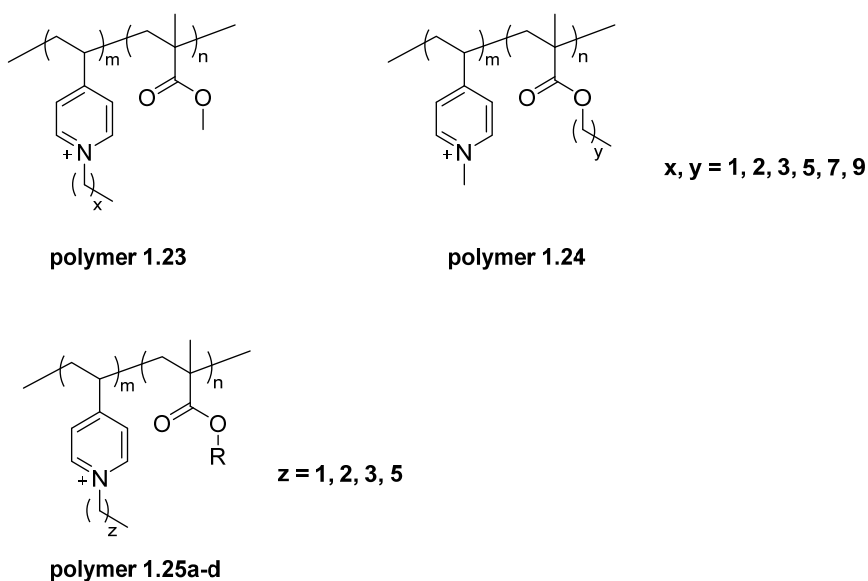


Figure 1.22 The effects of spatial distribution of hydrophobic and cationic groups.

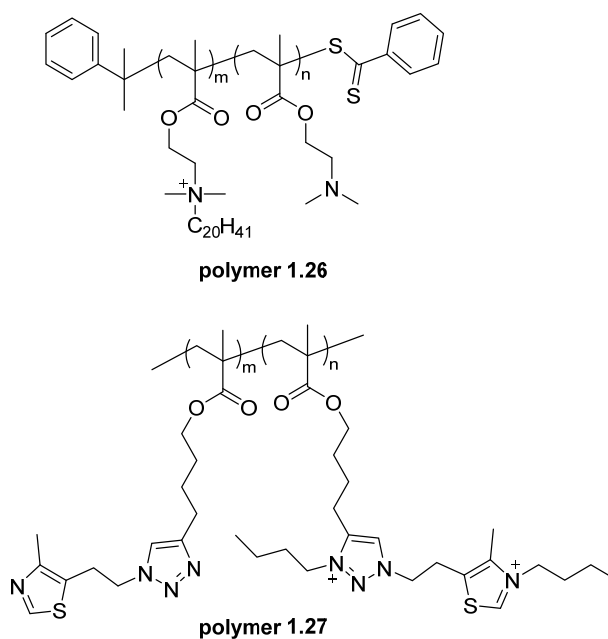


Figure 1.23 Polymethacrylates with hydrophobic groups directly linked to cationic centers.

There are also numerous other excellent antimicrobial polymeric materials reported by many intelligent chemists and material scientists. Amphiphilic balance is the primary factor to be optimized in order to mimic antimicrobial peptides and some fundamental

strategies have been made clear to us after long and extensive efforts by our research community especially those hallmarks by excellent pioneers. Briefly, hydrophilicity and hydrophobicity balance should be the key parameter to keep in mind although the balance is difficult to be tuned independently. Cyclic hydrophobic groups and unsaturated alkyl groups will preferably afford satisfactory results and neutrally hydrophilic moieties can give unexpected selectivity such as PEG and carbohydrates.^{39,84} Further, relatively low molecular weight demonstrated in most cases is a better choice for producing new materials.^{79,85} Also, hydrogen bonding can help to enhance the interaction between polymers and bacterial membranes.⁸⁶ In terms of cationic groups, primary amine mimicking lysine and guanidine mimicking arginine could afford polymers with great performance, and quaternized nitrogens involved in aromatic rings or π -conjugated rings are second choices.^{48c,87} Besides, the topology or morphology of polymeric materials are being taken into account for designing new materials since preliminary results showed surprising properties.⁸⁸

Nevertheless, it should also be noted that optimization of these parameters is dependent on the polymer platforms which means intensive efforts are still necessary to achieve highly selective compounds, case by case. Additionally, better understanding of the mechanism of actions will be beneficial although membrane interaction is believed to be the principal mode. Besides, unlike the daily applications such as food packing and water purification, antimicrobial agents to be applied in clinics should be strictly investigated before approved for marketing even though plenty of polymers behave quite well *in vitro*.

1.3 Problems and Research Objectives

1.3.1 Problems and Challenges of Current Antimicrobial Polymers

Although these polymers exhibited great biological activities, the majority of reported polymers, for instance, poly(meth)acrylates are carbon-carbon based backbones which are not degradable probably limiting their further *in vivo* applications.

To address this problem, Kuroda and others introduced degradable polyesters, polyurethanes as well as other fragile backbones into the field of antimicrobial polymeric materials.^{48d,87d,89} For example, Kuroda *et al.* reported self-immolative antimicrobial polymers by copolymerizing the previous polyacrylate with polyester which could automatically degrade although the biological profile still needs to be optimized further (Figure 1.24).^{89a}

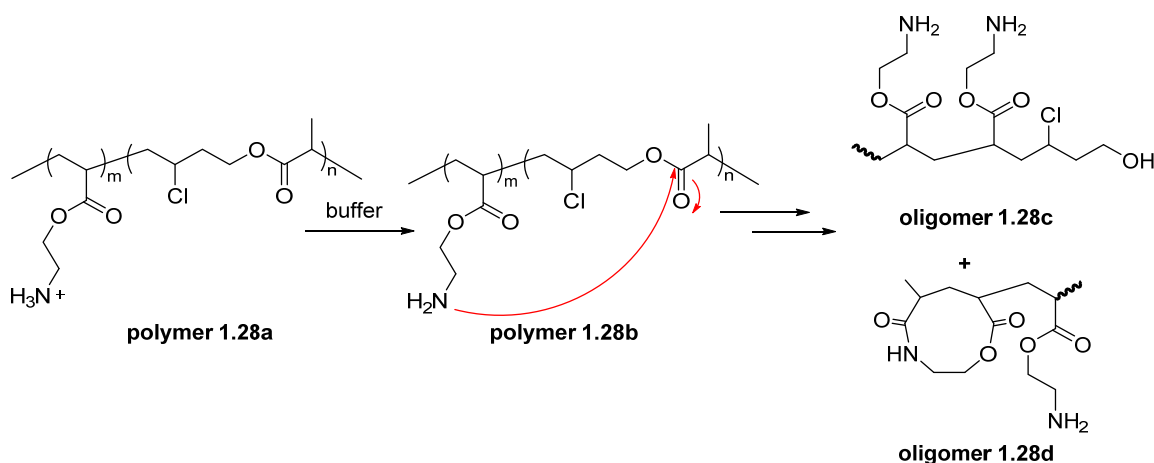


Figure 1.24 Self-degradable antibacterial polymers based on polyacrylates.

Nevertheless, the antimicrobial polymers reported are partially degradable and still toxic to host cells.

1.3.2 Research Objectives

Therefore, our objective is to develop antimicrobial polymers with degradability and low toxicities. Hopefully, new strategy for combatting drug resistance will be developed. Also, synthesizing polymeric materials with renewable natural resources, such as carbohydrates, will greatly relieve the burden of our environment.

1.4 References

- [1] G. J. Tortora, B. R. Funke, C. L. Case, *Microbiology: An Introduction*, 12 ed., Pearson Education, Inc, San Francisco, USA, **2016**.
- [2] J. Clardy, M. A. Fischbach, C. R. Currie, *Curr. Biol.* **2009**, *19*, R437.
- [3] M. L. Cohen, *Nature* **2000**, *406*, 762.
- [4] a) E. Y. Furuya, F. D. Lowy, *Nat. Rev. Microbiol.* **2006**, *4*, 36; b) H. F. Chambers, F. R. DeLeo, *Nat. Rev. Microbiol.* **2009**, *7*, 629; c) K. M. Overbye, J. F. Barrett, *Drug Discov. Today* **2005**, *10*, 45.
- [5] <http://www.who.int/medicines/publications/global-priority-list-antibiotic-resistant-bacteria/en/>.
- [6] a) C. Willyard, *Nature* **2017**, *543*, 15; b) G. M. Rossolini, F. Arena, P. Pecile, S. Pollini, *Curr. Opin. Pharm.* **2014**, *18*, 56.
- [7] a) G. A. Poland, R. M. Jacobson, I. G. Ovsyannikova, *Clin. Infect. Dis.* **2009**, *48*, 1254; b) D. P. Kontoyiannis, R. E. Lewis, *The Lancet* **2002**, *359*, 1135.
- [8] a) K. Hiramatsu, M. Igarashi, Y. Morimoto, T. Baba, M. Umekita, Y. Akamatsu, *Int. J. Antimicrob. Agents* **2012**, *39*, 478; b) E. D. Brown, G. D. Wright, *Nature* **2016**, *529*, 336.
- [9] G. J. Tortora, B. R. Funke, C. L. Case, *Microbiology: an introduction*, 11th ed., Pearson Education, Inc, San Francisco, USA, **2013**.
- [10] a) L. Zaffiri, J. Gardner, L. H. Toledo-Pereyra, *J. Invest. Surg.* **2012**, *25*, 67; b) N. C. Lloyd, H. W. Morgan, B. K. Nicholson, R. S. Ronimus, *Angew. Chem. Int. Ed.* **2005**, *44*, 941.
- [11] a) M. A. Kohanski, D. J. Dwyer, J. J. Collins, *Nat. Rev. Microbiol.* **2010**, *8*, 423; b) C. T. Walsh, T. A. Wencewicz, *J. Antibiot.* **2014**, *67*, 7.
- [12] J. T. Park, J. L. Strominger, *Science* **1957**, *125*, 99.
- [13] K. Kupferschmidt, *Science* **2016**, *352*, 758.

- [14] A. R. M. Coates, G. Halls, Y. Hu, *Brit. J. Pharmacol.* **2011**, 163, 184.
- [15] A. J. Alanis, *Arch. Med. Res.* **2005**, 36, 697.
- [16] a) J. M. A. Blair, M. A. Webber, A. J. Baylay, D. O. Ogbolu, L. J. V. Piddock, *Nat. Rev. Microbiol.* **2015**, 13, 42; b) I. T. Paulsen, M. H. Brown, R. A. Skurray, *Microbiol. Rev.* **1996**, 60, 575; c) S. Tamber, R. E. Hancock, *Front. Biosci* **2003**, 8, s472.
- [17] a) R. Bonnet, *Antimicrob. Agents Chemother.* **2004**, 48, 1; b) S. D. Lahiri, S. Mangani, T. Durand-Reville, M. Benvenuti, F. De Luca, G. Sanyal, J.-D. Docquier, *Antimicrob. Agents Chemother.* **2013**, 57, 2496.
- [18] A. Kumar, H. P. Schweizer, *Adv. Drug Deliv. Rev.* **2005**, 57, 1486.
- [19] C. Walsh, *Nature* **2000**, 406, 775.
- [20] R. H. Deurenberg, E. E. Stobberingh, *Infect. Genet. Evol.* **2008**, 8, 747.
- [21] a) I. M. Gould, M. Z. David, S. Esposito, J. Garau, G. Lina, T. Mazzei, G. Peters, *Int. J. Antimicrob. Agents* **2012**, 39, 96; b) I. M. Gould, R. Cauda, S. Esposito, F. Gudiol, T. Mazzei, J. Garau, *Int. J. Antimicrob. Agents* **2011**, 37, 202.
- [22] a) G. L. French, *Int. J. Antimicrob. Agents* **2010**, 36, S3; b) M. C. Jennings, K. P. C. Minbiole, W. M. Wuest, *ACS Infect. Dis.* **2015**, 1, 288.
- [23] <http://www.who.int/iris/handle/10665/44812>.
- [24] M. Baym, L. K. Stone, R. Kishony, *Science* **2016**, 351, aad3292.
- [25] J. A. Indrelie, W. R. Wilson, J. Y. Matsumoto, J. E. Geraci, J. A. Washington, *Antimicrob. Agents Chemother.* **1984**, 26, 909.
- [26] a) R. Watkins, K. Papp-Wallace, S. Drawz, R. Bonomo, *Front. Microbiol.* **2013**, 4, 392; b) R. N. Brogden, A. Carmine, R. C. Heel, P. A. Morley, T. M. Speight, G. S. Avery, *Drugs* **1981**, 22, 337.
- [27] G. Bushnell, F. Mitrani-Gold, L. M. Mundy, *Int. J. Infect. Dis.* **2013**, 17, e325.
- [28] a) M. Lopez, S. Köhler, J.-Y. Winum, *J. Inorg. Biochem.* **2012**, 111, 138; b) I. Nishimori, T. Minakuchi, D. Vullo, A. Scozzafava, C. T. Supuran, *Bioorg. Med. Chem.* **2011**, 19,

5023.

- [29] D. Vullo, V. D. Luca, A. Scozzafava, V. Carginale, M. Rossi, C. T. Supuran, C. Capasso, *Bioorg. Med. Chem.* **2013**, *21*, 1534.
- [30] a) C. Supuran, *Front. Pharmacol.* **2011**, *2*, 34; b) A. Maresca, A. Scozzafava, S. Köhler, J.-Y. Winum, C. T. Supuran, *J. Inorg. Biochem.* **2012**, *110*, 36; c) M. V. Buchieri, L. E. Riafrecha, O. M. Rodríguez, D. Vullo, H. R. Morbidoni, C. T. Supuran, P. A. Colinas, *Bioorg. Med. Chem. Lett.* **2013**, *23*, 740; d) C. T. Supuran, *Nat. Rev. Drug Discov.* **2008**, *7*, 168; e) I. Nishimori, T. Minakuchi, S. Onishi, D. Vullo, A. Scozzafava, C. T. Supuran, *J. Med. Chem.* **2007**, *50*, 381.
- [31] a) C. T. Supuran, *Curr. Med. Chem.* **2012**, *19*, 831; b) C. Capasso, C. T. Supuran, *Expert. Opin. Ther. Pat.* **2013**, *23*, 693.
- [32] P. Broxton, P. M. Woodcock, P. Gilbert, *J. Appl. Bacteriol.* **1983**, *54*, 345.
- [33] E.-R. Kenawy, S. D. Worley, R. Broughton, *Biomacromolecules* **2007**, *8*, 1359.
- [34] A. Muñoz-Bonilla, M. Fernández-García, *Eur. Polym. J.* **2015**, *65*, 46.
- [35] M. Zasloff, *Nature* **2002**, *415*, 389.
- [36] a) H. Steiner, D. Hultmark, Å. Engström, H. Bennich, H. G. Boman, *Nature* **1981**, *292*, 246; b) M. Zasloff, *Proc. Natl. Acad. Sci.* **1987**, *84*, 5449.
- [37] a) <http://aps.unmc.edu/AP/main.php>; b) G. Wang, X. Li, Z. Wang, *Nucleic Acids Res.* **2016**, *44*, D1087.
- [38] K. A. Brogden, *Nat. Rev. Microbiol.* **2005**, *3*, 238.
- [39] M. S. Ganewatta, C. Tang, *Polymer* **2015**, *63*, A1.
- [40] K. Matsuzaki, *Biochim. Biophys. Acta* **2009**, *1788*, 1687.
- [41] K. W. Bayles, *Nat. Rev. Microbiol.* **2013**, *12*, 63.
- [42] a) A. Schmidtchen, M. Pasupuleti, M. Malmsten, *Sci Adv. Colloid Interface Sci.* **2014**, *205*, 265; b) S. Ramesh, T. Govender, H. G. Kruger, B. G. Torre, F. Albericio, *J. Pept. Sci.* **2016**, *22*, 438.

- [43] A. Pessi, *J. Pept. Sci.* **2014**, 21, 379.
- [44] I. W. Hamley, *Biomacromolecules* **2014**, 15, 1543.
- [45] a) A. Di Grazia, F. Cappiello, H. Cohen, B. Casciaro, V. Luca, A. Pini, Y. P. Di, Y. Shai, M. L. Mangoni, *Amino Acids* **2015**, 47, 2505; b) G. Luca, M. Rossella De, C. Lucia, *Curr. Pharm. Des.* **2010**, 16, 3185; c) Y. Lan, J. T. Lam, G. K. H. Siu, W. C. Yam, A. J. Mason, J. K. W. Lam, *Tuberculosis* **2014**, 94, 678.
- [46] H. Khandelia, Y. N. Kaznessis, *Peptides* **2005**, 26, 2037.
- [47] P. Vlieghe, V. Lisowski, J. Martinez, M. Khrestchatisky, *Drug Discov. Today* **2010**, 15, 40.
- [48] a) N. Srinivas, P. Jetter, B. J. Ueberbacher, M. Werneburg, K. Zerbe, J. Steinmann, B. Van der Meijden, F. Bernardini, A. Lederer, R. L. A. Dias, P. E. Misson, H. Henze, J. Zumbunn, F. O. Gombert, D. Obrecht, P. Hunziker, S. Schauer, U. Ziegler, A. Käch, L. Eberl, K. Riedel, S. J. DeMarco, J. A. Robinson, *Science* **2010**, 327, 1010; b) Y. Pang, B. An, L. Lou, J. Zhang, J. Yan, L. Huang, X. Li, S. Yin, *J. Med. Chem.* **2017**, 60, 7300; c) H. Takahashi, G. A. Caputo, S. Vemparala, K. Kuroda, *Bioconj. Chem.* **2017**, 28, 1340; d) C. Ergene, E. F. Palermo, *Biomacromolecules* **2017**, 18, 3400; e) Y. Li, H. Wu, P. Teng, G. Bai, X. Lin, X. Zuo, C. Cao, J. Cai, *J. Med. Chem.* **2015**, 58, 4802.
- [49] a) E. A. Porter, X. Wang, H.-S. Lee, B. Weisblum, S. H. Gellman, *Nature* **2000**, 404, 565; b) A. Violette, S. Fournel, K. Lamour, O. Chaloin, B. Frisch, J.-P. Briand, H. Monteil, G. Guichard, *Chem. Biol.* **2006**, 13, 531.
- [50] R. P. Cheng, S. H. Gellman, W. F. DeGrado, *Chem. Rev.* **2001**, 101, 3219.
- [51] D. Liu, W. F. DeGrado, *J. Am. Chem. Soc.* **2001**, 123, 7553.
- [52] a) E. A. Porter, B. Weisblum, S. H. Gellman, *J. Am. Chem. Soc.* **2002**, 124, 7324; b) M. A. Schmitt, B. Weisblum, S. H. Gellman, *J. Am. Chem. Soc.* **2004**, 126, 6848.
- [53] M. A. Schmitt, B. Weisblum, S. H. Gellman, *J. Am. Chem. Soc.* **2007**, 129, 417.
- [54] a) R. Liu, X. Chen, S. P. Falk, K. S. Masters, B. Weisblum, S. H. Gellman, *J. Am. Chem.*

- Soc.* **2015**, 137, 2183; b) C. Mora-Navarro, J. Caraballo-León, M. Torres-Lugo, P. Ortiz-Bermúdez, *J. Pept. Sci.* **2015**, 21, 853.
- [55] a) S. Ng, B. Goodson, A. Ehrhardt, W. H. Moos, M. Siani, J. Winter, *Bioorg. Med. Chem.* **1999**, 7, 1781; b) B. Goodson, A. Ehrhardt, S. Ng, J. Nuss, K. Johnson, M. Giedlin, R. Yamamoto, W. H. Moos, A. Krebber, M. Ladner, M. B. Giacona, C. Vitt, J. Winter, *Antimicrob. Agents Chemother.* **1999**, 43, 1429.
- [56] W. Huang, J. Seo, S. B. Willingham, A. M. Czyzewski, M. L. Gonzalgo, I. L. Weissman, A. E. Barron, *PLoS One* **2014**, 9, e90397.
- [57] a) P. Armand, K. Kirshenbaum, R. A. Goldsmith, S. Farr-Jones, A. E. Barron, K. T. V. Truong, K. A. Dill, D. F. Mierke, F. E. Cohen, R. N. Zuckermann, E. K. Bradley, *Proc. Natl. Acad. Sci.* **1998**, 95, 4309; b) N. P. Chongsirawatana, J. A. Patch, A. M. Czyzewski, M. T. Dohm, A. Ivankin, D. Gidalevitz, R. N. Zuckermann, A. E. Barron, *Proc. Natl. Acad. Sci.* **2008**, 105, 2794; c) A. R. Statz, J. P. Park, N. P. Chongsirawatana, A. E. Barron, P. B. Messersmith, *Biofouling* **2008**, 24, 439.
- [58] a) N. P. Chongsirawatana, T. M. Miller, M. Wetzler, S. Vakulenko, A. J. Karlsson, S. P. Palecek, S. Mobashery, A. E. Barron, *Antimicrob. Agents Chemother.* **2011**, 55, 417; b) R. Kapoor, P. R. Eimerman, J. W. Hardy, J. D. Cirillo, C. H. Contag, A. E. Barron, *Antimicrob. Agents Chemother.* **2011**, 55, 3058.
- [59] A. Shin, E. Lee, D. Jeon, Y.-G. Park, J. K. Bang, Y.-S. Park, S. Y. Shin, Y. Kim, *Biochemistry* **2015**, 54, 3921.
- [60] T. Tashiro, *Macromol. Mater. Eng.* **2001**, 286, 63.
- [61] N. Kawabata, K. Yamazaki, T. Otake, I. Oishi, Y. Minekawa, *Epidemiol. Infect.* **1990**, 105, 633.
- [62] Y. Chen, S. D. Worley, J. Kim, C. I. Wei, T.-Y. Chen, J. I. Santiago, J. F. Williams, G. Sun, *Ind. Eng. Chem. Res.* **2003**, 42, 280.
- [63] a) D. Campoccia, L. Montanaro, C. R. Arciola, *Biomaterials* **2013**, 34, 8533; b) T. Wei,

- Z. Tang, Q. Yu, H. Chen, *ACS Appl. Mater. Interfaces* **2017**, 9, 37511; c) M. K. Kim, A. Zhao, A. Wang, Z. Z. Brown, T. W. Muir, H. A. Stone, B. L. Bassler, *Nat. Microbiol.* **2017**, 2, 17080.
- [64] a) J. C. Tiller, C.-J. Liao, K. Lewis, A. M. Klibanov, *Proc. Natl. Acad. Sci.* **2001**, 98, 5981; b) J. Haldar, D. An, L. Alvarez de Cienfuegos, J. Chen, A. M. Klibanov, *Proc. Natl. Acad. Sci.* **2006**, 103, 17667.
- [65] W. Sajomsang, U. R. Ruktanonchai, P. Gonil, C. Warin, *Carbohydr. Polym.* **2010**, 82, 1143.
- [66] K.-S. Huang, C.-H. Yang, S.-L. Huang, C.-Y. Chen, Y.-Y. Lu, Y.-S. Lin, *Int. J. Mol. Sci.* **2016**, 17.
- [67] I. Mukherjee, A. Ghosh, P. Bhadury, P. De, *ACS Omega* **2017**, 2, 1633.
- [68] a) G. N. Tew, D. Liu, B. Chen, R. J. Doerksen, J. Kaplan, P. J. Carroll, M. L. Klein, W. F. DeGrado, *Proc. Natl. Acad. Sci.* **2002**, 99, 5110; b) H. Tang, R. J. Doerksen, T. V. Jones, M. L. Klein, G. N. Tew, *Chem. Biol.* **2006**, 13, 427.
- [69] S. Choi, A. Isaacs, D. Clements, D. Liu, H. Kim, R. W. Scott, J. D. Winkler, W. F. DeGrado, *Proc. Natl. Acad. Sci.* **2009**, 106, 6968.
- [70] a) L. Arnt, G. N. Tew, *J. Am. Chem. Soc.* **2002**, 124, 7664; b) L. Arnt, K. Nüsslein, G. N. Tew, *J. Polym. Sci. A Polym. Chem.* **2004**, 42, 3860; c) L. Arnt, J. R. Rennie, S. Linser, R. Willumeit, G. N. Tew, *J. Phys. Chem. B* **2006**, 110, 3527.
- [71] J. Hua, R. W. Scott, G. Diamond, *Mol. Oral Microbiol.* **2010**, 25, 426.
- [72] a) M. F. Ilker, K. Nüsslein, G. N. Tew, E. B. Coughlin, *J. Am. Chem. Soc.* **2004**, 126, 15870; b) Z. M. Al-Badri, A. Som, S. Lyon, C. F. Nelson, K. Nüsslein, G. N. Tew, *Biomacromolecules* **2008**, 9, 2805; c) G. J. Gabriel, A. E. Madkour, J. M. Dabkowski, C. F. Nelson, K. Nüsslein, G. N. Tew, *Biomacromolecules* **2008**, 9, 2980.
- [73] F. Sgolastra, B. M. deRonde, J. M. Sarapas, A. Som, G. N. Tew, *Acc. Chem. Res.* **2013**, 46, 2977.

- [74] S. Colak, C. F. Nelson, K. Nüsslein, G. N. Tew, *Biomacromolecules* **2009**, *10*, 353.
- [75] a) J. A. Patch, A. E. Barron, *J. Am. Chem. Soc.* **2003**, *125*, 12092; b) I. S. Radzishhevsky, S. Rotem, D. Bourdetsky, S. Navon-Venezia, Y. Carmeli, A. Mor, *Nat. Biotechnol.* **2007**, *25*, 657.
- [76] a) A. Hayen, M. A. Schmitt, F. N. Ngassa, K. A. Thomasson, S. H. Gellman, *Angew. Chem. Int. Ed.* **2004**, *43*, 505; b) M. A. Schmitt, S. H. Choi, I. A. Guzei, S. H. Gellman, *J. Am. Chem. Soc.* **2005**, *127*, 13130.
- [77] a) K. Kuroda, G. A. Caputo, *Wiley Interdiscip. Rev. Nanomed. Nanobiotechnol.* **2013**, *5*, 49; b) H. Takahashi, E. F. Palermo, K. Yasuhara, G. A. Caputo, K. Kuroda, *Macromol. Biosci.* **2013**, *13*, 1285.
- [78] K. Matyjaszewski, J. Spanswick, *Mater. Today* **2005**, *8*, 26.
- [79] K. Kuroda, W. F. DeGrado, *J. Am. Chem. Soc.* **2005**, *127*, 4128.
- [80] a) E. F. Palermo, K. Kuroda, *Biomacromolecules* **2009**, *10*, 1416; b) K. Kuroda, G. A. Caputo, W. F. DeGrado, *Chem. Eur. J.* **2009**, *15*, 1123; c) E. F. Palermo, S. Vemparala, K. Kuroda, *Biomacromolecules* **2012**, *13*, 1632; d) X. Yang, K. Hu, G. Hu, D. Shi, Y. Jiang, L. Hui, R. Zhu, Y. Xie, L. Yang, *Biomacromolecules* **2014**, *15*, 3267.
- [81] a) K. E. S. Locock, T. D. Michl, J. D. P. Valentin, K. Vasilev, J. D. Hayball, Y. Qu, A. Traven, H. J. Griesser, L. Meagher, M. Haeussler, *Biomacromolecules* **2013**, *14*, 4021; b) A. Punia, A. Mancuso, P. Banerjee, N.-L. Yang, *ACS Macro Lett.* **2015**, *4*, 426; c) M. Álvarez-Paino, A. Muñoz-Bonilla, F. López-Fabal, J. L. Gómez-Garcés, J. P. A. Heuts, M. Fernández-García, *Biomacromolecules* **2015**, *16*, 295.
- [82] V. Sambhy, B. R. Peterson, A. Sen, *Angew. Chem. Int. Ed.* **2008**, *47*, 1250.
- [83] a) Y. Chen, P. A. Wilbon, Y. P. Chen, J. Zhou, M. Nagarkatti, C. Wang, F. Chu, A. W. Decho, C. Tang, *RSC Adv.* **2012**, *2*, 10275; b) R. Tejero, D. López, F. López-Fabal, J. L. Gómez-Garcés, M. Fernández-García, *Biomacromolecules* **2015**, *16*, 1844.
- [84] a) S. Chakraborty, R. Liu, J. J. Lemke, Z. Hayouka, R. A. Welch, B. Weisblum, K. S.

- Masters, S. H. Gellman, *ACS Macro Lett.* **2013**, 2, 753; b) D. S. S. M. Uppu, M. Bhowmik, S. Samaddar, J. Haldar, *Chem. Commun.* **2016**, 52, 4644.
- [85] a) K. Lienkamp, K.-N. Kumar, A. Som, K. Nüsslein, G. N. Tew, *Chem. Eur. J.* **2009**, 15, 11710; b) B. P. Mowery, A. H. Lindner, B. Weisblum, S. S. Stahl, S. H. Gellman, *J. Am. Chem. Soc.* **2009**, 131, 9735; c) C. A. Hae Cho, C. Liang, J. Perera, J. Liu, K. G. Varnava, V. Sarojini, R. P. Cooney, D. J. McGillivray, M. A. Brimble, S. Swift, J. Jin, *Biomacromolecules* **2018**, 19, 1389.
- [86] a) D. S. S. M. Uppu, M. M. Konai, U. Baul, P. Singh, T. K. Siersma, S. Samaddar, S. Vemparala, L. W. Hamoen, C. Narayana, J. Haldar, *Chem. Sci.* **2016**, 7, 4613; b) D. S. S. M. Uppu, S. Samaddar, J. Hoque, M. M. Konai, P. Krishnamoorthy, B. R. Shome, J. Haldar, *Biomacromolecules* **2016**, 17, 3094.
- [87] a) A. Punia, E. He, K. Lee, P. Banerjee, N.-L. Yang, *Chem. Commun.* **2014**, 50, 7071; b) S. E. Exley, L. C. Paslay, G. S. Sahukhal, B. A. Abel, T. D. Brown, C. L. McCormick, S. Heinhorst, V. Koul, V. Choudhary, M. O. Elasri, S. E. Morgan, *Biomacromolecules* **2015**, 16, 3845; c) V. W. L. Ng, J. P. K. Tan, J. Leong, Z. X. Voo, J. L. Hedrick, Y. Y. Yang, *Macromolecules* **2014**, 47, 1285; d) W. Chin, C. Yang, V. W. L. Ng, Y. Huang, J. Cheng, Y. W. Tong, D. J. Coady, W. Fan, J. L. Hedrick, Y. Y. Yang, *Macromolecules* **2013**, 46, 8797.
- [88] a) T.-K. Nguyen, S. J. Lam, K. K. K. Ho, N. Kumar, G. G. Qiao, S. Egan, C. Boyer, E. H. H. Wong, *ACS Infect. Dis.* **2017**, 3, 237; b) S. J. Lam, N. M. O'Brien-Simpson, N. Pantarat, A. Sulistio, E. H. H. Wong, Y.-Y. Chen, J. C. Lenzo, J. A. Holden, A. Blencowe, E. C. Reynolds, G. G. Qiao, *Nat. Microbiol.* **2016**, 1, 16162; c) R. Namivandi-Zangeneh, R. J. Kwan, T.-K. Nguyen, J. Yeow, F. L. Byrne, S. H. Oehlers, E. H. H. Wong, C. Boyer, *Polym. Chem.* **2018**, 9, 1735.
- [89] a) M. Mizutani, E. F. Palermo, L. M. Thoma, K. Satoh, M. Kamigaito, K. Kuroda, *Biomacromolecules* **2012**, 13, 1554; b) S. Mankoci, R. L. Kaiser, N. Sahai, H. A. Barton,

A. Joy, *ACS Biomater. Sci. Eng.* **2017**, 3, 2588; c) D. N. Amato, D. V. Amato, O. V. Mavrodi, W. B. Martin, S. N. Swilley, K. H. Parsons, D. V. Mavrodi, D. L. Patton, *ACS Macro Lett.* **2017**, 6, 171.

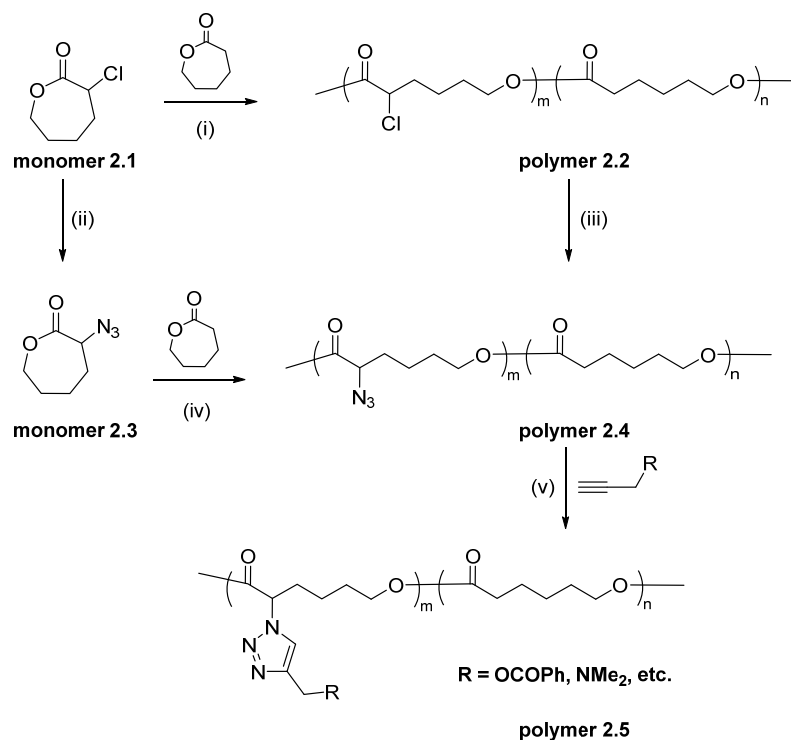
Chapter 2

Synthesis of Antibacterial Glycosylated Polycaprolactones with Reduced Toxicities

2.1 Introduction

The antimicrobial polymers, inspired by the cationic amino acids residues in AMPs, generally have cationic groups to facilitate their adsorption to negatively charged bacterial membranes.¹ Many antibacterial polymers have been synthesized, such as polynorbornenes,² polycarbonates,³ poly(β -lactam),⁴ polypeptides⁵ and polyacrylate derivatives.⁶ However, most synthetic antimicrobial polymers are consisting of non-degradable carbon-based backbones, limiting their potential in clinical applications. Aliphatic polyesters constitute a class of biodegradable polymers and their roles as scaffolds for biodegradable antibacterial polymers have been rarely investigated.^{3a,3e,7} Although antibacterial polycarbonates have been reported and appear to be a good example of degradable antibacterial polymers, PCL (poly-(ϵ -caprolactone)) has more efficient degradation behavior compared to polycarbonates.⁸ Also, antibacterial polymers employing using PCL as backbone are rarely studied.⁹

As a well-known biodegradable polyester, PCL has attracted considerable attention for the past decades, but the major drawback is the lack of side functional groups which limited their further applications. Fortunately, functional ϵ -caprolactone with pendant chloride groups was reported by Riva and coworkers which could be further converted into azido groups, rendering post-modification possible through copper-catalyzed click reaction (Scheme 2.1).¹⁰ Besides, the backbone of cationic antibacterial polymers is known to profoundly affect the resultant biological properties. Therefore, these interesting and attractive results had inspired us to design new antibacterial polymers based on polycaprolactones.



Scheme 2.1 Functional PCLs prepared by combining ring-opening polymerization and CuAAC reaction. i) 2,2-dibutyl-2-stanna-1,3-dioxepane (DSDOP), toluene, rt, 4 h; ii) NaN₃, DMF, 45 °C, 3 days; iii) NaN₃, DMF, rt, overnight; iv) DSDOP, toluene, rt, 4 h; v) CuI, DBU, THF, 35 °C, 4 h.

Click chemistry has drawn considerable attention since first defined by Sharpless, which is not a certain reaction but a few reactions comprising a set of criteria making this approach possess incomparable advantages.¹¹ As defined by Sharpless, click reactions usually occur in mild conditions with high efficiency and show outstanding tolerance of functional groups, endowing them great potential in broader applications. There are several good click reactions available, and CuAAC reaction has been extensively applied in polymerization technique.¹²

Cationic groups such as quaternary ammonium, guanidinium as well as imidazolium salts have gained considerable attention in antimicrobial applications.¹³ Amongst them,

imidazoliums have been extensively applied in organic synthesis as ionic liquids because of their special physiochemical properties.¹⁴ Moreover, imidazoliums applied in antimicrobial polymers has demonstrated great potency against a wide range of pathogens, owing to their relatively high hydrophilicity and especially permanent charges.^{3c,15}

Furthermore, like natural AMPs, most cationic polymers are hemolytic or cytotoxic to human cells,¹⁶ limiting their further applications. Thus, studies have been widely pursued to manipulate the antimicrobial activity and biocompatibility of the synthetic polymers through various factors such as hydrophobicity from alkyl chain, hydrophilicity from different types of cationic groups and neutral polar subunits as well as polymer compositions.^{2a,6a,6b,17} In particular, the balance between hydrophilicity and hydrophobicity of the entire polymer is most crucial to the selectivity. This can be achieved by adding alkyl chains to increase hydrophobicity and biocompatible compounds such as poly(ethylene glycol) and carbohydrate.¹⁸

Glycopolymers were widely studied because of their multivalent interactions with cells since the first glycopolymer with pendant lactose was reported by Kobayashi and coworkers.¹⁹ During the past decades, plenty of efforts were dedicated to synthesizing glycopolymers with great diversity, and different strategies and various polymerization techniques especially living polymerization processes were employed to facilitate the synthesis including ring-opening polymerization.²⁰ Although bacterial lectins have not been researched as extensively as those of animals, interactions of bacterial adhesion lectins with mannose was studied by Knight and coworkers.²¹ Besides their recognition

features, another advantage of carbohydrates is their biocompatibility. Narain and coworkers successfully produced a set of methacrylate-based glycopolymers via RAFT polymerization. More than 80% cell viability was achieved when the cells were incubated with glycopolymer-functionalized quantum dots.²²

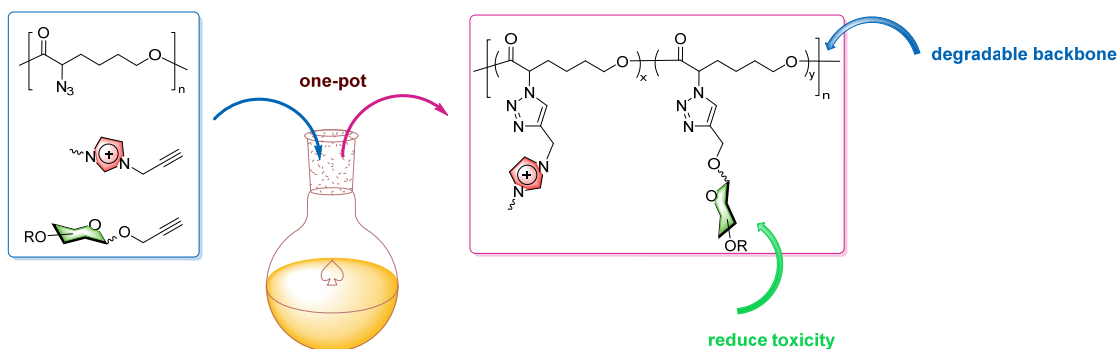


Figure 2.1 Design of new antibacterial polymers based on PCL bearing imidazoliums and carbohydrates.

Therefore, with the aim of finding new biodegradable antimicrobial compounds and investigating the possible effects of carbohydrates on the biological activities, we proposed to design a series of new antibacterial polymers based on polycaprolactone. PCL with pendant azido groups can be successfully prepared via ring-opening polymerization, and the side groups are readily to be functionalized with imidazoliums and carbohydrates through CuAAC click chemistry in one-pot (Figure 2.1). The composition of imidazolium and carbohydrate in final polymers can be controlled by their feeding ratio in the click step attributed to the high efficiency of CuAAC reaction.

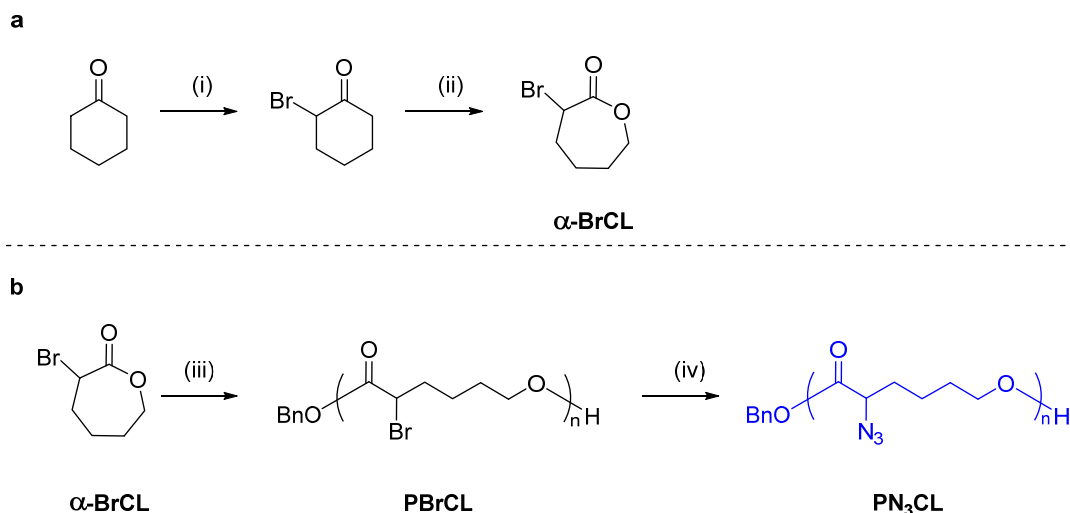
2.2 Results and Discussion

Briefly, a series of glycosylated polycaprolactones bearing imidazolium groups have been prepared by combination of ring-opening polymerization and CuAAC reaction. The antibacterial activity and toxicity of resultant polymers were examined, and promising candidate has been identified by screening, which is a typical procedure for the development of antibacterial polymers. To systematically study the structure-activity relationship, various carbohydrates and imidazoliums were incorporated by grafting onto the backbone in one-pot.

2.2.1 Synthesis of Poly(azido- ϵ -caprolactone) (PN₃CL) with Clickable Side Groups.

The functionalizable monomer of α -bromo- ϵ -caprolactone was synthesized using previously reported procedure²³ and functionalizable poly(ϵ -caprolactone) were synthesized by reported procedure with some modifications (Scheme 2.2).²⁴

Briefly, cyclohexanone was converted into α -bromocyclohexanone by bromination with N-bromosuccinimide (NBS) followed by Baeyer-Villiger oxidation with 3-chloroperoxybenzoic acid (*m*-CPBA) as the oxidant, producing the monomer α -bromo- ϵ -caprolactone (α -BrCL) in moderate yield (41%). With the monomer in hand, the poly(α -bromo- ϵ -caprolactone) (PBrCL) was prepared by ring-opening polymerization using benzyl alcohol (BnOH) as initiator and tin(II) 2-ethylhexanoate (Sn(Oct)₂) as catalyst.



Scheme 2.2 Synthesis of PCL with editable side groups starting from cyclohexanone. a) Monomer synthesis: i) NBS, NH_4OAc , Et_2O , rt, 30 min, 67%; ii) *m*-CPBA, DCM, rt, 24 h, 41%; b) Polymer synthesis: iii) BnOH , $\text{Sn}(\text{Oct})_2$, 80 °C, 48 h, 83%; iv) NaN_3 , DMF, rt, overnight, 93%.

The antibacterial activities and toxicity of cationic polymers have been found to be influenced by molecular weights. Polymers with moderate molecular weights have generally been found active against bacteria with moderate toxicities.^{5a,16,25} Thus, various functionalized polycaprolactone derivatives with moderate molecular weight of about 4 kDa to 5 kDa were targeted by controlling the feeding ratio. More specifically, the feeding ratio of $\alpha\text{-BrCL}$ and BnOH was 30 and the resulted polymer poly(α -bromo- ϵ -caprolactone) (PBrCL) was obtained in 83% yield. Furthermore, the degree of polymerization (DP) was calculated from the integration of signals at 7.37 ppm (benzyl end groups) and 3.88-4.53 ppm ($-\text{OCH}_2-$ and $-\text{CH}(\text{Br})-$) in ^1H NMR, and the DP was 25. Considering the 83% yield, we can conclude that the targeted molecular weight was successfully obtained in a controlled manner (Figure 2.2a).

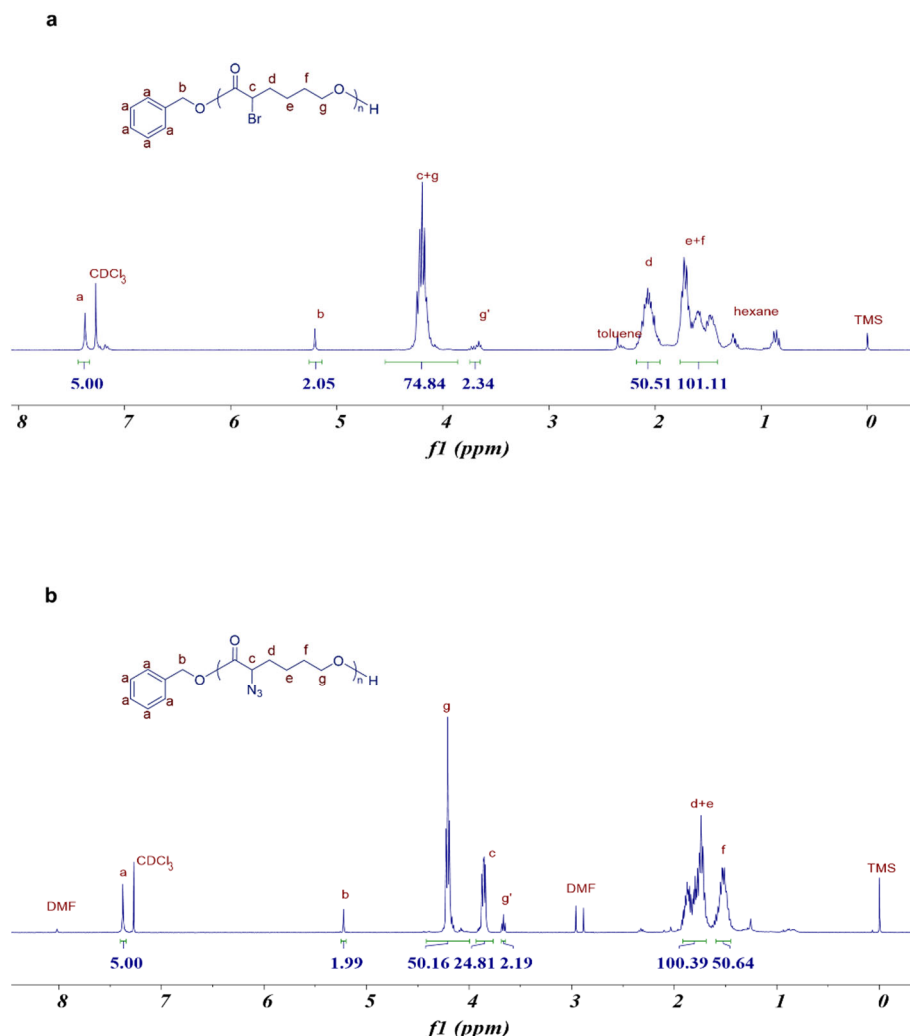


Figure 2.2 ^1H -NMR spectra of resultant PCLs in CDCl_3 . a) ^1H -NMR of PBrCL; b) ^1H -NMR of PN_3CL .

The GPC results has shown the polymer gave unimodal signal and the PDI was 1.29 (Figure 2.3). Subsequently, the bromo substituents on PBrCL were converted into azido groups by reacting with sodium azide (NaN_3) in DMF at room temperature. The resulted poly(α -azido- ϵ -caprolactone) (PN_3CL) was characterized with ^1H NMR and the ratio of the integration of signals at 4.41-4.40 ppm ($-\text{OCH}_2-$) and 3.78-3.97 ppm ($-\text{CH}(\text{N}_3)-$) indicates the complete conversion of bromo groups to azido groups (Figure 2.2b). The DP calculated from ^1H NMR and PDI determined by GPC had almost no change which were

25 and 1.30 respectively, suggesting the negligible transesterification or hydrolysis in the process.

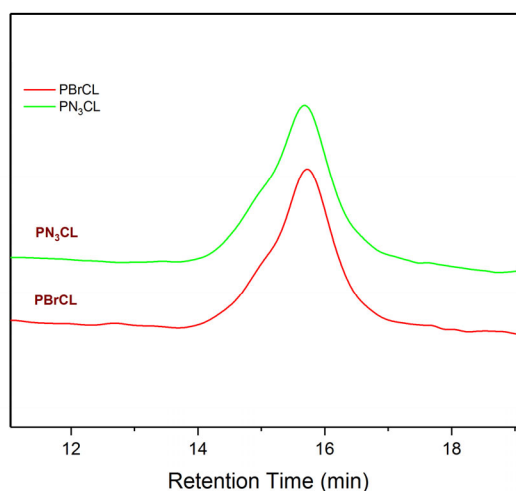
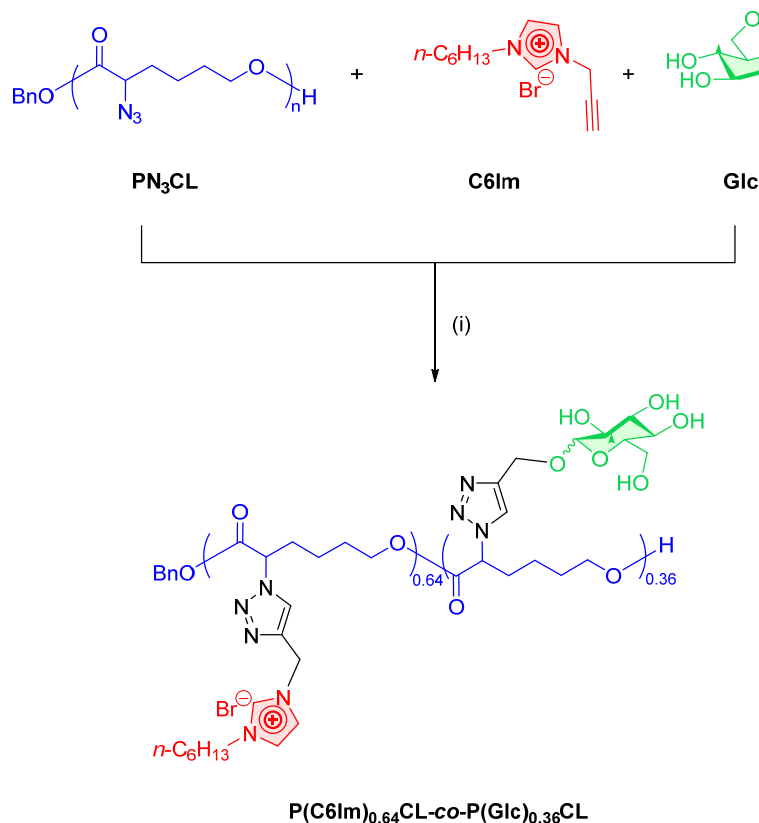


Figure 2.3 GPC traces of resultant PCLs in THF.

2.2.2 Conjugation of Poly(α -azido- ϵ -caprolactone) with Imidazoliums and Carbohydrates via CuAAC Click Chemistry.

The post-modification of the obtained PN₃CL was conducted using CuAAC click reaction via a modified literature procedure.^{24b} Briefly, the click reaction was carried out utilizing the CuI/triethylamine combination in anhydrous and degassed DMF at a slightly elevated temperature of 40 °C because of poor solubility of cationic compounds and carbohydrates at room temperature. As an example, albeit not the first trial, a functionalized PCL modified with 1-propargyl-3-hexyl-imidazolium bromide (C6Im) and prop-2-ynyl-D-glucopyranoside (Glc) was synthesized successfully in one-pot reaction (Scheme 2.3).



Scheme 2.3 Synthesis of $\text{P(C6Im)}_{0.64}\text{-co-P(Glc)}_{0.36}\text{CL}$ in a one-pot reaction: i) CuI , Et_3N , DMF, $40\text{ }^\circ\text{C}$, overnight (Glc = Glucose), 95%.

Besides, in order to investigate the structure-activity relationship especially the carbohydrate effects, a library of PCLs was synthesized. The signal of proton on triazole ring (8.2 ppm for sugars and 8.3 for imidazolium) is different from the signals of protons on the imidazolium ring (8.9 ppm and 7.6 ppm), and thus the ratios of sugars and imidazoliums can be calculated from the integrals in ^1H NMR of resultant polymers (Figure 2.4). And the polymer in previous example was calculated to possess 64% imidazolium and 36% glucoside, coded as $\text{P(C6Im)}_{0.64}\text{CL-co-P(Glc)}_{0.36}\text{CL}$ (Figure 2.4b).

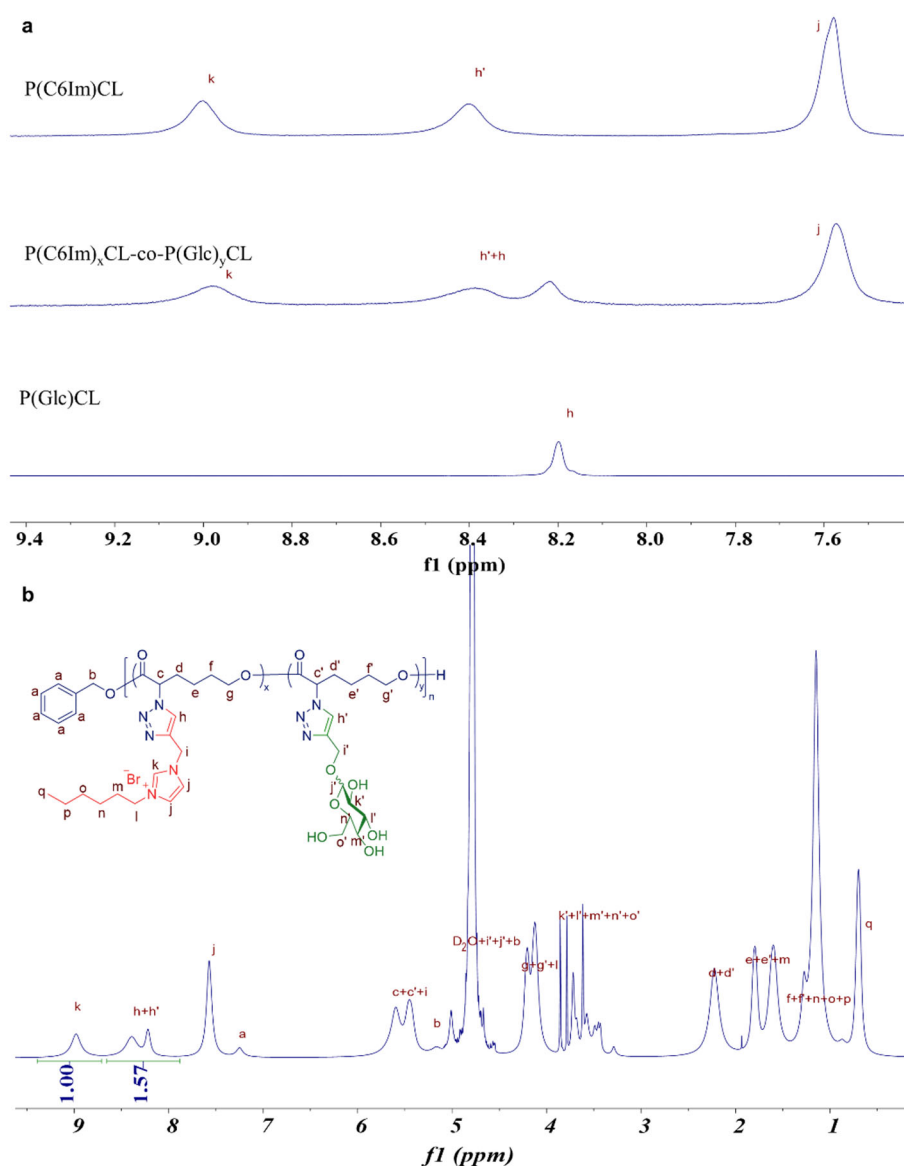


Figure 2.4 Calculating the ratio of grafted imidazolium and carbohydrate in final polymer by the integrals in ^1H -NMR (D_2O). a) Characteristic signals in resulting PCLs: signals j and k are from imidazolium ring while h and h' are from the formed triazole rings, $\text{Ratio(Im/Glc)} = I_k / (I_{h+h'} - I_k)$; b) Polymer calculated to possess 64% imidazolium and 36% glucoside, coded as $\text{P(C6Im)}_{0.64}\text{CL-co-P(Glc)}_{0.36}\text{CL}$.

It is noteworthy that the actual content of resulting polymers is very close to the designed feeding ratio of grafting agents (Table 2.1)

Table 2.1 Representative designed ratios and actual ratios of resulting polymers by one-pot click reaction.

Sample	Ratio (IM: Carbohydrate)	
	Designed	Actual ^a
P(C8Im) _{0.63} CL-co-P(Glc) _{0.37} CL	67:33	63:37
P(C8Im) _{0.48} CL-co-P(Glc) _{0.52} CL	50:50	48:52
P(C8Im) _{0.37} CL-co-P(Glc) _{0.63} CL	33:67	37:63
P(C8Im) _{0.2} CL-co-P(Glc) _{0.8} CL	20:80	20:80
P(C6Im) _{0.76} CL-co-P(Glc) _{0.24} CL	80:20	76:24
P(C6Im) _{0.64} CL-co-P(Glc) _{0.36} CL	70:30	64:36
P(C6Im) _{0.5} CL-co-P(Glc) _{0.5} CL	50:50	50:50
P(C6Im) _{0.38} CL-co-P(Glc) _{0.62} CL	40:60	38:62
P(C6Im) _{0.29} CL-co-P(Glc) _{0.71} CL	30:70	29:71
P(C6Im) _{0.33} CL-co-P(Gal) _{0.67} CL	40:60	33:67
P(C6Im) _{0.35} CL-co-P(Man) _{0.65} CL	40:60	35:65
P(C6Im) _{0.33} CL-co-P(GlcNAc) _{0.67} CL	40:60	33:67

^a Determined by NMR

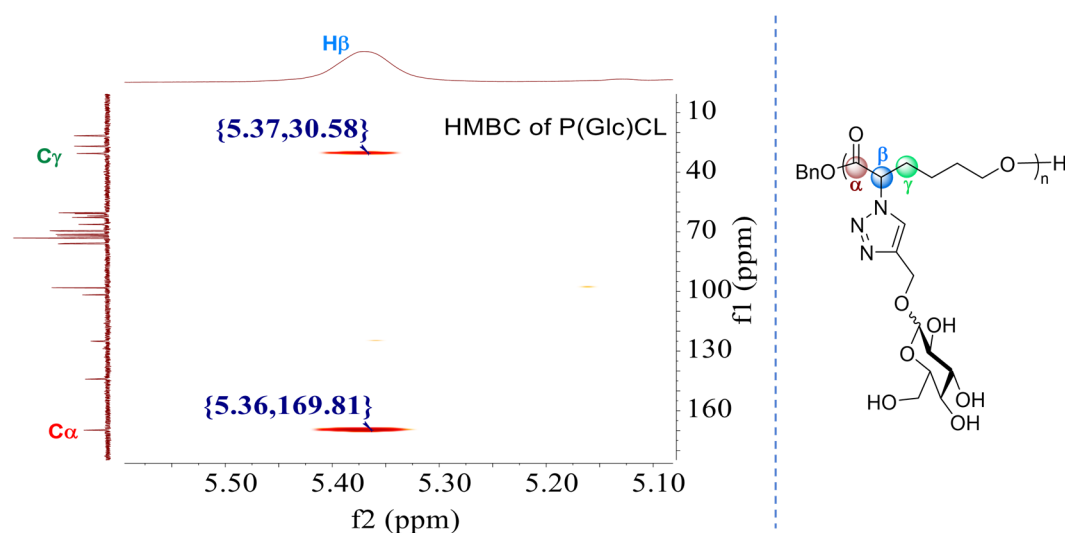


Figure 2.5 HMBC of P(Glc)CL.

Also, some proton signals on the main chain of PCL are isolated from the others, which could be confirmed by 2D NMR and applied in calculating the click efficiency as well as molecular weight (Figure 2.5-2.8).

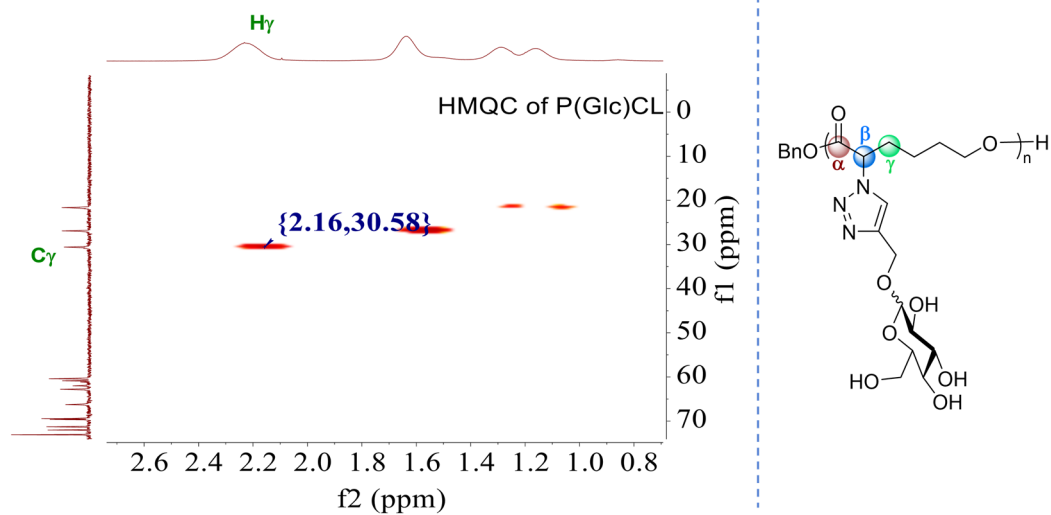


Figure 2.6 HMQC of P(Glc)CL.

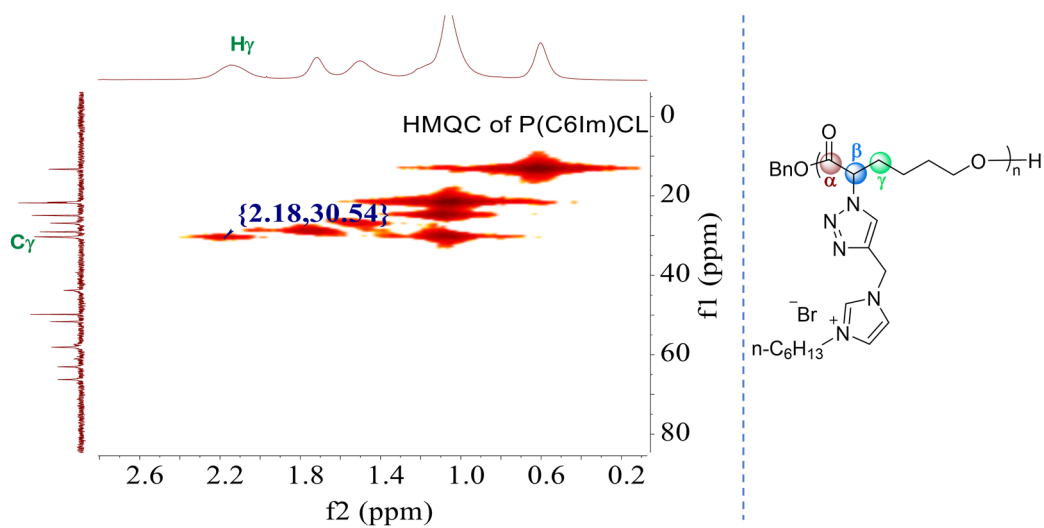


Figure 2.7 HMQC of P(C6Im)CL.

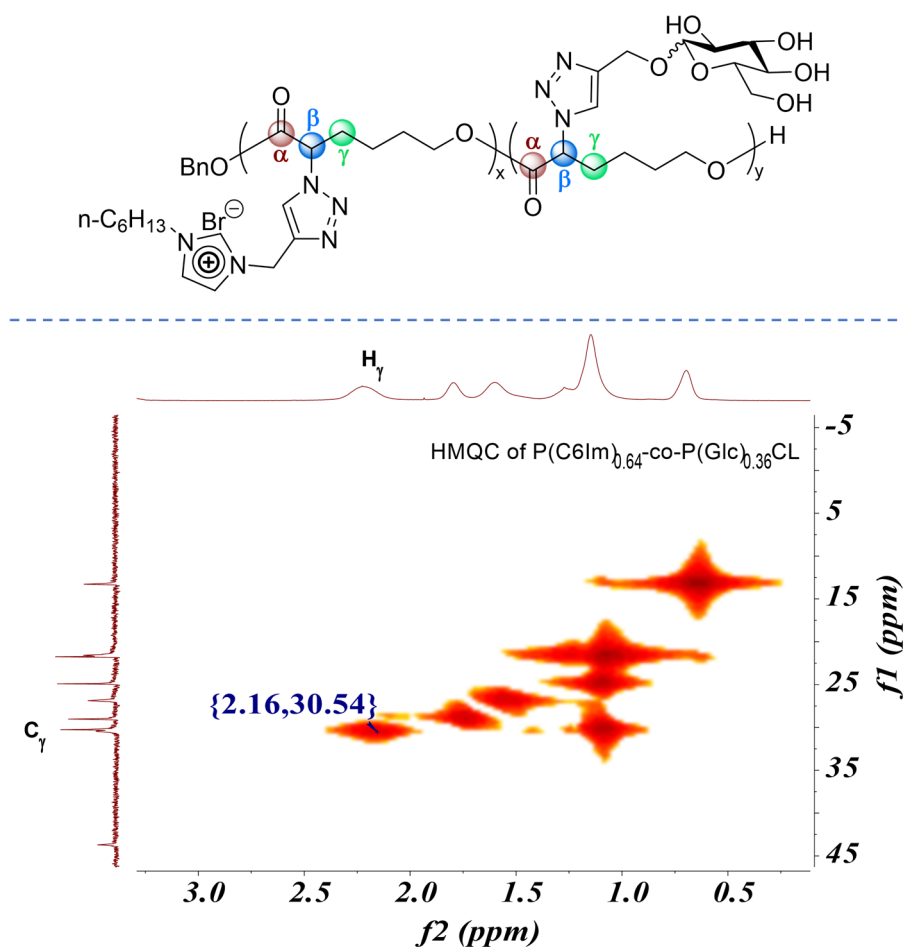


Figure 2.8 HMQC of P(C6Im)_{0.64}CL-co-P(Glc)_{0.36}CL.

The HMBC of P(Glc)CL indicates H_β coupled with the adjacent carbonyl C_α and C_γ, proving H_β is on the adjacent carbon C_β of carbonyl group. With the information from HMQC of P(Glc)CL, H_γ has coupled with only C_γ, proving it is the only proton connected with carbon C_γ. Furthermore, the H_γ only coupled with the C_γ in the HMQC of PCLs bearing imidazolium as well, indicating H_γ is the isolated proton signal in the main chain. Therefore, the molecular weight of the polymers can be calculated from both ¹H NMR and GPC (Table 2.2).

Table 2.2 Molecular weight and PDI determined by NMR and GPC.

Entry	Sample	Molecular Weight		PDI ^a
		M _n , NMR (kDa)	M _n , GPC ^a (kDa)	
P1	P(EDA)CL	10.3	2.1	1.06
P2	P(Arg)CL	7.0	2.0	1.05
P3	P(C4Im)CL	9.1	2.0	1.06
P4	P(C6Im)CL	9.9	1.8	1.09
P5	P(C8Im)CL	10.8	1.9	1.07
P6	P(C10Im)CL	11.5	1.8	1.07
P7	P(C8Im) _{0.63} CL- <i>co</i> -P(Glc) _{0.37} CL	11.5	1.8	1.08
P8	P(C8Im) _{0.48} CL- <i>co</i> -P(Glc) _{0.52} CL	9.0	1.7	1.07
P9	P(C8Im) _{0.37} CL- <i>co</i> -P(Glc) _{0.63} CL	7.8	1.6	1.13
P10	P(C8Im) _{0.2} CL- <i>co</i> -P(Glc) _{0.8} CL	9.8	4.6 ^b	1.47 ^b
P11	P(C6Im) _{0.76} CL- <i>co</i> -P(Glc) _{0.24} CL	8.6	1.9	1.06
P12	P(C6Im) _{0.64} CL- <i>co</i> -P(Glc) _{0.36} CL	10.3	1.9	1.08
P13	P(C6Im) _{0.5} CL- <i>co</i> -P(Glc) _{0.5} CL	8.5	1.7	1.10
P14	P(C6Im) _{0.38} CL- <i>co</i> -P(Glc) _{0.62} CL	8.3	1.5	1.20
P15	P(C6Im) _{0.29} CL- <i>co</i> -P(Glc) _{0.71} CL	9.4	1.2	1.27
P16	P(C6Im) _{0.33} CL- <i>co</i> -P(Gal) _{0.67} CL	10.6	1.7	1.15
P17	P(C6Im) _{0.35} CL- <i>co</i> -P(Man) _{0.65} CL	10.2	1.4	1.23
P18	P(C6Im) _{0.33} CL- <i>co</i> -P(GlcNAc) _{0.67} CL	10.1	1.6	1.23
P19	P(Arg) _{0.5} CL-P(Glc) _{0.5} CL	5.6	1.8	1.12
P20	P(Glc)CL	9.3	12.8 ^b	1.49 ^b
P21	P(Man)CL	11.5	10.3 ^b	1.39 ^b
P22	P(Gal)CL	9.2	10.9 ^b	1.48 ^b
P23	P(GlcNAc)CL	14.1	14.6 ^b	1.38 ^b

^a Determined by aqueous GPC (0.05M NaCl solution) system using pullulan standards as the reference without otherwise noted. ^b Determined by DMF GPC (1% LiBr) system using narrow polystyrene standards as the reference.

Generally, the molecular weight by GPC is based on the hydrodynamic volume in the solution, therefore it depends on mobile phase, flow rate, column, standard reference samples, etc. Unexpectedly, the molecular weight of our polymer calculated by NMR are much higher than that determined by aqueous GPC. The polymers in aqueous solutions probably shrink a lot because of their amphiphilic structures. This could be proved by the GPC results of some samples using DMF as eluent, however, most polymers could not be

properly soluble in DMF. Besides, all the polymers gave unimodal peaks, suggesting the uniform grafting of imidazolium and carbohydrates groups (Figure 2.9 and 2.10).

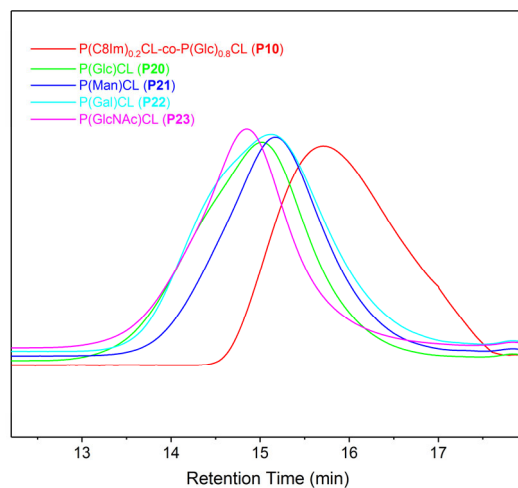


Figure 2.9 GPC traces of resultant polymers in DMF.

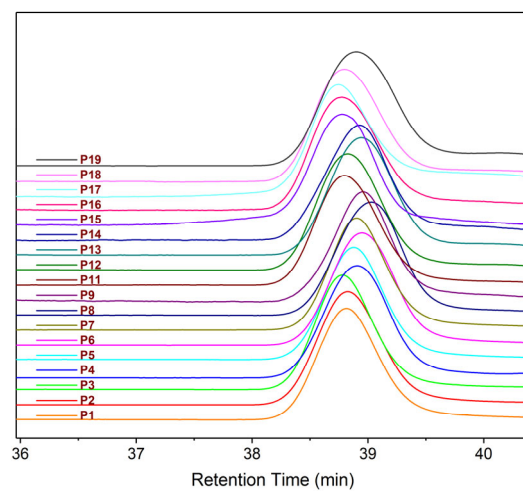


Figure 2.10 GPC traces of resultant polymers in aqueous media.

2.2.3 Antibacterial Activities and Toxicity of the Resulting Poly(ϵ -caprolactone).

The antibacterial efficacy of the resulting PCLs was first evaluated by employing both Gram-negative (*Escherichia coli* (*E. coli*) and *Pseudomonas aeruginosa* (*P. aeruginosa*)) and Gram-positive bacteria (*Staphylococcus aureus* (*S. aureus*) and methicillin-resistant *Staphylococcus aureus* (MRSA)). The minimum inhibitory concentration (MIC), or the lowest concentration of compound needed to prevent visible growth of bacteria, of various polymer derivatives were measured against the different bacterial strains. We measured hemolytic toxicity as the concentration causing 50% hemolysis of human red blood cells (HC₅₀). We measured the selectivity of the functionalized PCLs as the ratio between HC₅₀ and MIC values (Herein, MIC values against *S. aureus* was used). Toxicity towards a typical mammalian cell (3T3 fibroblasts) at 100 and 200 $\mu\text{g/mL}$ (several times the MICs) was also measured.

Since the type of cationic groups significantly affect the antibacterial activity as well as toxicity,²⁶ we first screened several types of cationic groups without carbohydrate involved, including primary amine, guanidine group as well as imidazolium (Table 2.3, P1-P4). The results suggested that imidazolium and arginine are better groups compared to primary amine considering both activity and toxicity.

Table 2.3 Antibacterial and hemolytic activity and mammalian cell biocompatibility of synthesized PCLs.

Entry	Sample	MIC ($\mu\text{g/mL}$)				HC ₅₀ ($\mu\text{g/mL}$) ^a	Selectivity ^b HC ₅₀ /MIC	MTT (Cell viability, %)	
		<i>S. aureus</i>	MRSA	<i>E. coli</i>	<i>P. aeruginosa</i>			100 $\mu\text{g/mL}$	200 $\mu\text{g/mL}$
P1	P(EDA)CL	32	256	64	64	4513	141	22	6
P2	P(Arg)CL	32	32	16	64	>12500	>390	36	14
P3	P(C4Im)CL	32	32	32	128	1158	36	81	27
P4	P(C6Im)CL	4	4	8	32	687	172	20	6
P5	P(C8Im)CL	8	8	16	32	332	42	18	9
P6	P(C10Im)CL	32	16	64	128	24	1	4	4
P7	P(C8Im) _{0.63} CL- <i>co</i> - P(Glc) _{0.37} CL	8	8	32	32	149	19	31	6
P8	P(C8Im) _{0.48} CL- <i>co</i> - P(Glc) _{0.52} CL	8	16	32	64	346	43	32	5
P9	P(C8Im) _{0.37} CL- <i>co</i> - P(Glc) _{0.63} CL	16	32	16	256	386	24	48	7
P10	P(C8Im) _{0.2} CL- <i>co</i> - P(Glc) _{0.8} CL	128	256	512	>512	1361	11	98	95
P11	P(C6Im) _{0.76} CL- <i>co</i> - P(Glc) _{0.24} CL	4	8	16	64	139	35	33	6
P12	P(C6Im) _{0.64} CL- <i>co</i> - P(Glc) _{0.36} CL	8	8	16	64	337	42	38	6

Table 2.3 (continued)

Entry	Sample	MIC ($\mu\text{g/mL}$)				HC ₅₀ ($\mu\text{g/mL}$) ^a	Selectivity ^b HC ₅₀ /MIC	MTT (Cell viability, %)	
		<i>S. aureus</i>	MRSA	<i>E. coli</i>	<i>P. aeruginosa</i>			100 $\mu\text{g/mL}$	200 $\mu\text{g/mL}$
P13	P(C6Im) _{0.5} CL-co-P(Glc) _{0.5} CL	16	32	64	256	1497	47	80	35
P14	P(C6Im) _{0.38} CL-co-P(Glc) _{0.62} CL	32	32	128	512	1796	56	84	45
P15	P(C6Im) _{0.29} CL-co-P(Glc) _{0.71} CL	64	128	256	>512	>12500	>195	92	72
P16	P(C6Im) _{0.33} CL-co-P(Gal) _{0.67} CL	32	64	64	256	1380	43	85	51
P17	P(C6Im) _{0.35} CL-co-P(Man) _{0.65} CL	64	64	128	512	>12500	>195	90	82
P18	P(C6Im) _{0.33} CL-co-P(GlcNAc) _{0.67} CL	64	64	64	512	5782	90	96	93
P19	P(Arg) _{0.5} CL-co-P(Glc) _{0.5} CL	64	64	64	128	>12500	>195	83	58
P20	P(Glc)CL	>512	>512	>512	>512	>12500	-	99	96

^a Values obtained from the plotted hemolysis curve. ^b Calculated based on the MIC values of *S. aureus* 29213.

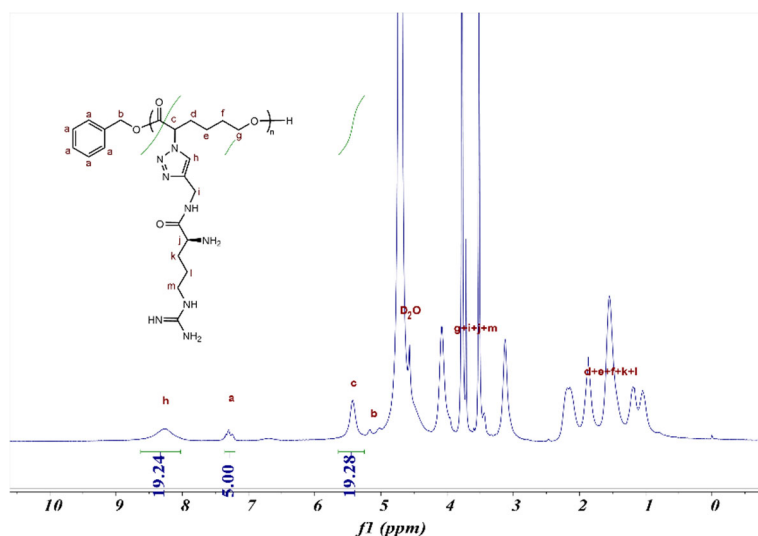


Figure 2.11 ^1H -NMR spectra of P(Arg)CL (P2) in D_2O .

However, the polycaprolactone bearing arginine appeared to undergo self-degradation, remarkable loss of molecular weight has been observed by NMR, rendering great difficulties on controlling the final composition (Table 2.3, P2 and P19 and Figure 2.11). Therefore, we proceeded to study the structure-activity relationship based on imidazolium-carrying polymers.

As imidazolium was considered as best cationic group, different imidazolium salts with variable alkyl tail length were grafted onto the PCLs. All the resultant PCL derivatives have good efficacy against both Gram-negative and Gram-positive bacteria (Table 2.3, P3-P6). Among these PCLs, polymers possessing imidazolium with intermediate length (6 or 8) carbon tails have better antibacterial activities than those possessing shorter and longer carbon chains (P4 and P5 vs P3 and P6).

With the exception of P3, the other imidazolium functionalized PCLs had relatively high toxicity towards mammalian cells. The hemolytic activities of P3 to P5 were reasonable, with a selectivity index of 172 and 42 for P4 and P5 respectively. P6 is too hemolytic, likely because the side chain with 10 carbons is too long.

To determine whether increasing the hydrophilicity of the polymers can improve the toxicity profile of the polymers^{18c}, carbohydrates were introduced into two series with 8 and 6 alkyl side chains (*i.e.*, P7 to P10 and P11 to P18 respectively) and their effects were systematically studied with different molar ratios and various carbohydrates.

Comparing P5 with their glycosylated derivatives (P7 to P10), the MIC values against Gram-negative strains increased significantly with increasing ratios of carbohydrate in the polymers whereas the MIC values went up less significantly for Gram-positive bacteria. It is probably due to the impermeability of the outer membranes of Gram-negative bacteria to large hydrophilic molecules (Table 2.3, P7-P10).²⁷ However, the C8-Im derivatives' hemolysis and cytotoxicity did not decrease until the sugar content is rather large (*i.e.*, with P10).

On the other hand, for similar ratios of carbohydrate and imidazolium, PCLs bearing C6-Im has higher MICs than those possessing C8-Im despite their lower hemolysis and lower 3T3 toxicity (Table 2.3, P8 vs P13 and P9 vs P14). As with P5 derivatives (*i.e.* P7-P10), the MIC increased much less significantly with Gram-positive bacteria when the ratio of glycosylated substitution was increased. However, their toxicity to 3T3 cells, as well as their hemolytic toxicity, was significantly reduced. For example, P15 has fairly balanced profiles of bactericidal activities against Gram-positive bacterial and good selectivity

indices for 3T3 and red blood cells. Additionally, more Gram-positive strains including *B. subtilis*, *Enterococcus faecalis*, *Enterococcus faecium* and MRSA USA300, together with a panel of other clinical MRSA strains from local hospitals, were used to evaluate selected compounds (Table 2.4). Comparable results to those in Table 1 were obtained, indicating they (including P13 which has good 3T3 and red blood cell compatibility, together with MICs) are potentially bactericidal towards deadly MRSA strains. Thus, we can conclude, the alkyl side chain length, and content of imidazolium in these PCL-backbone polymers are crucial to the antibacterial activity. Interestingly, only the shorter C6-Im can achieve a more balanced MIC and selectivity values possibly because the PCL backbone is relatively hydrophobic. Also, with the decreasing ratios of imidazolium in the intermediate range (Table 2.3, P7-P9, and P11-P14), the MIC values increased moderately for Gram-positive bacteria but dramatically for Gram-negative bacteria. Overall, the hemolysis of the PCL-Im derivatives are generally quite good (with selectivity ratios of at least 40 even for P5).

Furthermore, to study the effects of different carbohydrates, various sugars (Glucose, Galactose, Mannose, Glucosamine) were attached in comparable molar ratios. No significant difference was observed in MIC values (Table 2.3, P15-P18).

Table 2.4 Antibacterial activity of selected polymers against other Gram-positive strains including resistant strains

Entry	MIC ^a (µg/mL)										
	<i>B. subtilis</i> 6633	<i>E. faecalis</i> 29212	<i>E. faecium</i> 19434	MRSA USA300	MRSA 1	MRSA 2	MRSA 3	MRSA 4	MRSA 5	MRSA 6	MRSA 7
P8	8	16	8	8	8	8	16	8	16	16	8
P9	32	32	32	32	16	32	64	16	64	32	32
P13	8	64	16	32	16	16	128	16	32	32	32
P14	16	64	32	32	16	16	128	16	32	64	32
P15	64	256	64	128	64	64	256	64	128	128	128
P16	16	64	32	32	32	32	128	32	32	64	64
P17	32	128	32	64	64	64	256	32	64	64	64
P18	32	128	32	64	32	32	128	32	64	64	64

^a *B. subtilis*, *E. faecalis*, *E. faecium*, MRSA BAA40, MRSA USA300 were purchased from ATCC. MRSA 1-7 were clinical strains isolated from local hospital (TTSH).

However, it is noteworthy that PCLs with C6-Im bearing Glucose and Mannose are relatively less hemolytic probably attributed to their difference in polarity (Table 2.3 and Figure 2.12b), and C6-Im with Glucose, Mannose and Glucosamine had markedly improved 3T3 compatibility (Figure 2.13b).

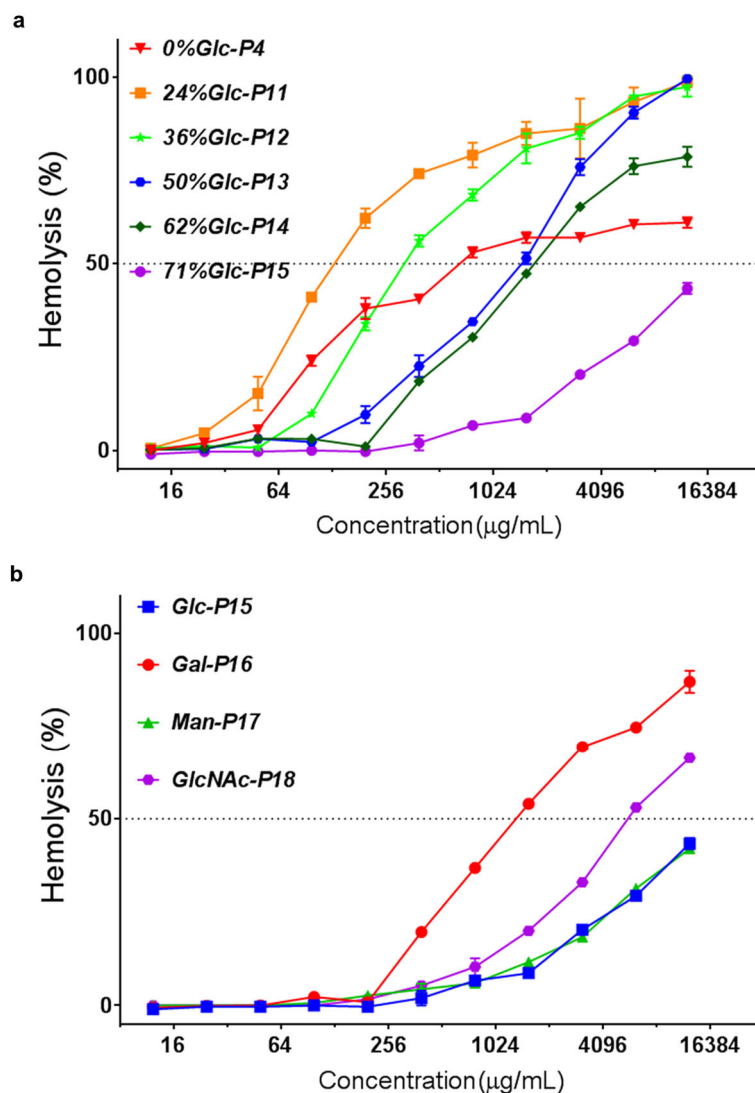


Figure 2.12 Dose-dependent hemolytic activity of resultant PCLs. a) PCLs bearing different ratios of Glucose; b) PCLs bearing different carbohydrates (Glucose, Galactose, Mannose and Glucosamine). Glc = Glucose, Gal = Galactose, Man = Mannose, GlcNAc = N-acetylglucosamine.

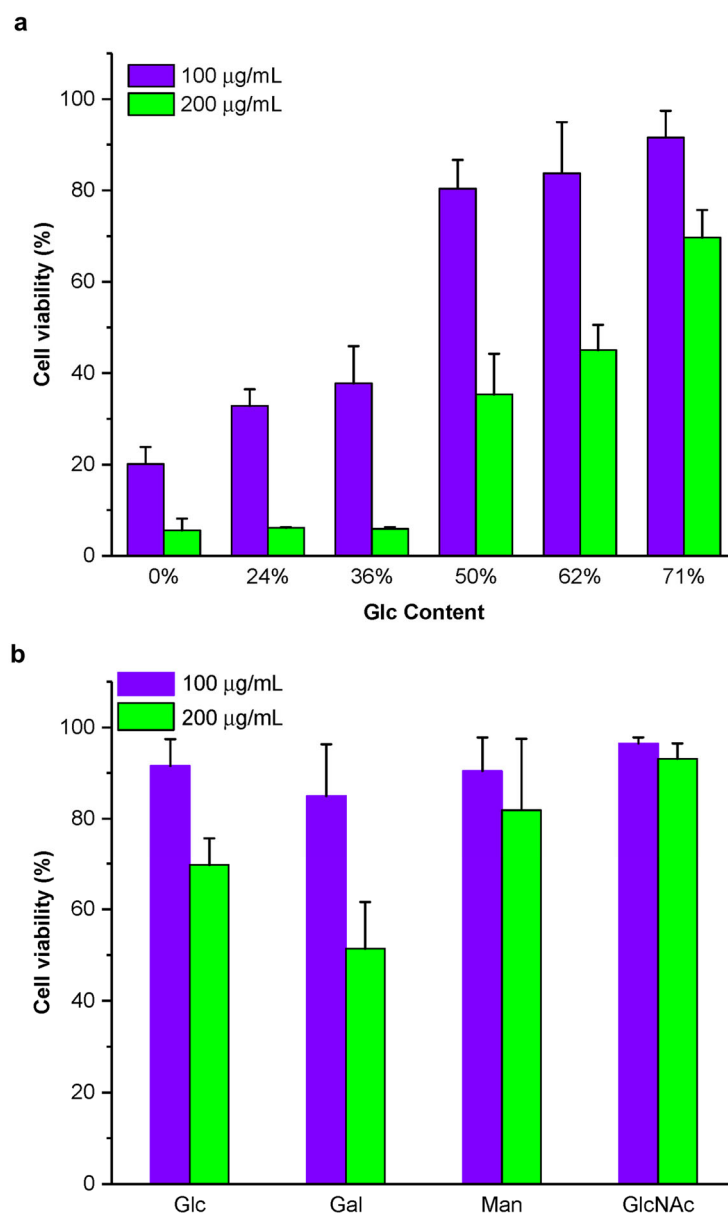


Figure 2.13 3T3 fibroblast cell viability after incubated with functionalized PCLs: a) Cell viability of PCLs bearing different ratios of C6-imidazolium and Glc; b) Cell viability of PCLs bearing different carbohydrates with comparable ratios.

With regard to selectivity against bacteria over red blood cells, P15 and P17 showed the best results (>195), followed by P4 (>172) and P18 (>90). However, considering both the

hemolytic selectivity and cytotoxicity, P17 ($P(C6Im)_{0.35}CL-co-P(Man)_{0.65}CL$) was believed to have the most satisfactory balance in this polymer system.

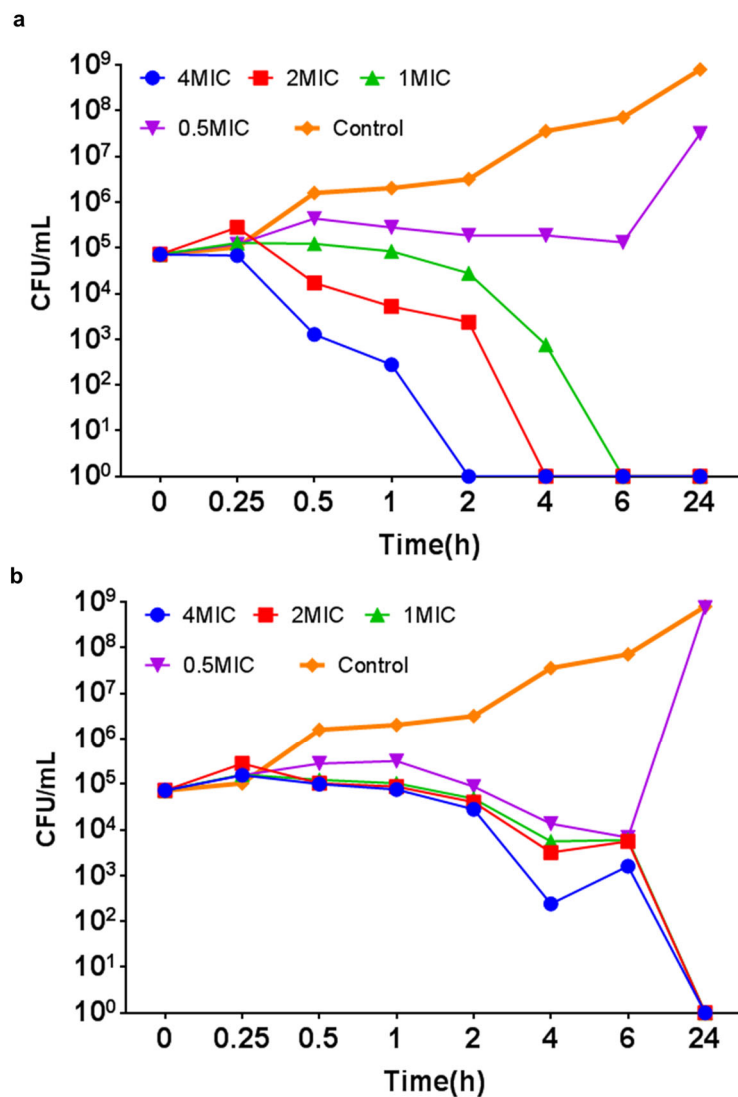


Figure 2.14 Killing kinetics against MRSA BAA40: a) P17; b) Vancomycin.

With this promising compound in hand, the killing kinetics of the compound was studied and compared against vancomycin, which is the last resort antibiotics against MRSA infection. By exposing MRSA BAA40 to a series of concentrations of synthesized polymer and vancomycin, rapid bactericidal effects were observed at $1\times MIC$ concentration

of our polymer whereas vancomycin could not kill the bacteria within 6 h even at 4×MIC concentration (Figure 2.14a and 2.14b). Another MRSA strain tested (USA300) has revealed the same trend although some regrowth could be observed at lower concentration probably due to slight degradation of antibacterial agents (Figure 2.15a and 2.15b).

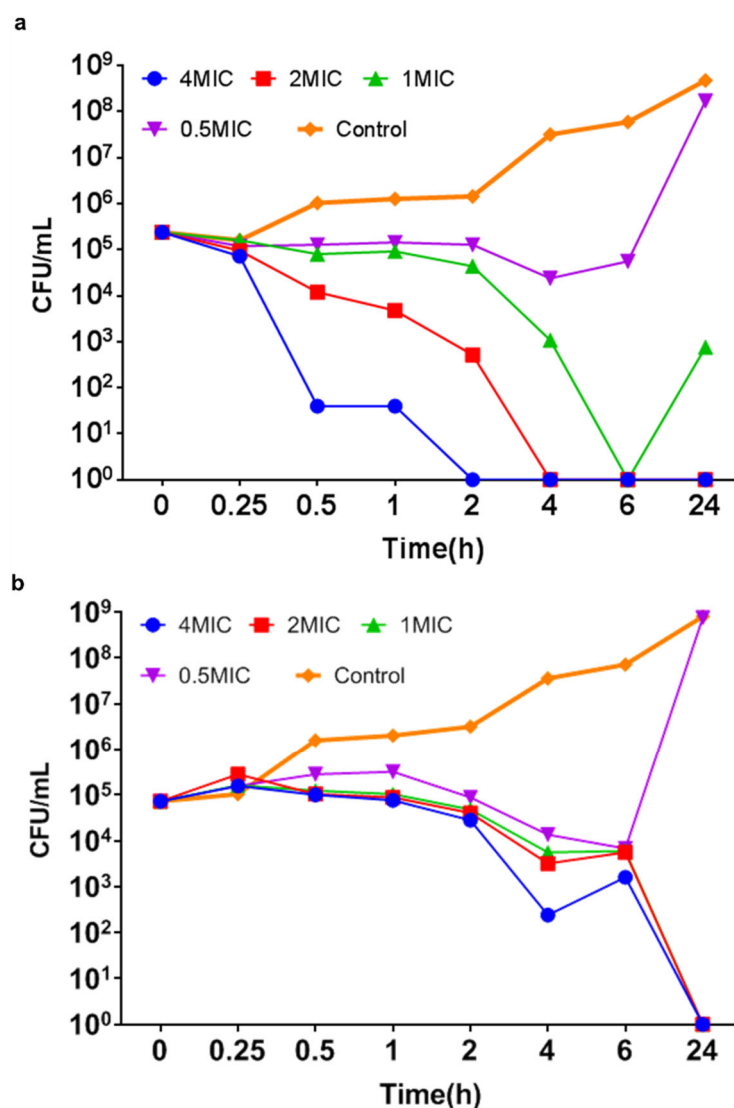


Figure 2.15 Killing kinetics against MRSA USA300: a) P17; b) Vancomycin.

2.2.4 Degradation and Killing Kinetics

Besides, to examine the degradability of our polymers, a model study was carried out with P17 in physiological pH condition at 37 °C. The preliminary results indicated that the polymers are hydrolytically degradable (Figure 2.16).

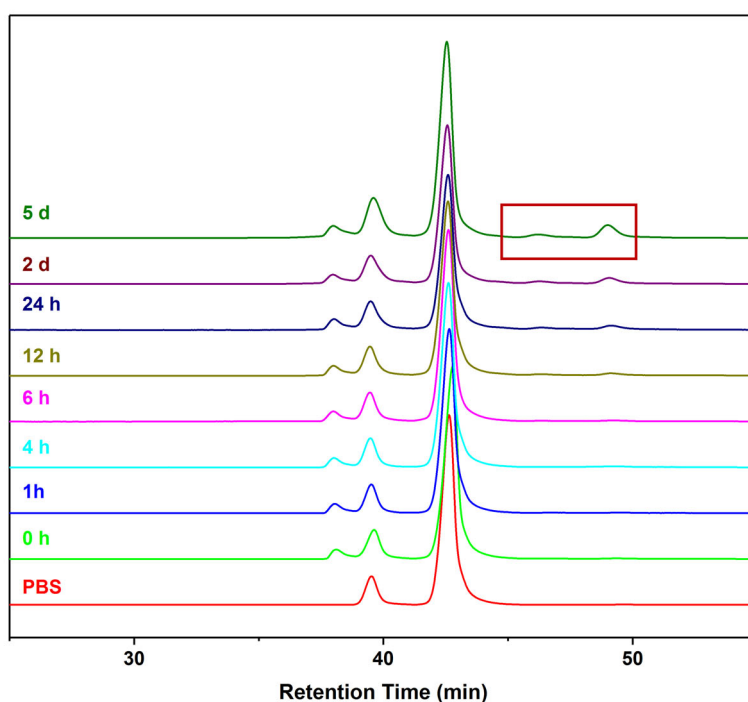


Figure 2.16 Degradation of P17 in PBS at 37 °C monitored by aqueous GPC.

In addition, no noticeable degradation occurred before inhibiting bacteria and significant loss of activity after degradation was observed (Figure 2.17). This feature endows the polymers with great advantages over enzymatically degradable polymers, rendering such polymers more promising in further applications.

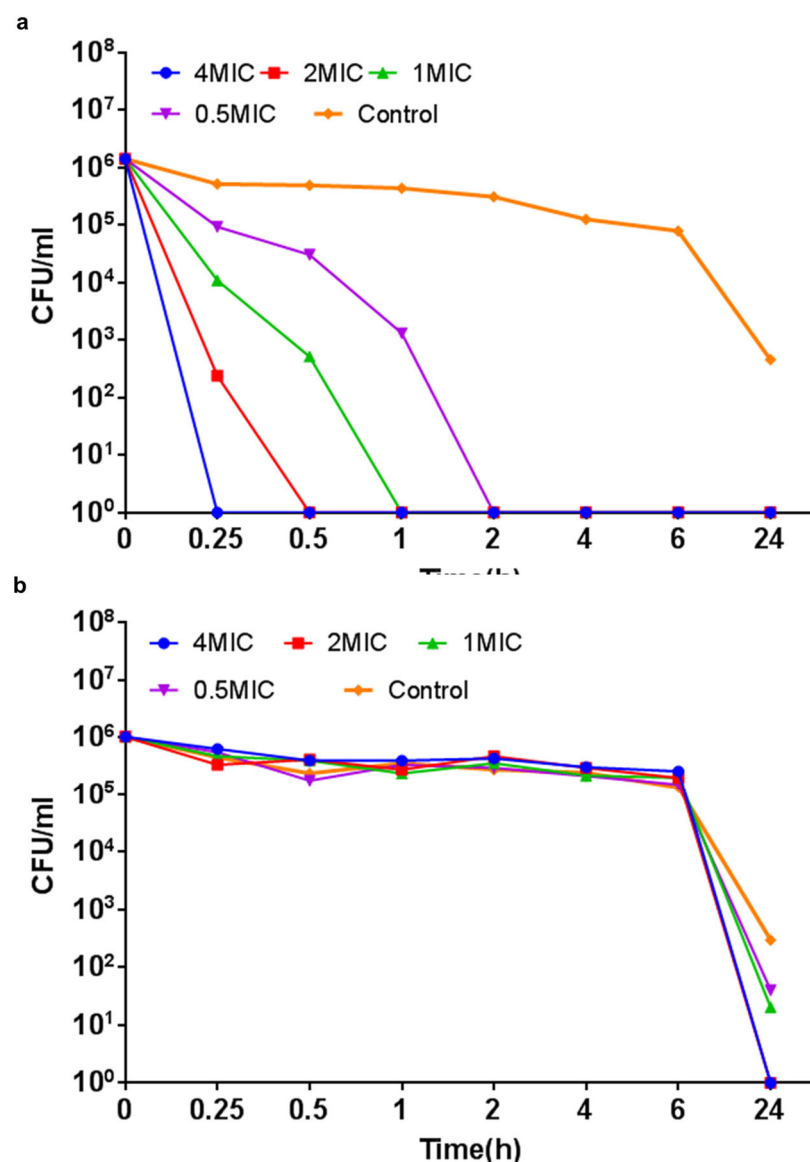


Figure 2.17 Killing kinetics against MRSA BAA40 in PBS. a) P17; b) Degraded mixture after 5 days.

Compared with bacteriostatic antibiotics, cationic polymers are preferred in many situations against resistant bacteria, biofilm bacteria or persistent bacteria where clinical studies have proven the therapeutic efficacy of bactericidal agents.²⁸ Moreover, cationic polymers could minimize the emergence of resistance in early clinical usage, due to minimal bacteria survival and mutation.²⁹ This could be an advantage of our polymer

series due to its true sterilization effect within a short period of time at a relatively low concentration.²⁹ Thus, the PCL bearing Mannose and imidazolium could be a potentially effective antibacterial agent in clinical applications.

2.3 Conclusion

We have successfully synthesized a new biodegradable series of polymers: poly(ϵ -caprolactone)-graft-alkylimidazolium-graft-carbohydrates via ring-opening polymerization followed by clicking with alkyne-imidazoliums and alkyne-carbohydrates. The actual ratio of alkyne-Im to alkyne-carbohydrates clicked on PCL was achieved through careful control of reagent ratios. The synthesized PCLs have good antibacterial efficacy towards Gram-positive bacteria. However, the hemolytic and 3T3 toxicities of these PCL derivatives were generally high for the PCL graft alkyl-Im polymers. These toxicities can be improved upon addition of carbohydrates, at the expense of some bacteria activity. Through our screening efforts, we have successfully identified a candidate polymer, P17, $P(C6Im)_{0.35}CL-CO-P(Man)_{0.65}CL$, that demonstrated good MICs with very low toxicities against red blood cells and 3T3 cells. This candidate compound was demonstrated to have faster killing kinetics when compared against vancomycin. In conclusion, we have developed a new class of clinically relevant antibacterial polymers that is biodegradable, potent and biocompatible, paving the way for clinical applications of antibacterial polymers in the future.

2.4 Experimental Section

2.4.1 Materials

Chemicals and solvents are purchased from Alfa-Aesar, Sigma-Aldrich and VWR and used without further purification unless otherwise noted. Anhydrous toluene (over sodium/benzophenone), tetrahydrofuran (THF, over sodium/benzophenone) and dichloromethane (DCM, over calcium hydride) were freshly distilled under nitrogen atmosphere before use. All the other anhydrous solvents were purchased from Sigma-Aldrich and used as received. Amino acids derivatives and coupling reagents were purchased from GL Biochem Co. (Shanghai, China). Deuterated solvents are obtained from Cambridge Isotope Laboratories and used as received. Thin layer chromatography (TLC) with Merck TLC silica gel 60 F254 plate was used to monitor reaction. UV, potassium permanganate and iodine staining were used to visualize compounds on TLC plates. Flash column chromatography with silica gel 60 (0.010-0.063 mm) was applied for the purification of organic compounds. Benzyl alcohol (Alfa-Aesar, 99%) was stirred with sodium at room temperature and distilled under nitrogen and stored in Schlenk flask in desiccator until further use. H₂SO₄-silica was prepared according to the reported procedure and stored in desiccator until further use.³⁰ Regenerated cellulose dialysis tubing (MWCO 3500 Da) was purchased from Fisher Scientific. Deionized water was obtained from a Merck Millipore Integral 3 water purification system. For biological studies, NIH 3T3 fibroblasts were purchased from Millipore, Singapore. All broth and agar were purchased from Becton Dickinson Company (Franklin Lakes, US) and used as received. Bacteria strains used (*Escherichia coli* ATCC8739, *Staphylococcus aureus*

ATCC29213, *Pseudomonas aeruginosa* PAO1, *Bacillus subtilis* ATCC6633, *Enterococcus faecalis* ATCC29212, *Enterococcus faecium* ATCC 19434 and drug-resistant *Staphylococcus aureus* MRSA BAA40, MRSA USA300) were purchased from ATCC. Drug-resistant *Staphylococcus aureus* MRSA 1-7 were clinical strains isolated from local hospital (TTSH).

2.4.2 Instruments for characterization

^1H and ^{13}C and 2D NMR spectra were recorded on Bruker Avance 300, Bruker Avance 400, Bruker AVIII 400 and JEOL JNM-ECA 400 spectrometers using deuterated solvents as reference. Mass spectra were obtained using an Agilent 6230 TOF LC/MS with an electrospray (ESI) source with purine and HP-0921 as an internal calibrates. Organic phase gel permeation chromatography (GPC) was carried out on a Shimadzu liquid chromatography system equipped with a Shimadzu refractive index detector (RID-10A) and two Agilent Polargel columns operating at 40 °C using DMF (with 1 wt % LiBr) or THF as the eluent at a flow rate of 1 mL/min using polystyrene kit as standard. Aqueous phase GPC was carried out on an Agilent liquid chromatography system equipped with an Agilent refractive index detector with two Shodex OHpak columns operating at 40 °C using 0.05M NaCl solution as the eluent at a flow rate of 0.5 mL/min using pullulan kit as standard to determine M_n , M_w , and polydispersity index ($\text{PDI} = M_w/M_n$).

2.4.3 Synthesis of monomer and polymers

Synthesis of α -bromo- ϵ -caprolactone (α -BrCL).

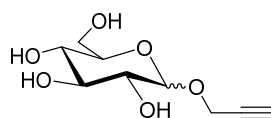
The α -bromo- ϵ -caprolactone (α -BrCL) was synthesized according to the literature procedure started from cyclohexanone.³¹ Briefly, Cyclohexanone (14.7 g, 0.15 mol) was dissolved in dry diethyl ether (150 mL) followed by the addition of N-bromosuccinimide (NBS, 28.0 g, 0.158 mol). The solution was stirred and ammonium acetate (1.16 g, 0.015 mol) was added portion-wise. After stirring for 0.5 h at room temperature, the solid was filtered off and the filtrate was washed with water, dried over Na_2SO_4 , concentrated and subject to flash column chromatography, giving pale yellow liquid α -bromo-cyclohexanone (17.8 g, 67%). To the solution of α -bromo-cyclohexanone (10.0 g, 56 mmol) in anhydrous dichloromethane (DCM, 200 mL), 3-chloroperoxybenzoic acid (*m*-CPBA, 25.7 g, 85 mmol, ca. 70% with water) was added and the solution was stirred at room temperature for 24 h. The mixture was cooled to $-20\text{ }^\circ\text{C}$ and filtered. The filtrate was washed successively with $\text{Na}_2\text{S}_2\text{O}_3$ and saturated NaHCO_3 solution thoroughly until no acid could be detected by TLC. The organic layer was dried over Na_2SO_4 , concentrated and subject to flash column chromatography, affording the desired monomer α -bromo- ϵ -caprolactone in 41% yield (4.4 g). ^1H NMR (400 MHz, CDCl_3) δ 4.85 (dd, $J = 6.2, 3.6$ Hz, 1H), 4.77 – 4.63 (m, 1H), 4.37 – 4.20 (m, 1H), 2.20 – 2.11 (m, 2H), 2.11 – 1.93 (m, 2H), 1.92 – 1.76 (m, 2H). ^{13}C NMR (125 MHz, CDCl_3) δ 169.8, 69.7, 48.2, 31.8, 29.1, 25.2. MS (ESI) m/z calcd. for $\text{C}_6\text{H}_{10}^{79}\text{BrO}_2$ $[\text{M}+\text{H}]^+$ 192.99, found 192.96, calcd. for $\text{C}_6\text{H}_{10}^{81}\text{BrO}_2$ $[\text{M}+\text{H}]^+$ 194.98, found 194.96.

Synthesis of poly(α -azido- ϵ -caprolactone) (PN_3CL).

The poly(α -azido- ϵ -caprolactone) (**PN₃CL**) was synthesized according to the reported procedure with some modifications (Scheme 2).²⁴ To the solution of α -bromo- ϵ -caprolactone (8.7 g, 45 mmol) in anhydrous toluene (20 mL), benzyl alcohol (BnOH, 162 mg, 1.5 mmol) and tin(II) 2-ethylhexanoate (Sn(Oct)₂, 648 mg, 1.6 mmol) were added sequentially. The mixture in the Schlenk flask was subject to three cycles of freeze-pump-thaw cycles, sealed under nitrogen and stirred at 80 °C for 48 h before quenched with highly diluted HCl in methanol. The resulted mixture was diluted with DCM and precipitated with hexane, centrifuged and dried under vacuum, giving the poly(α -azido- ϵ -caprolactone) (**PBrCL**) in 83% yield (7.2 g). ¹H NMR (300 MHz, CDCl₃) δ 7.37 (m, *Ar-H* from Bn-), 5.21 (s, PhCH₂-), 4.53 – 3.88 (m, –OCH₂- and –CH(Br)-), 3.66 (t, –CH₂OH), 2.24 – 1.91 (m, –CH(Br)CH₂-), 1.85 – 1.37 (m, –CH(Br)CH₂CH₂CH₂-). ¹³C NMR (75 MHz, CDCl₃) δ 169.7, 65.5, 45.7, 34.3, 27.8, 23.8. $M_{n,NMR} = 4.8$ kDa, $M_{n,GPC} = 4.4$ kDa, PDI = 1.29. To a solution of **PBrCL** (7.5 g, 39 mmol of repeating unit) in DMF (120 mL) was added sodium azide (NaN₃, 5.1 g, 78 mmol), the mixture was stirred at room temperature overnight before concentrated under vacuum. The concentrated solution was diluted with toluene followed by centrifugation to remove the insoluble solid. The supernatant was concentrated and dried in vacuo afterwards to afford the final desired **PN₃CL** (5.6 g, 93%). ¹H NMR (400 MHz, CDCl₃) δ 7.38 (m, *Ar-H* from Bn-), 5.22 (s, PhCH₂-), 4.40 – 4.11 (m, –OCH₂-), 3.97 – 3.78 (m, –CH(N₃-), 3.67 (t, –CH₂OH), 1.94 – 1.68 (m, –CH(Br)CH₂CH₂CH₂-), 1.62 – 1.44 (m, –CH(Br)CH₂CH₂CH₂-). ¹³C NMR (100 MHz, CDCl₃) δ 170.4, 65.4, 61.9, 30.9, 28.1, 22.3. $M_{n,NMR} = 4.0$ kDa, $M_{n,GPC} = 4.6$ kDa, PDI = 1.30.

General procedure for modification of PN₃CL with grafting compounds.

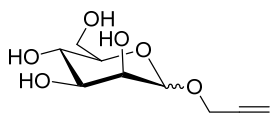
The modification of PN₃CL was modified from literature procedure.^{24b} All the modification reactions were conducted using a similar procedure, therefore, the procedure of modification with 1-propargyl-3-butyl-imidazolium bromide is taken as an example herein. To the solution of PN₃CL (129 mg, 1.0 equiv. azide group) and 1-propargyl-3-butyl-imidazolium bromide (212 mg, 1.05 equiv) in DMF (5 mL), anhydrous triethylamine (8.4 mg, 0.1 equiv.) was added and the mixture was subject to two freeze-pump-thaw cycles before the addition of CuI (15.8 mg, 0.1 equiv.). The mixture was subject to another two freeze-pump-thaw cycles before sealed under argon and stirred at 40 °C overnight. The resulted mixture was diluted with water and transferred into dialysis tubing directly followed by dialyzed against highly diluted EDTA solution (0.25 mg/ L) for 2 days and deionized water for another one day. Puffy solid could be obtained after lyophilization.

2.4.4 Synthesis of grafting compounds**Prop-2-ynyl-D-glucopyranoside³⁰**

H₂SO₄-silica was prepared according to the protocol described in Singh's report: to a slurry of silica gel (10 g, silica gel 60, 0.010-0.063 mm) in ether (50 mL) was added conc.H₂SO₄ (3 mL) with shaking for 5 min. The solvent was evaporated under reduced pressure, resulting in free flowing H₂SO₄-silica which was dried at 110 °C overnight and stored in desiccator until further use. D-Glucose (10.0 g, 55.5 mmol) was suspended in

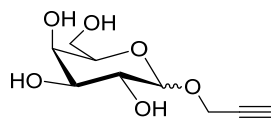
propargyl alcohol (16.1 mL, 278 mmol) and stirred at 65°C. 550 mg of H₂SO₄–silica catalyst was added to the mixture and the reaction mixture was stirred at 65°C overnight and monitored with TLC. After the complete conversion of D-glucose, the reaction mixture was transferred to a silica gel column and the excess propargyl alcohol was eluted with pure dichloromethane followed by elution of the desired glycoside with CH₂Cl₂–MeOH mixture, affording the product in 37% yield. ¹H NMR (400 MHz, methanol-*d*₄, α/β =3:1) δ 5.04 (d, *J* = 3.7 Hz, α-H1, 1H), 4.50 (d, *J* = 7.9 Hz, β-H1, 1H), 4.36 – 4.33 (m, 2H, both isomers), 3.96 – 3.81 (m, 1H, both isomers), 3.77 – 3.64 (m, 2H, both isomers), 3.64 – 3.57 (m, 1H, both isomers), 3.52 – 3.22 (m, 2H, both isomers), 2.93 – 2.90 (m, 1H, both isomers). MS (ESI) *m/z* calcd for C₁₈H₂₈NaO₁₂ [2M+Na]⁺ 459.15, found 459.25. ¹H NMR and MS revealed formation of the desired glycoside anomeric mixture matching the spectral data reported in literature.

Prop-2-ynyl-D-mannopyranoside³²



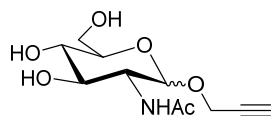
Prop-2-ynyl-D-mannopyranoside was prepared using the same procedure for Prop-2-ynyl-D-glucopyranoside. Prop-2-ynyl-D-mannopyranoside was obtained as white solid (Yield: 34%). ¹H NMR (400 MHz, methanol-*d*₄, α/β >10:1) δ 4.97 (s, 1H), 4.38 – 4.17 (m, 2H), 3.96 – 3.77 (m, 2H), 3.77 – 3.59 (m, 3H), 3.56 – 3.46 (m, 1H), 2.95 – 2.81 (m, 1H). MS (ESI) *m/z* calcd for C₁₈H₂₈NaO₁₂ [2M+Na]⁺ 459.15, found 459.16. ¹H NMR and MS revealed formation of the desired glycoside anomeric mixture.

Prop-2-ynyl-D-galactopyranoside³³

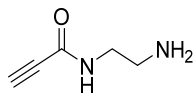


Prop-2-ynyl-D-galactopyranoside was prepared using the same procedure for Prop-2-ynyl-D-glucopyranoside. Prop-2-ynyl-D-galactopyranoside was obtained as white solid (Yield: 31%). ¹H NMR (400 MHz, methanol-*d*₄, α/β =5:1) δ 5.07 (d, *J* = 3.8 Hz, 1H), 4.51 – 4.26 (m, 1H), 3.96 (d, *J* = 2.9 Hz, 1H), 3.90 – 3.72 (m, 4H), 3.63 – 3.50 (m, 1H), 2.91 (t, *J* = 2.5 Hz, 1H). MS (ESI) *m/z* calcd for C₁₈H₂₈NaO₁₂ [2M+Na]⁺ 459.15, found 459.20. ¹H NMR and MS revealed formation of the desired glycoside anomeric mixture.

Prop-2-ynyl-2-acetylamino-2-deoxy-D-glucopyranoside³⁴



Prop-2-ynyl-2-acetylamino-2-deoxy-D-glucopyranoside was prepared using the same procedure for Prop-2-ynyl-D-glucopyranoside. Prop-2-ynyl-2-acetylamino-2-deoxy-D-glucopyranoside was obtained as pale-yellow solid (Yield: 23%). ¹H NMR (400 MHz, methanol-*d*₄, α/β =5:1) δ 5.01 (d, *J* = 3.6 Hz, α-H1, 1H), 4.62 (d, *J* = 8.4 Hz, β-H1, 1H), 4.40 – 4.22 (m, 2H), 4.01 – 3.90 (m, 1H), 3.90 – 3.80 (m, 1H), 3.76 – 3.64 (m, 2H), 3.64 – 3.57 (m, 1H), 3.44 – 3.36 (m, 1H), 2.88 (t, *J* = 2.5 Hz, 1H), 2.01 (s, 3H). MS (ESI) *m/z* calcd for C₂₂H₃₄N₂NaO₁₂ [2M+Na]⁺ 541.20, found 541.28. ¹H NMR and MS revealed formation of the desired glycoside anomeric mixture.

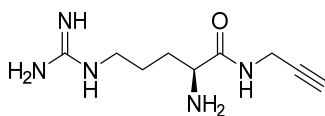
N-(2-aminoethyl)propiolamide

Monosubstituted N-Boc-ethylenediamine was prepared following the method in literature with modification.³⁵ To an ice-cooled solution of ethylenediamine (1.2 g, 20 mmol) in anhydrous THF, a solution of di-tertbutyl decarbonate (1.09 g, 5 mmol) in THF was added dropwise, and the mixture was stirred for extra 30 min before warmed up to room temperature. The resulting mixture was stirred overnight at room temperature before removing the solvent under reduced pressure. The residue was dissolved in ethyl acetate and washed with brine, dried and concentrated to give desired product as colorless oil. ¹H NMR (400 MHz, CDCl₃) δ 5.19 (s, 1H), 3.22 – 3.09 (m, 2H), 2.76 (t, *J* = 5.7 Hz, 2H), 2.33 (s, 2H), 1.38 (s, 9H).

The coupling between propiolic acid and monosubstituted N-Boc-ethylenediamine was carried out according to reported procedure with modification.³⁶ To the solution of propiolic acid (350 mg, 5 mmol) in DCM, EDCI (1.20 g, 6.25 mmol) was added and stirred at room temperature for 1 h. After cooling in ice bath, the solution of monosubstituted N-Boc-ethylenediamine (800 mg, 5 mmol) in DCM was added to the mixture dropwise, warmed up and stirred for another 12 h. The reaction mixture was washed with brine and water successively before dried over Na₂SO₄. The crude product was subjected to flash column chromatography using EA-Hexane as eluent, affording the product as light-yellow solid. ¹H NMR (400 MHz, CDCl₃) δ 6.29 (s, 1H), 4.92 (s, 1H), 3.43 – 3.30 (m, 4H), 2.79 (s, 1H), 1.42 (s, 9H).

The product in previous step was subjected to deprotection using TFA/DCM (1:1) as solvent. After stirring overnight, the solvent was evaporated under reduced pressure and the residue was final product. The product has good purity and used without further purification. ^1H NMR (400 MHz, methanol- d_4) δ 3.37 (s, 1H), 3.24 – 3.16 (m, 2H), 3.02 – 2.92 (m, 2H). MS (ESI) m/z calcd for $\text{C}_5\text{H}_9\text{N}_2\text{O}$ $[\text{M}+\text{H}]^+$ 113.07, found 113.29.

(S)-2-amino-5-guanidino-N-(prop-2-yn-1-yl)pentanamide³⁷

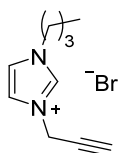


Alkynylated arginine derivative was prepared with modifications.³⁸ To a solution of Boc-Arg(Pbf)-OH (1.05 g, 2.0 mmol) and HATU (950 mg, 2.5 mmol) in dry DMF, DIPEA (0.99 mL, 6.0 mmol) was added and the mixture was stirred for 30 min under N_2 at room temperature before propargylamine (137.5 mg, 2.5 mmol) was added. The resulting mixture was stirred for another 24 h followed by dilution with ethyl acetate. The solution was washed with 1M HCl solution, saturated NaHCO_3 and water. The organic layer was dried over Na_2SO_4 , filtered, concentrated and subjected to column chromatography using EA-hexane as eluent, giving pale yellow solid (Yield: 64%). ^1H NMR (500 MHz, CDCl_3) δ 7.34 (s, 1H), 6.27 (s, 3H), 5.71 – 5.39 (m, 1H), 4.20 (s, 1H), 4.12 - 3.88 (m, 2H), 3.27 (s, 2H), 2.96 (s, 2H), 2.51 (s, 3H), 2.50 (s, 3H), 2.18 (t, J = 2.5 Hz, 1H), 2.09 (s, 3H), 1.93 - 1.78 (m, 2H), 1.78 – 1.52 (m, 2H), 1.46 (s, 6H), 1.41 (s, 9H).

The alkynylated arginine from previous step was subjected to deprotection in TFA/water (95:5) mixture at room temperature. The mixture was stirred overnight before

removing the solvent under reduced pressure. The residue was dissolved in water and washed with chloroform until no UV active compound observed in the chloroform extracts. The aqueous layer was concentrated to give desired product as light-yellow oil. ^1H NMR (400 MHz, Deuterium Oxide) δ 4.08 – 3.87 (m, 3H), 3.18 (t, J = 6.8 Hz, 2H), 2.58 (t, J = 2.5 Hz, 1H), 1.96 – 1.81 (m, 2H), 1.67 – 1.54 (m, 2H). MS (ESI) m/z calcd for $\text{C}_9\text{H}_{18}\text{N}_5\text{O}$ $[\text{M}+\text{H}]^+$ 211.15, found 212.19.

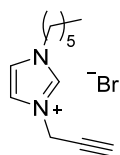
1-Propargyl-3-butyl-1,3-diazanyl-2,4-cyclopentadiene bromide³⁹



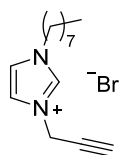
N-Butyl imidazole was prepared following the method in literature with modifications.⁴⁰ To the suspension of imidazole (6.0 g, 88 mmol) in acetonitrile (50 mL) was added KOH pellets (9.9 g, 177 mmol), the mixture was stirred for 30min followed by the addition of 1-bromobutane (9.7 mL, 90 mmol). The reaction mixture was refluxed for 4 h before cooled to room temperature. The solvent was removed under reduced pressure and the residue was dissolved in ethyl acetate and washed with water and brine. The organic phase was dried over Na_2SO_4 , filtered and concentrated under reduced pressure and subjected to flash column using MeOH-EtOAc as eluent affording the desired product in 81% yield. ^1H NMR (400 MHz, Chloroform- d) δ 7.42 (s, 1H), 7.01 (s, 1H), 6.87 (s, 1H), 3.89 (t, J = 7.1 Hz, 2H), 1.83 – 1.67 (m, 2H), 1.37 – 1.23 (m, 2H), 0.90 (t, J = 7.4 Hz, 3H).

The 1-Propargyl-3-butyl-1,3-diazanyl-2,4-cyclopentadiene bromide was synthesized according to the procedure in the literature with modification.⁴¹ To the 1-butyylimidazole

(1.0 g, 8.1 mmol) solution in ethanol (40 mL), propargyl bromide (1.0 g, 8.5 mmol) was added and the reaction mixture was refluxed for 24h before cooled down to room temperature. The solvent was removed under reduced pressure and the residue was washed with diethyl ether and dried in vacuo, giving pale yellow oil. ^1H NMR (400 MHz, methanol- d_4) δ 9.29 (s, 1H), 7.93 – 7.53 (m, 2H), 5.27 (d, J = 2.6 Hz, 2H), 4.36 (t, J = 7.4 Hz, 2H), 3.38 (t, J = 2.6 Hz, 1H), 2.03 – 1.92 (m, 2H), 1.56 – 1.40 (m, 2H), 1.06 (t, J = 7.4 Hz, 3H). MS (ESI) m/z calcd for $\text{C}_{10}\text{H}_{15}\text{N}_2$ $[\text{M}-\text{Br}]^+$ 163.12, found 163.20.

1-Propargyl-3-hexyl-1,3-diazanyl-2,4-cyclopentadiene bromide⁴¹

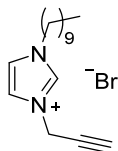
1-Propargyl-3-hexyl-1,3-diazanyl-2,4-cyclopentadiene bromide was produced in the same procedure. ^1H NMR (400 MHz, methanol- d_4) δ 9.44 (s, 1H), 8.06 – 7.71 (m, 2H), 5.40 (d, J = 2.6 Hz, 2H), 4.46 (t, J = 7.4 Hz, 2H), 3.47 (t, J = 2.6 Hz, 1H), 2.25 – 1.90 (m, 2H), 1.61 – 1.33 (m, 4H), 1.06 (t, J = 7.4 Hz, 3H). MS (ESI) m/z calcd for $\text{C}_{12}\text{H}_{19}\text{N}_2$ $[\text{M}-\text{Br}]^+$ 191.15, found 191.23.

1-Propargyl-3-octyl-1,3-diazanyl-2,4-cyclopentadiene bromide⁴¹

1-Propargyl-3-octyl-1,3-diazanyl-2,4-cyclopentadiene bromide was produced in the same procedure. ^1H NMR (400 MHz, methanol- d_4) δ 9.33 (s, 1H), 7.95 – 7.60 (m, 2H), 5.29 (d, J = 2.3 Hz, 2H), 4.36 (t, J = 7.4 Hz, 2H), 3.37 (t, J = 2.6 Hz, 1H), 2.15 – 1.80 (m, 2H), 1.50 –

1.23 (m, 6H), 0.96 (t, $J = 7.4$ Hz, 3H). MS (ESI) m/z calcd for $C_{14}H_{23}N_2$ $[M-Br]^+$ 219.19, found 219.29.

1-Propargyl-3-decyl-1,3-diazanyl-2,4-cyclopentadiene bromide⁴¹



1-Propargyl-3-decyl-1,3-diazanyl-2,4-cyclopentadiene bromide was produced in the same procedure. 1H NMR (400 MHz, methanol- d_4) δ 9.28 (s, 1H), 7.81 (s, 2H), 5.26 (d, $J = 2.5$ Hz, 2H), 4.34 (t, $J = 7.4$ Hz, 2H), 3.37 (t, $J = 2.6$ Hz, 1H), 2.18 – 1.88 (m, 2H), 1.56 – 1.25 (m, 8H), 0.96 (t, $J = 7.4$ Hz, 3H). MS (ESI) m/z calcd for $C_{16}H_{27}N_2$ $[M-Br]^+$ 247.22, found 247.34.

2.4.5 Degradability examination.

The degradation ability of polymers was conducted using the selected sample as a model. Polymer was incubated in phosphate-buffered-saline (PBS, pH = 7.4) at 37 °C. Aliquots were taken out at certain time intervals and monitored directly by GPC.

2.4.6 Minimum inhibitory concentration (MIC) determination.

Minimum inhibition concentrations (MICs) were measured following standard broth dilution method with minor modification.⁴² Bacterial cells were grown overnight in Mueller-Hinton broth (MHB, Difco®, Becton, Dickinson and Company) at 37 °C. The bacteria were 1:100 subcultured in MHB to a mid-exponential phase and diluted to 5×10^5 CFU·mL⁻¹ in fresh MHB. Stock solutions of PCLs were prepared in the MHB medium at a concentration of 1024 $\mu\text{g} \cdot \text{mL}^{-1}$. The solutions were 2-fold serially diluted in MHB medium,

and 50 μL of each dilution was placed in each well of 96-well microplates (Nunc™, ThermoScientific) followed by the addition of 50 μL of the bacterial suspension. The plate was mixed in a shaker incubator for 10 min before incubated at 37 °C for 18 h, and the absorbance at 600 nm was measured with a microplate reader (TECAN, infinite F200). A positive control without polymer and a negative control without bacteria were included. MIC was determined as the lowest concentration of the compound that inhibited the growth of bacteria by more than 90%. All tests were done in three independent tests with duplicate per test.

2.4.7 Hemolysis studies.

Fresh human blood was collected from a healthy donor (IRB-2015-03-040) and used within the same day. Human blood was drawn directly into K2-EDTA-coated Vacutainer tubes to prevent coagulation of blood and stored at 4 °C for 30 min. 1 mL blood was mixed with 9mL PBS and centrifuged at 1,000 rpm for 5 min. Supernatant was discarded and red blood cells (RBCs) were collected. The RBCs were washed with PBS three times and resuspended to a final concentration of 5% (v/v) in PBS. A two-fold dilution series of polymer in PBS solution was prepared, 50 μL red blood cell suspension was mixed with 50 μL polymer solution in each well and incubated for 1 h at 37 °C in an inoculation shaker with continuous shaking at 150 rpm. The 96 well plates were centrifuged at 1,000 rpm for 10 min. After centrifugation, 80 μL centrifuge supernatant samples were transferred to a new 96-well plate and diluted with 80 μL PBS, and hemolytic activity was calculated by measuring absorbance at 540 nm using a 96-well plate spectrophotometer (Benchmark Plus, BIO-RAD). PBS buffer (pH 7.4) was used as a negative hemolysis control, and Triton

X-100 (0.1% v/v in PBS) was used as a positive control. The percentage of hemoglobin release was calculated from the following equation: Hemolysis (%) = $[(O_p - O_b)/(O_t - O_b)] \times 100\%$ where O_p is the absorbance for the polymer, O_b is the absorbance for the negative control (PBS), and O_t is the absorbance for the positive control of Triton X-100. All data were obtained from the mean value of three replicates.

2.4.8 Cytotoxicity assays.

The mammalian cell biocompatibility study was tested towards 3T3 fibroblast cell using 3-(4,5-dimethylthiazol-2-yl)-2,5-diphenyltetrazolium bromide (MTT) in colorimetric assay. 3T3 cells (ATCC) were cultured in Dulbecco's Modified Eagle's Medium (DMEM, Gibco) supplemented with 10% fetal bovine serum (FBS) and 1% antibiotics (penicillin/streptomycin). The cells in tissue culture flask were cultured at 37 °C in a humidified incubator with 5% CO₂ until 80% confluence was reached. 3T3 cells were harvested from the confluence flask by trypsinization. Cell number was determined using a hemocytometer and 10⁴ cells/well were seeded into a 96-well tissue culture plate and incubated at 37 °C in a humidified incubator with 5% CO₂ for 24h. Polymer in culture medium solutions at 100 µg/mL and 200 µg/mL were added into the 96-well plate seeded with cells and incubated at 37 °C in a humidified incubator with 5% CO₂ incubator for 24 h. Cells incubated with only DMEM were used as positive nontoxic controls. Afterwards, the culture medium containing polymer was removed, and each well was washed with PBS prior to the addition of MTT solution (1 mg·mL⁻¹ in DMEM). After another 4 h of incubation, the MTT solution was aspirated and 100 µL dimethyl sulfoxide (DMSO) was

added into each well, and the plate was shaken at 150 rpm for 10 minutes, after which the absorbance of each well was measured at 570 nm using a microplate reader spectrophotometer (BIO-RAD, Benchmark Plus). The cell viability results were expressed as percentages relative to the absorbance obtained in the control experiment.

$$\% \text{ Cell viability} = \frac{\text{Average abs of treated cells}}{\text{Average abs of controls}} \times 100\%$$

2.4.9 Bacteria killing kinetics.

Time kill study was conducted by incubating bacteria with different concentrations of polymer/antibiotics and determining CFU·mL⁻¹ at various time points. Bacterial cells were grown overnight in Mueller-Hinton broth medium at 37 °C. After subculturing to a mid-exponential phase, bacteria were diluted to 5×10⁵ CFU·mL⁻¹ in fresh MHB. Polymer or antibiotic were added to 1000 µL bacteria in MHB suspension in Eppendorf tubes to achieve a final polymer/antibiotic concentration of 4×MIC, 2×MIC, 1×MIC and 0.5×MIC respectively. Bacteria in MHB suspension without addition of polymer were used as positive control. The bacteria suspensions with polymers were incubated in an inoculation shaker at 37 °C with continuous shaking. Aliquots were taken at different time intervals (0, 0.25, 0.5, 1, 2, 4, 6, and 24 h) and ten-fold serial diluted in PBS for plating. The diluted aliquots were plated on LB agar and incubated at 37 °C and CFU of each sample was determined after 20 h. The killing model for the comparison with polymer degradation was carried out in PBS with same conditions except no medium. Two independent experiments with duplicate for each test were performed for each polymer/pathogen combination, and the resulting average values are plotted on CFU·mL⁻¹ against time.

2.5 References

- [1] a) K. A. Brogden, *Nat. Rev. Microbiol.* **2005**, 3, 238; b) G. N. Tew, R. W. Scott, M. L. Klein, W. F. DeGrado, *Acc. Chem. Res.* **2010**, 43, 30.
- [2] a) Z. M. Al-Badri, A. Som, S. Lyon, C. F. Nelson, K. Nüsslein, G. N. Tew, *Biomacromolecules* **2008**, 9, 2805; b) M. F. Ilker, K. Nüsslein, G. N. Tew, E. B. Coughlin, *J. Am. Chem. Soc.* **2004**, 126, 15870; c) G. J. Gabriel, A. E. Madkour, J. M. Dabkowski, C. F. Nelson, K. Nüsslein, G. N. Tew, *Biomacromolecules* **2008**, 9, 2980; d) K. Lienkamp, A. E. Madkour, A. Musante, C. F. Nelson, K. Nüsslein, G. N. Tew, *J. Am. Chem. Soc.* **2008**, 130, 9836.
- [3] a) F. Nederberg, Y. Zhang, J. P. K. Tan, K. Xu, H. Wang, C. Yang, S. Gao, X. D. Guo, K. Fukushima, L. Li, J. L. Hedrick, Y.-Y. Yang, *Nat. Chem.* **2011**, 3, 409; b) Z. X. Voo, M. Khan, K. Narayanan, D. Seah, J. L. Hedrick, Y. Y. Yang, *Macromolecules* **2015**, 48, 1055; c) V. W. L. Ng, J. P. K. Tan, J. Leong, Z. X. Voo, J. L. Hedrick, Y. Y. Yang, *Macromolecules* **2014**, 47, 1285; d) W. Chin, G. Zhong, Q. Pu, C. Yang, W. Lou, P. F. De Sessions, B. Periaswamy, A. Lee, Z. C. Liang, X. Ding, S. Gao, C. W. Chu, S. Bianco, C. Bao, Y. W. Tong, W. Fan, M. Wu, J. L. Hedrick, Y. Y. Yang, *Nat. Commun.* **2018**, 9, 917; e) A. Nimmagadda, X. Liu, P. Teng, M. Su, Y. Li, Q. Qiao, N. K. Khadka, X. Sun, J. Pan, H. Xu, Q. Li, J. Cai, *Biomacromolecules* **2017**, 18, 87.
- [4] a) B. P. Mowery, S. E. Lee, D. A. Kissounko, R. F. Epand, R. M. Epand, B. Weisblum, S. S. Stahl, S. H. Gellman, *J. Am. Chem. Soc.* **2007**, 129, 15474; b) R. Liu, X. Chen, S. P. Falk, B. P. Mowery, A. J. Karlsson, B. Weisblum, S. P. Palecek, K. S. Masters, S. H. Gellman, *J. Am. Chem. Soc.* **2014**, 136, 4333; c) R. Liu, X. Chen, S. P. Falk, K. S. Masters, B. Weisblum, S. H. Gellman, *J. Am. Chem. Soc.* **2015**, 137, 2183.
- [5] a) C. Zhou, X. Qi, P. Li, W. N. Chen, L. Mouad, M. W. Chang, S. S. J. Leong, M. B. Chan-Park, *Biomacromolecules* **2010**, 11, 60; b) M. Xiong, M. W. Lee, R. A. Mansbach, Z. Song, Y. Bao, R. M. Peek, C. Yao, L.-F. Chen, A. L. Ferguson, G. C. L. Wong, J.

- Cheng, *Proc. Natl. Acad. Sci.* **2015**, 112, 13155.
- [6] a) K. Kuroda, W. F. DeGrado, *J. Am. Chem. Soc.* **2005**, 127, 4128; b) I. Ivanov, S. Vemparala, V. Pophristic, K. Kuroda, W. F. DeGrado, J. A. McCammon, M. L. Klein, *J. Am. Chem. Soc.* **2006**, 128, 1778; c) S. Varun, P. B. R., S. Ayusman, *Angew. Chem. Int. Ed.* **2008**, 47, 1250.
- [7] a) J. Wang, Y. P. Chen, K. Yao, P. A. Wilbon, W. Zhang, L. Ren, J. Zhou, M. Nagarkatti, C. Wang, F. Chu, X. He, A. W. Decho, C. Tang, *Chem. Commun.* **2012**, 48, 916; b) Y. Li, K. Fukushima, D. J. Coady, A. C. Engler, S. Liu, Y. Huang, J. S. Cho, Y. Guo, L. S. Miller, J. P. K. Tan, P. L. R. Ee, W. Fan, Y. Y. Yang, J. L. Hedrick, *Angew. Chem. Int. Ed.* **2012**, 52, 674.
- [8] a) J. H. Jung, M. Ree, H. Kim, *Catal. Today* **2006**, 115, 283; b) J. G. Sanchez, A. Tsuchii, Y. Tokiwa, *Biotechnol. Lett.* **2000**, 22, 849; c) H. Pranamuda, R. Chollakup, Y. Tokiwa, *Appl. Environ. Microb.* **1999**, 65, 4220.
- [9] H. Bakhshi, S. Agarwal, *J. Mater. Chem. B* **2017**, 5, 6827.
- [10] R. Riva, S. Schmeits, F. Stoffelbach, C. Jérôme, R. Jérôme, P. Lecomte, *Chem. Commun.* **2005**, 5334.
- [11] H. C. Kolb, M. G. Finn, K. B. Sharpless, *Angew. Chem. Int. Ed.* **2001**, 40, 2004.
- [12] a) Z.-h. Huang, Y.-y. Zhou, Z.-m. Wang, Y. Li, W. Zhang, N.-c. Zhou, Z.-b. Zhang, X.-l. Zhu, *Chin. J. Polym. Sci.* **2017**, 35, 317; b) U. Tunca, *J. Polym. Sci. A Polym. Chem.* **2014**, 52, 3147; c) W. H. Binder, R. Sachsenhofer, *Macromol. Rapid Commun.* **2008**, 29, 952.
- [13] Y. Xue, H. Xiao, Y. Zhang, *Int. J. Mol. Sci.* **2015**, 16.
- [14] a) T. Itoh, *Chem. Rev.* **2017**, 117, 10567; b) R. L. Vekariya, *J. Mol. Liq.* **2017**, 227, 44.
- [15] W. Qian, J. Texter, F. Yan, *Chem. Soc. Rev.* **2017**, 46, 1124.
- [16] K. Kenichi, C. G. A., D. W. F., *Chem. Eur. J.* **2009**, 15, 1123.
- [17] a) L. Karen, M. A. E., K. Kushi-Nidhi, N. Klaus, T. G. N., *Chem. Eur. J.* **2009**, 15, 11715; b) E. Tarik, S. Abhigyan, R. J. R., N. C. F., U. Yelena, N. Klaus, C. E. Bryan,

- T. G. N., *Macromol. Chem. Phys.* **2008**, 209, 516.
- [18] a) S. Colak, C. F. Nelson, K. Nüsslein, G. N. Tew, *Biomacromolecules* **2009**, 10, 353;
b) Y. Chuan, K. Sangeetha, L. Jie, L. Shaoqiong, L. Xiaohua, C. D. J., C. Wei, D. L. Gennaro, S. Amit, H. J. L., Y. Y. Yan, *Adv. Healthc. Mater.* **2016**, 5, 1272; c) E. H. H. Wong, M. M. Khin, V. Ravikumar, Z. Si, S. A. Rice, M. B. Chan-Park, *Biomacromolecules* **2016**, 17, 1170; d) M. Álvarez-Paino, A. Muñoz-Bonilla, F. López-Fabal, J. L. Gómez-Garcés, J. P. A. Heuts, M. Fernández-García, *Biomacromolecules* **2015**, 16, 295; e) S. Venkataraman, Y. Zhang, L. Liu, Y.-Y. Yang, *Biomaterials* **2010**, 31, 1751; f) A. I. Lopez, R. Y. Reins, A. M. McDermott, B. W. Trautner, C. Cai, *Mol. BioSyst.* **2009**, 5, 1148.
- [19] Y. Miura, Y. Hoshino, H. Seto, *Chem. Rev.* **2016**, 116, 1673.
- [20] K. Aoi, K. Tsutsumiuchi, E. Aoki, M. Okada, *Macromolecules* **1996**, 29, 4456.
- [21] J. Bouckaert, J. Berglund, M. Schembri, E. De Genst, L. Cools, M. Wuhrer, C.-S. Hung, J. Pinkner, R. Slättegård, A. Zavialov, D. Choudhury, S. Langermann, S. J. Hultgren, L. Wyns, P. Klemm, S. Oscarson, S. D. Knight, H. De Greve, *Mol Microbiol* **2005**, 55, 441.
- [22] a) X. Jiang, M. Ahmed, Z. Deng, R. Narain, *Bioconjugate Chem* **2009**, 20, 994; b) M. Ahmed, Z. Deng, R. Narain, *Acs Appl Mater Interfaces* **2009**, 1, 1980.
- [23] G. Ma, D. Li, J. Wang, X. Zhang, H. Tang, *Aust. J. Chem.* **2013**, 66, 1576.
- [24] a) X. Ning, W. Rui, D. Fu-Sheng, L. Zi-Chen, *J. Polym. Sci. A Polym. Chem.* **2009**, 47, 3583; b) R. Riva, S. Schmeits, C. Jérôme, R. Jérôme, P. Lecomte, *Macromolecules* **2007**, 40, 796.
- [25] G. J. Gabriel, J. A. Maegerlein, C. F. Nelson, J. M. Dabkowski, T. Eren, K. Nüsslein, G. N. Tew, *Chem. Eur. J.* **2009**, 15, 433.
- [26] a) E. F. Palermo, K. Kuroda, *Biomacromolecules* **2009**, 10, 1416; b) R. Tejero, D. López, F. López-Fabal, J. L. Gómez-Garcés, M. Fernández-García, *Biomacromolecules* **2015**, 16, 1844.

- [27] a) M. F. Richter, B. S. Drown, A. P. Riley, A. Garcia, T. Shirai, R. L. Svec, P. J. Hergenrother, *Nature* **2017**, 545, 299; b) A. H. Delcour, *Biochim. Biophys. Acta* **2009**, 1794, 808.
- [28] G. A. Pankey, L. D. Sabath, *Clin. Infect. Dis.* **2004**, 38, 864.
- [29] C. W. Stratton, *Emerg. Infect. Dis.* **2003**, 9, 10.
- [30] R. Singh, A. J. Varma, *Green Chem.* **2012**, 14, 348.
- [31] G. Ma, D. Li, J. Wang, X. Zhang, H. Tang, *Aust. J. Chem.* **2013**, 66, 1576.
- [32] Q. Zhang, S. Slavin, M. W. Jones, A. J. Haddleton, D. M. Haddleton, *Polym. Chem.* **2012**, 3, 1016.
- [33] B. P. Krishnan, S. Ramakrishnan, K. M. Sureshan, *Chem. Commun.* **2013**, 49, 1494.
- [34] D. Yan, J. Naughton, M. Clyne, P. V. Murphy, *Carbohydr. Res.* **2012**, 360, 1.
- [35] C. Douat-Casassus, N. Marchand-Geneste, E. Diez, N. Gervois, F. Jotereau, S. Quideau, *J. Med. Chem.* **2007**, 50, 1598.
- [36] S. Srinivasachari, K. M. Fichter, T. M. Reineke, *J. Am. Chem. Soc.* **2008**, 130, 4618.
- [37] N. Yaakov, Y. Chaikin, E. Wexselblatt, Y. Tor, A. Vaskevich, I. Rubinstein, *Chem. Eur. J.* **2017**, 23, 10148.
- [38] L. Gallego-Yerga, M. Lomazzi, V. Franceschi, F. Sansone, C. Ortiz Mellet, G. Donofrio, A. Casnati, J. M. García Fernández, *Org. Biomol. Chem.* **2015**, 13, 1708.
- [39] L. Boffa, E. C. Gaudino, K. Martina, L. Jicsinszky, G. Cravotto, *New J. Chem.* **2010**, 34, 2013.
- [40] J.-Y. Cheng, Y.-H. Chu, *Tetrahedron Lett.* **2006**, 47, 1575.
- [41] C. Zhou, Y.-H. Li, Z.-H. Jiang, K.-D. Ahn, T.-J. Hu, Q.-H. Wang, C.-H. Wang, *Chin. Chem. Lett.* **2016**, 27, 681.
- [42] I. Wiegand, K. Hilpert, R. E. W. Hancock, *Nat. Protoc.* **2008**, 3, 163.

Chapter 3

Construction of pH Sensitive Functional Polymers via ROMP^{1,*}

^{*}Reproduced from Ref 1 with permission from the Royal Society of Chemistry

3.1 Introduction

Owing to the high controllability, ROMP polymers have been widely applied in many fields, including biologically active compounds.² For instance, ROMP polymers bearing carbohydrates have extensively investigated by Kiessling and coworkers in biological processes.³ Moreover, it is noteworthy that the Tew group has extensively employed poly(oxa)norbornenes as scaffolds in the development of antimicrobial polymers which has been discussed in previous introduction part (Figure 3.1).⁴

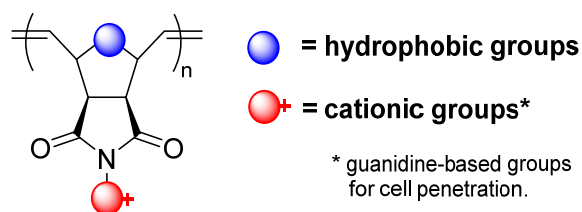


Figure 3.1 Antimicrobial ROMP polymers developed by Tew *et al.*

Albeit powerful, polymers prepared via ROMP are primarily consisting of carbon-carbon based building blocks which is non-degradable, limiting their further applications. To address this, scientists have paid remarkable efforts on producing copolymers which are partially degradable owing to the fragile units involved.⁵ For example, biodegradable poly(lactide) chains were grafted to polynorbornene backbone, affording polymeric materials with degradable side chains.⁶ Besides, PCL chains and peptide sequences were also employed as side chains in producing such copolymers (Figure 3.2).⁷

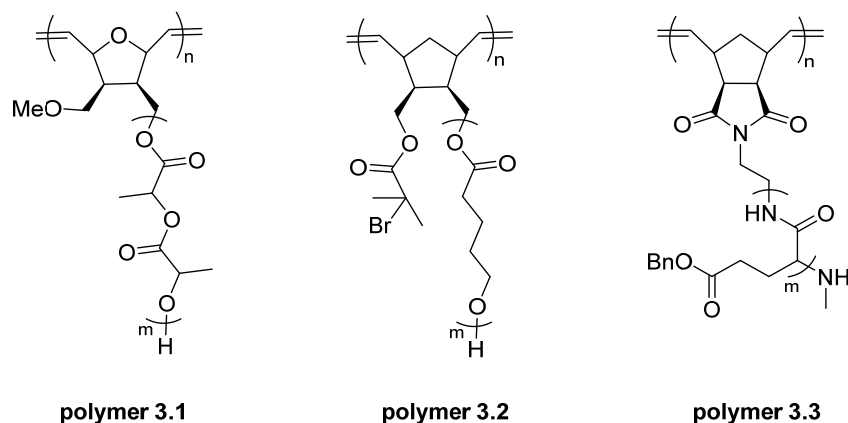


Figure 3.2 ROMP polymers with degradable side chains.

In addition, macrocyclic olefin possessing acid-labile acetal linkage was subjected to copolymerization with norbornene derivatives, affording block copolymers with sequential addition procedure. The degradability of copolymers was demonstrated by the successful preparation of end-functionalized homopolymers (Figure 3.3).^{5c}

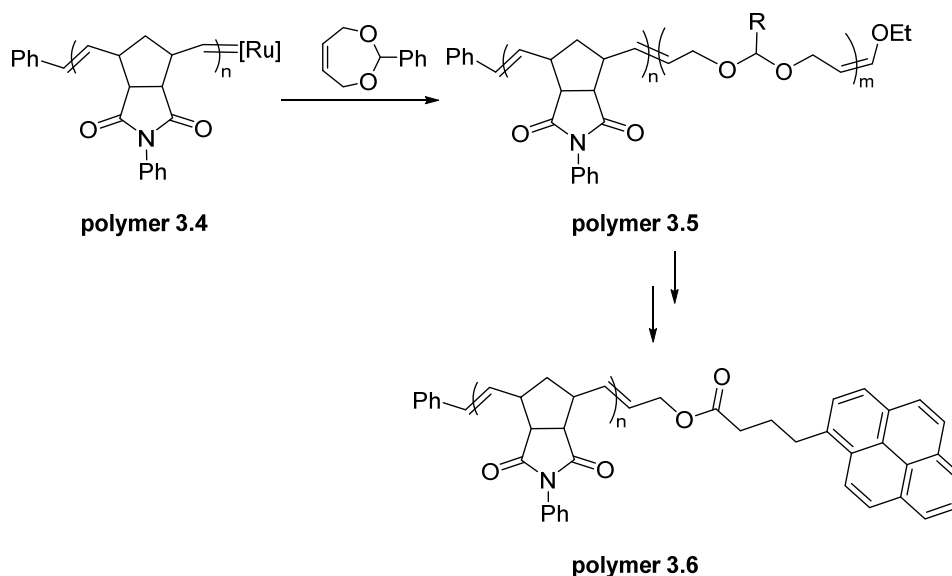


Figure 3.3 Synthesis of end-functionalized polynorbornene derivatives through degradation of block copolymer.

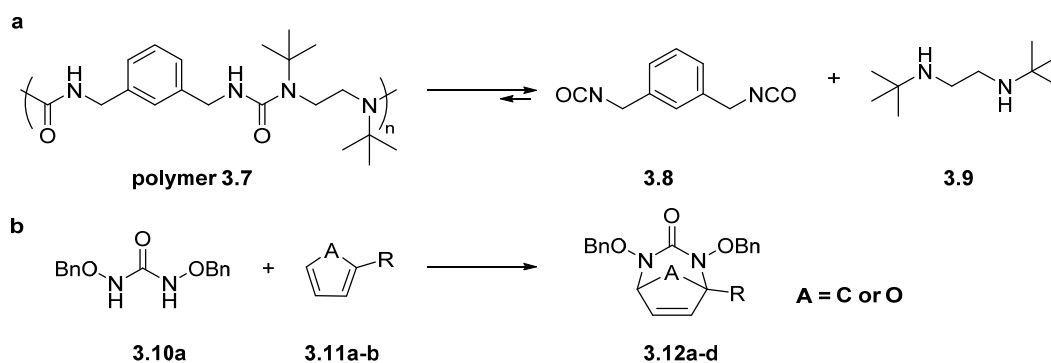


Figure 3.4 Urea-based compounds. a) Hydrolytically degradable polyurea; b) Facile synthesis of urea-based bicyclic olefins.

Nevertheless, fully degradable polymers that could be completely torn into small fragments are rarely reported on ROMP polymers. Recently, Cheng and coworkers reported a series of degradable polyurea which could hydrolytically degrade in short time (Figure 3.4a).⁸ Besides, Jeffrey et al. reported a facile approach to prepare bicyclic olefins containing urea substructure as well as hemiaminal ether linkage (Figure 3.4b).⁹

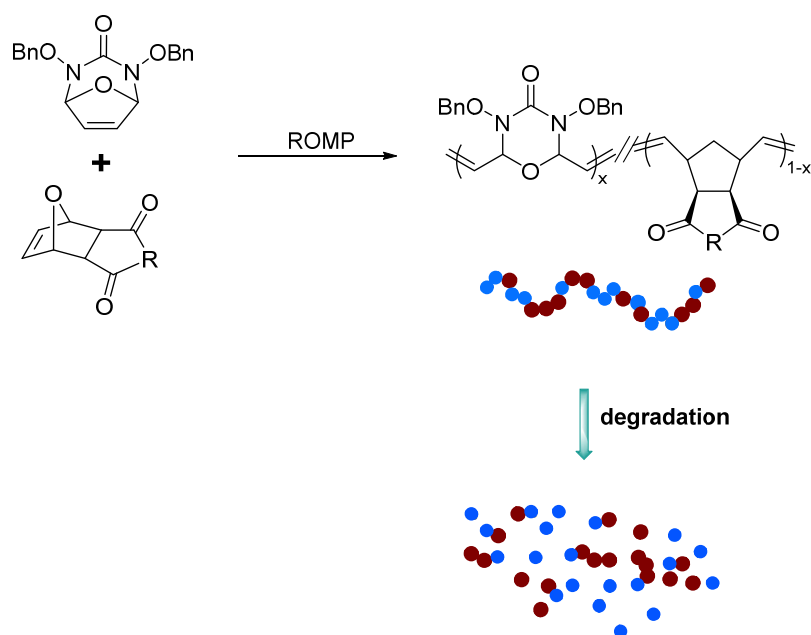


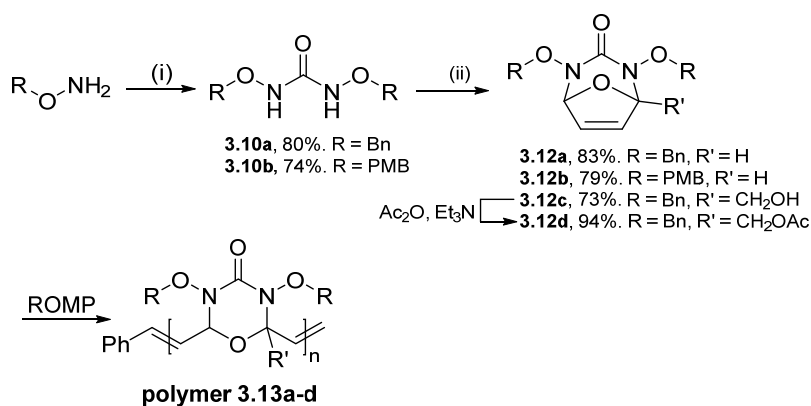
Figure 3.5 Introducing labile olefins into ROMP systems to prepare fully degradable polymers.

Therefore, we envisioned that this scaffold could be introduced into ROMP systems, affording fully degradable polymers which would be beneficial to further antibacterial applications (Figure 3.5).

3.2 Results and Discussion

Briefly, a series of ROMP polymers with both acid and base sensitivity have been prepared, including homopolymers and copolymers. The degradation behavior of homopolymers from urea-based bicyclic olefins has been studied both in acidic and basic media. In addition, a series of functionalized norbornenes have been successfully copolymerized with urea-based monomers. The critical composition for the successful degradation of copolymers has been identified through systematical study. Several functional copolymers have been successfully prepared with preliminary trial in antibacterial application.

3.2.1 Synthesis of homopolymers

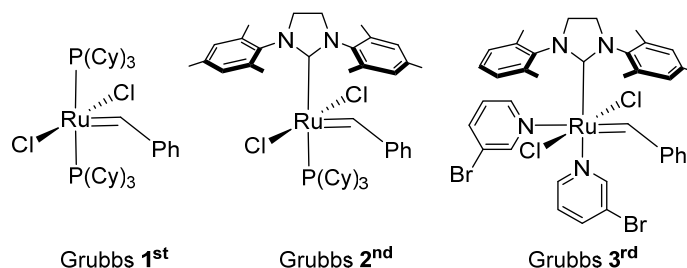


Scheme 3.1 Synthesis of monomers and polymers. i) CDI, imidazole, DCM, 0 °C-rt, ii) TFP, TFP-Na, $\text{PhI}(\text{OAc})_2$, furans, CH_3CN , 0 °C. PMB = *p*-methoxybenzyl.

The bicyclic olefin monomers based on urea were synthesized using Jeffrey's procedure.⁹ Specifically, precursors **3.10a** and **3.10b** were prepared and allowed to undergo [4+3] cycloaddition, giving monomer **3.12a** and **3.12b**, respectively. Besides, since

hindrance is vital to the degradability of urea-based scaffold,^{8a} hindered monomer **3.12c** and **3.12d** were also prepared with substituted furan derivative (Scheme 3.1).

Table 3.1 Optimize the homopolymerization of oxadiazinone monomers.



Entry ^a	Catalyst	[M] ₀ /[C] ₀ ^b	Yield (%) ^c	<i>M</i> _n ^{GPC} (×10 ³ g/mol) ^d	PDI ^e
1	Grubbs 3 rd	50	88	6.4	1.6
2	Grubbs 2 nd	50	91	19.1	1.7
3	Grubbs 2 nd	100	88	36.4	1.9
4	Grubbs 1 st	50	98	10.5	1.1
5	Grubbs 1 st	100	96	19.6	1.2
6	Grubbs 1 st	200	87	38.0	1.6
7	Grubbs 1 st	50 ^f	93	9.1	1.1
8	Grubbs 1 st	50 ^g	84	21.7	1.1

^a All reactions were carried out using monomer **3.12a** with initial concentration of 1.0 mol/L under argon atmosphere in THF at 25 °C without otherwise noted; ^b [M]₀/[C]₀ = Initial monomer to catalyst loading; ^c Isolated yield; ^d *M*_n = number-average molecular weight; ^e PDI = polydispersity index, (*M*_w/*M*_n), determined by GPC; ^f Initial concentration = 2.0 mol/L; ^g Monomer **3.12b** was employed.

With monomers in hand, the monomer **3.12a** was subjected to typical conditions using Grubbs 3rd generation catalyst which is reported to be a fast initiator for ROMP.¹⁰ Besides, monomer **3.12a** was taken as a model substrate for screening the conditions of ROMP and reactions were carried out with different Grubbs catalysts and monomer to catalyst ratios (Table 3.1). Unexpectedly, broad molecular weight distribution of polyoxadiazinone

(polymer **3.13a**) was obtained with Grubbs 3rd generation catalyst although a single peak was observed in GPC (Table 3.1, entry 1 and Figure 3.6).

Similarly, Grubbs 2nd generation catalyst also gave relatively high polydispersity index (Table 3.1, entry 2 and 3). Surprisingly, the Grubbs 1st generation catalyst could offer polymer in excellent yield with much lower PDI compared to the other two catalysts (Table 1, entry 4 and 5). It is noteworthy that the polymerization with M_0/C of 200 gave polymer with wider molecular weight distribution, which is probably the consequence of back-biting, a typical drawback of ROMP (Table 3.1, entry 6).¹¹ Moreover, polymers were obtained in comparable molecular weight with different initial monomer concentrations, indicating the fast initiation process (Table 3.1, entry 4 and 7). These results indicated that Grubbs 1st catalyst is more suitable for this monomer scaffold.

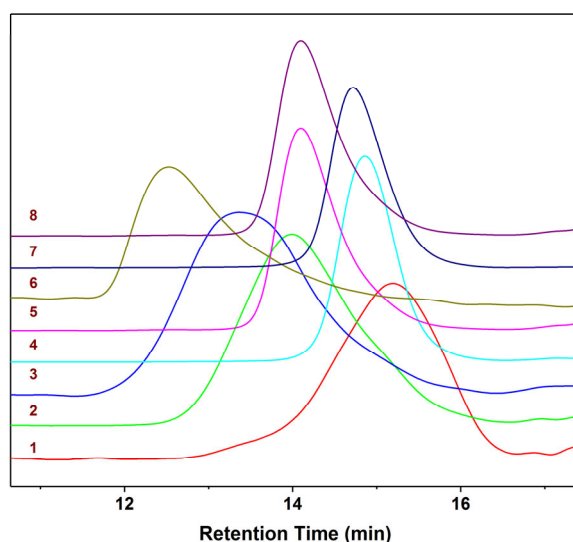


Figure 3.6 GPC traces of polymers in Table 3.1.

Moreover, other monomers prepared were also subjected to polymerization with the optimized conditions. Unfortunately, only monomer **3.12b** could polymerize smoothly (Table 3.1, entry 8), whereas the monomer **3.12c** was unable to polymerize under the same conditions. Although Grubbs catalysts have been reported to be compatible with hydroxyl group, the free hydroxyl group was still protected with acetate and subjected to polymerization under optimized condition. However, monomer **3.12d** was also reluctant to undergo polymerization. These results suggested that bulkiness in the monomer can significantly affect the polymerization process, probably because the catalyst cannot approach the hindered double bond.

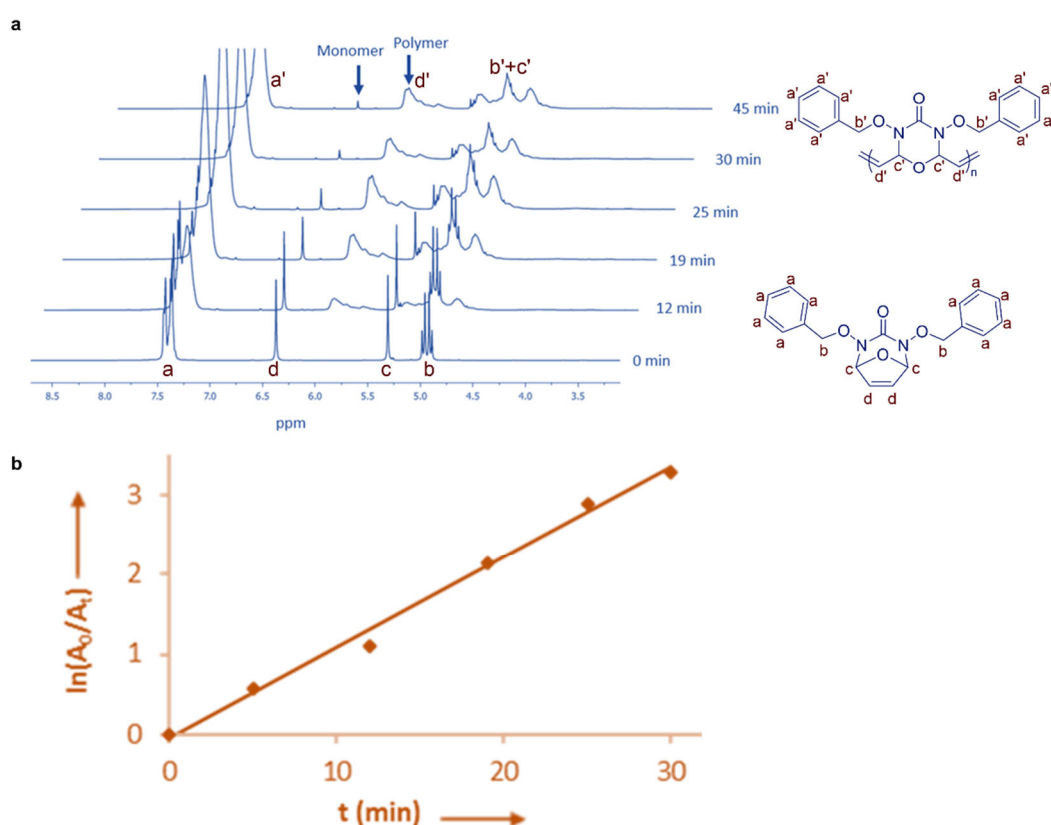


Figure 3.7 Polymerization kinetics. a) Monitored by ¹H-NMR *in situ* (CD₂Cl₂; b) Polymerization follows the 1st order reaction kinetics.

In addition, the polymerization kinetics was also studied by employing monomer **3.12a** as a model substrate. More specifically, the progress of polymerization was monitored by ^1H -NMR spectroscopy. The decrease of peak area at 6.36 ppm for olefinic signal in the monomer and the increase of peak area at 5.80 ppm indicated successful polymerization (Figure 3.7a). In addition, the plot of $\ln[A_0/A_t]$ against time gave a straight line, which suggested that the polymerization reaction follows the pseudo first-order reaction kinetics (Figure 3.7b). Moreover, the M_n vs M_0/C plot indicates the molecular weight increases linearly with the increasing monomer/catalyst ratio, further proving the fast initiation and chain-growth process in the polymerization (Figure 3.8).¹²

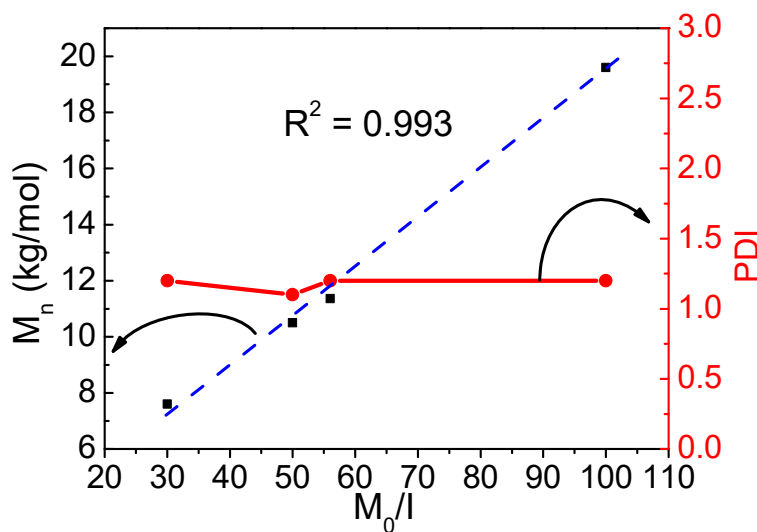


Figure 3.8 Linear dependence of M_n (dash line) on monomer-to-initiator ratio (M_0/I) and polydispersity (PDI, solid line).

3.2.2 Degradation behavior of homopolymers

Even if the hindered monomers could not be prepared successfully, *polymer 3.13a* was subjected to the study of degradation behavior. The decomposition pattern of *polymer 3.13a* in both acidic and basic media were investigated.

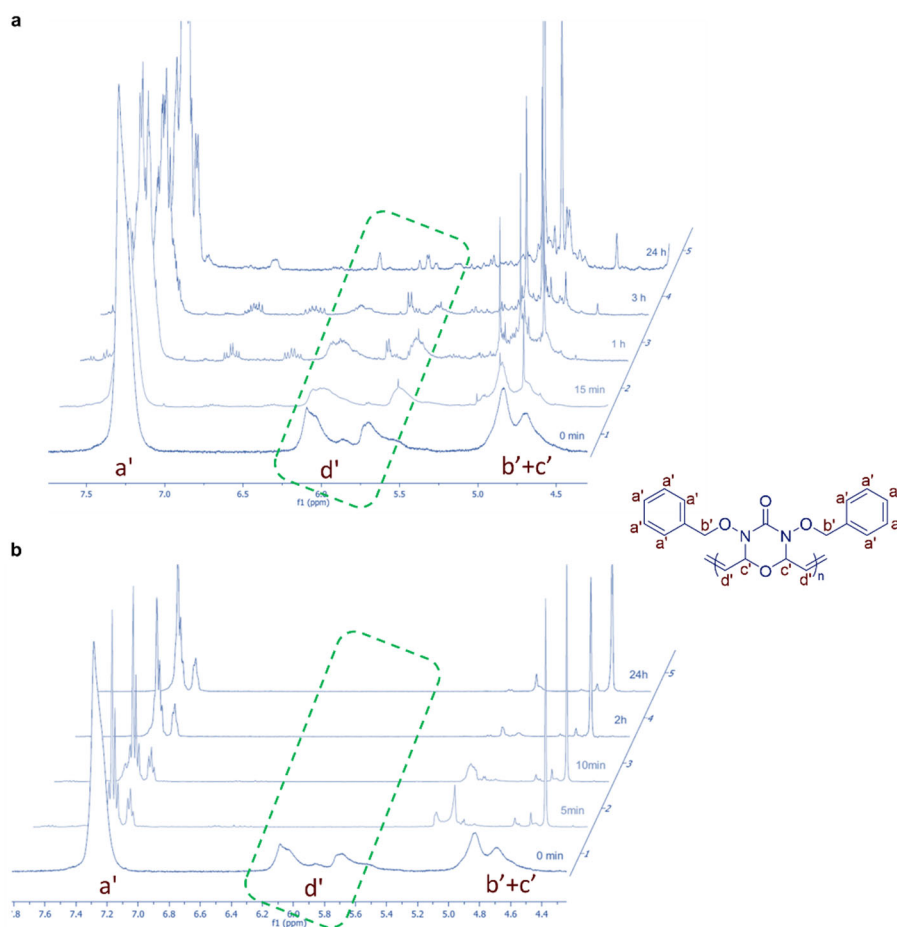


Figure 3.9 Degradation of *polymer 3.13a* in solutions monitored by ^1H -NMR (Acetone- d_6). a) pH = 1; b) pH = 13.5.

To be specific, *polymer 3.13a* was dissolved in a range of pH solutions and the degradation was monitored by ^1H -NMR for 24 hours at room temperature. The

characteristic peak of polymer at 5.80 ppm disappeared completely in solutions with pH 1 and pH 13.5 (Figure 3.9).

The time-dependent degradation of *polymer 3.13a* is visualized by plots of A_t/A_0 against time (Figure 3.10).

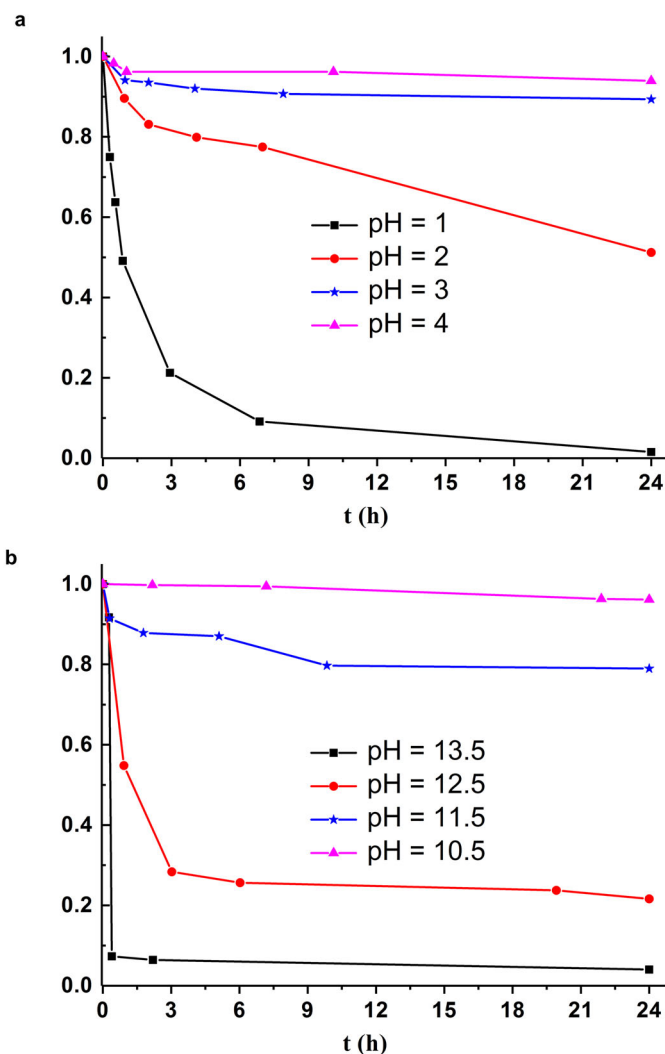


Figure 3.10 Degradation of *polymer 3.13a* in solutions with different pH. a) Acidic; b) Basic.

Besides, the degradation processes at pH 1 and pH 12.5 were also monitored by GPC which showed the same trend as that monitored by ^1H -NMR, indicating NMR could be

applied in evaluating degradation behaviour (Figure 3.11). No significant degradation was observed at pH values between 3.0 and 4.0 over 24 hours of exposure.

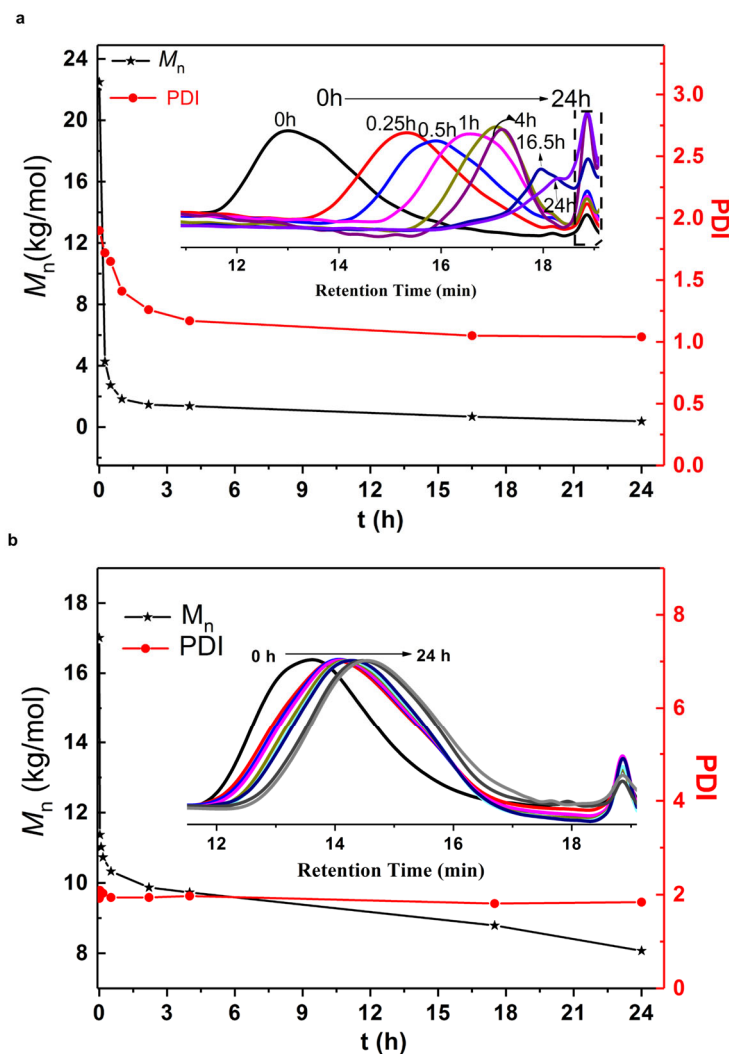


Figure 3.11 Degradation of *polymer 3.13a* in solutions monitored by GPC. a) pH = 1; b) pH = 12.5.

Still, the polymer was vulnerable under specific conditions such as pH 1 and at room temperature, with 63% decomposition within 30 minutes and complete decomposition in 24 hours. The disintegration of *polymer 3.13a* was moderate at pH 2 and 52%

decomposition was observed over 24 hours. Interestingly, *polymer 3.13a* also degraded under basic conditions and 92% decomposition was observed at pH 13.5 within 5 minutes. Similarly, degradation was also observed at pH 12.5 with comparatively slower rate. The disintegration of the polymer backbone was even slower at pH 11.5 whilst no significant decomposition was observed at pH 10.5. Therefore, it can be concluded that polyoxadiazinone is a unique class of degradable ROMP polymer which is stable at neutral pH but labile in specific acidic or basic environments, implying the versatility of oxadiazinone scaffold in producing more degradable polymers via ROMP.

3.2.3 Introducing degradability into functional copolymers

The oxanorbornene and norbornene monomers have been used extensively for ROMP with a variety of applications but the corresponding polymers are unaffected by acids or bases.¹³ Hence, it would be interesting to produce degradable poly(oxa)norbornene and polynorbornene by introducing oxadiazinone into the backbone. As such, a series of (oxo)norbornene-based monomers (**3.14a-g**) were prepared and copolymerized with monomer **3.12a** (Figure 3.12).

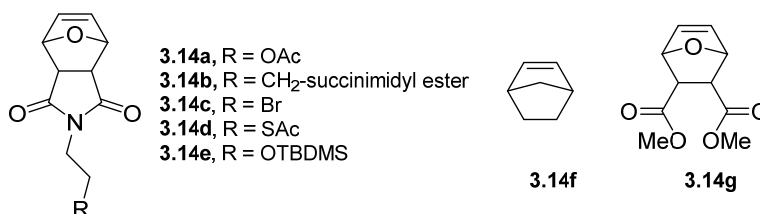
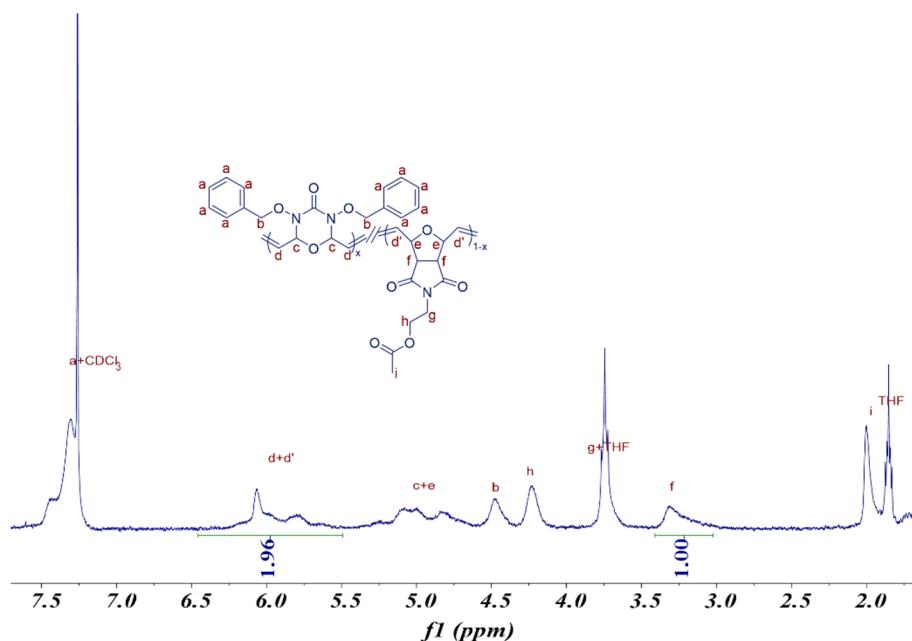


Figure 3.12 Structures of co-monomers **3.14a-g**.

Table 3.2 Copolymerization of oxadiazinone monomer and (oxa)norbornenes.

Entry ^a	Polymer	Monomers	Polymer Composition (5:X) ^b	M_n^{GPC} ($\times 10^3$ g/mol) ^c	PDI ^d
1	12a(49)-co-14a(51)	12a and 14a	49:51	12.9	1.2
2	12a(37)-co-14b(63)	12a and 14b	37:63	55.2	1.8
3	12a(10)-co-14b(90)	12a and 14b	10:90	12.2	1.6
4	12a(81)-co-14c(19)	12a and 14c	81:19	31.5	1.9
5	12a(66)-co-14c(34)	12a and 14c	66:34	27.7	2.0
6	12a(47)-co-14c(53)	12a and 14c	47:53	16.6	2.0
7	12a(83)-co-14d(17)	12a and 14d	83:17	8.6	1.3
8	12a(60)-co-14d(40)	12a and 14d	60:40	9.2	1.3
9	12a(32)-co-14d(68)	12a and 14d	32:68	8.8	1.2
10	12a(69)-co-14e(31)	12a and 14e	69:31	39.5	1.8
11	12a(49)-co-14e(51)	12a and 14e	49:51	26.8	2.6
12	12a(31)-co-14e(69)	12a and 14e	31:69	36.5	2.7
13	12a(36)-co-14f(64)	12a and 14f	36:64	15.0	1.8
14	12a(73)-co-14g(27)	12a and 14g	73:27	48.8	2.0
15	12a(39)-co-14g(61)	12a and 14g	39:61	10.8	1.2
16	12a(27)-co-14g(73)	12a and 14g	27:73	40.6	1.7
17	12a(9)-co-14g(91)	12a and 14g	9:91	12.7	1.2

^a All the reactions were performed under argon atmosphere in optimal conditions; ^b Determined by ¹H-NMR; ^c M_n = number-average molecular weight; ^d PDI = polydispersity index (M_w/M_n), determined by GPC.

**Figure 3.13** Calculation of monomer ratios in copolymer 12a(49)-co-14a(51), ratio(12a:14a)

$$=(I_{d+d'}-I_f)/I_f.$$

Satisfactorily, the copolymerization of **3.12a** and **3.14a** was successfully accomplished by mixing equimolar monomers in the optimal conditions, giving the polymer **12a(49)-co-14a(51)** with narrow molecular weight distribution, in which the ratio could be calculated by ¹H-NMR easily (Table 3.2, entry 1 and Figure 3.13).

Similarly, other copolymers were synthesized with **3.12a** and different functionalized monomers using Grubbs 1st generation catalyst with the previously optimized conditions. The bulky groups, like *N*-succinimidyl ester, have direct effect on the polymerization process and the molecular weight dropped significantly as the percentage of bulky monomer **3.14b** in the backbone was increased (Table 3.2, entry 2 vs 3). Similar steric effect was observed for monomer **3.14e**, and the value of PDI increased drastically from 1.8 to 2.7 when the percentage of bulky monomer increased from 31% to 69% (Table 3.2, entry 10-12). These results further proved the speculation that double bond in hindered oxadiazinone monomer, such as monomer **3.12c** and **3.12d**, is unapproachable for Grubbs catalysts. However, when the less bulky bromo substituted monomer **3.14c** was subjected to copolymerization, polymers with broad molecular weight distribution were obtained and the reason is unclear (Table 3.2, entry 4-6). The more controlled copolymerization was observed with monomer **3.14d** compared to monomers **3.14b**, **3.14c** and **3.14e** (Table 3.2, entry 7-9). Hence, the molecular weight and polydispersity of such copolymers depend heavily on the nature of substituents on the co-monomers.

In addition, to further study the copolymerization pattern of the monomer **3.12a** and norbornene-based monomers, monomer **3.12a** and monomer **3.14a** were taken as model substrates. The reactivity ratios were calculated using the Fineman-Ross copolymerization

equation and plotting (Figure 3.14).¹⁴ The slope of the straight line corresponds to r_2 (**3.14a**) = 0.52, indicating a preferred homopolymerization of **3.14a** versus cross propagation, and the Y-intercept represents r_1 having a value of 0.11, suggesting a preferred copolymerization of **3.12a** versus cross propagation. It can be concluded that the copolymerization of the two monomers tends to be non-ideal azeotropic copolymerization ($r_1 < 1, r_2 < 1$), but lies between alternating and random copolymerization, further implying the feasibility of introducing the degradability into functional polynorbornene systems.

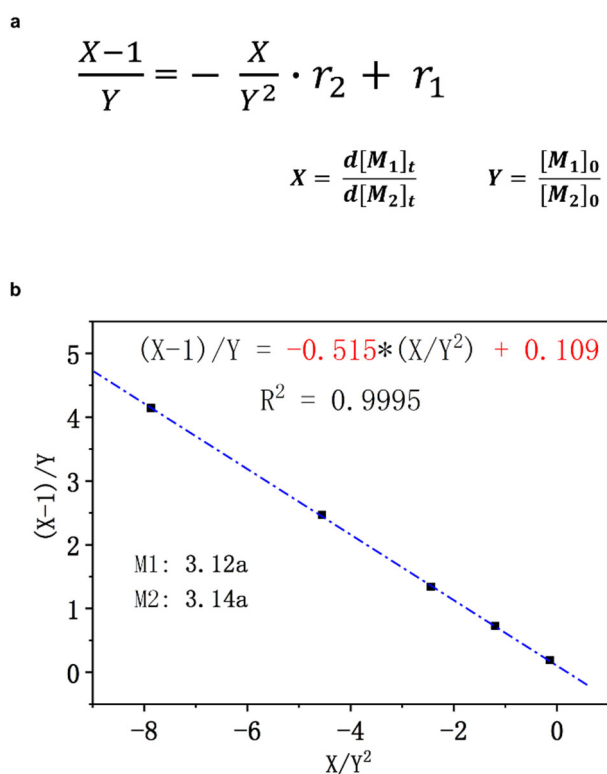


Figure 3.14 Calculation of reactivity ratios. a) Fineman-Ross copolymerization equation (X is molar ratio of monomers in copolymer, Y is molar ratio of monomers feed); b) Plot of copolymerization of monomers **3.12a** and **3.14a**.

The composition pattern of copolymer was also examined with COSY correlation by comparing individual homopolymers, copolymer and block copolymer of **3.12a** and **3.14a** (Figure 3.15 and 3.16). The strong correlation between two olefin protons at 6.09 ppm and 5.80 ppm shows a clear sign that **12a(49)-co-14a(51)** is not block copolymer. Moreover, such COSY correlation is missing in both individual polymers.

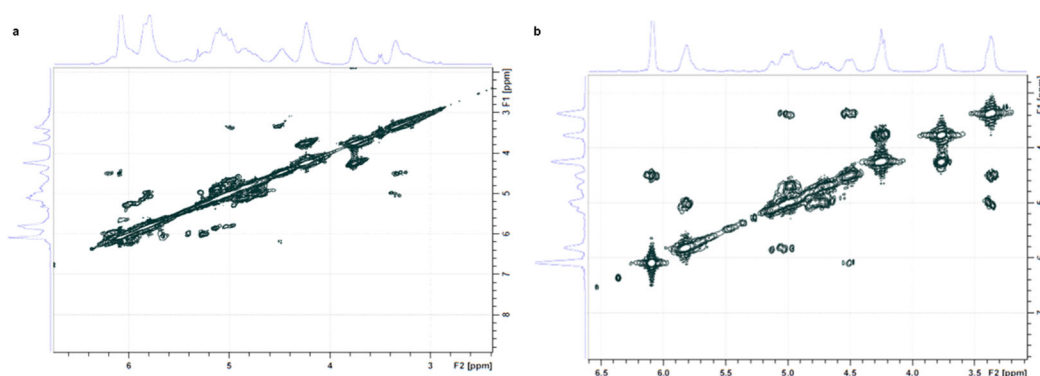


Figure 3.15 ^1H - ^1H COSY NMR of copolymers (CDCl_3). a) Copolymer **12a(49)-co-14a(51)**; b) Block copolymer **12a-block-14a**.

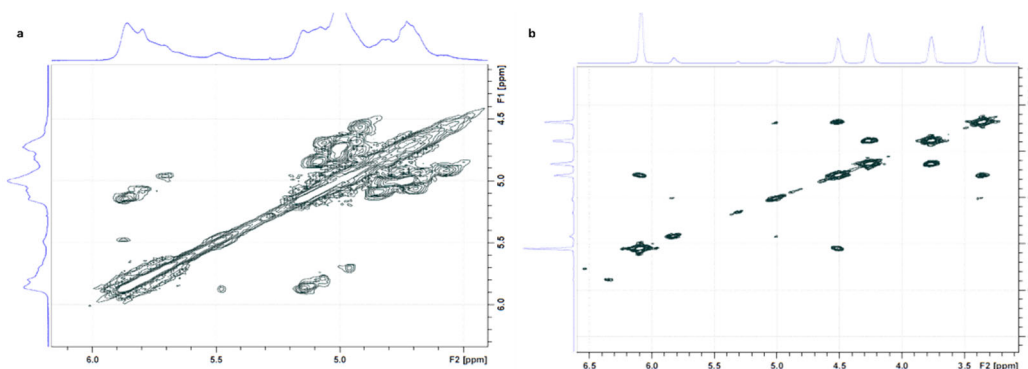


Figure 3.16 ^1H - ^1H COSY NMR of homopolymers (CDCl_3). a) polymer **3.13a**; b) polymer **3.15**.

After successful incorporation of polyoxadiazinone into the backbone of functional poly(oxa)norbornenes, the degradability of copolymers was examined. Specifically, the copolymer **12a(49)-co-14a(51)** was treated with different pH solutions and monitored with

^1H -NMR. For pH 1, 80% degradation was observed after 96 hours, on the other hand, decomposition was very fast at pH 13.5 and 87% polymer was degraded within 5 minutes (Figure 3.17).

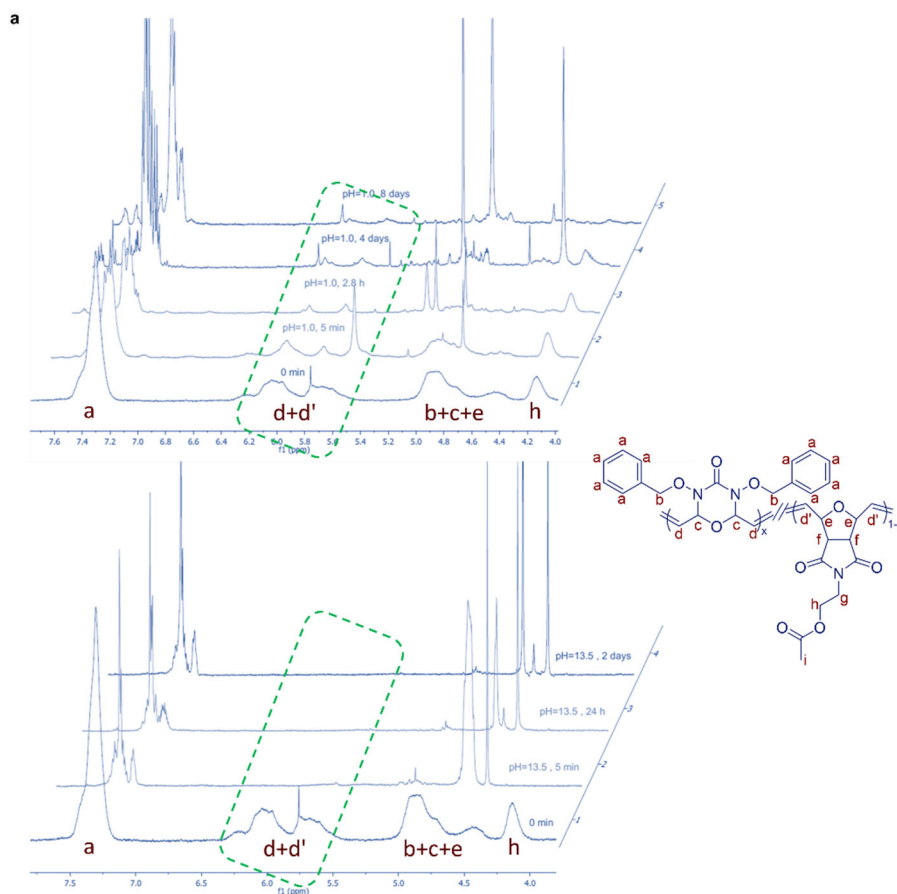
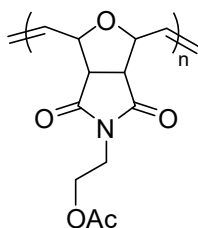


Figure 3.17 Degradation of copolymer **12a(49)-co-14a(51)**, monitored by ^1H -NMR (Acetone- d_6). a) pH = 1; b) pH = 13.5.



polymer 3.15

Figure 3.18 Structure of homopolymer from monomer **3.14a**.

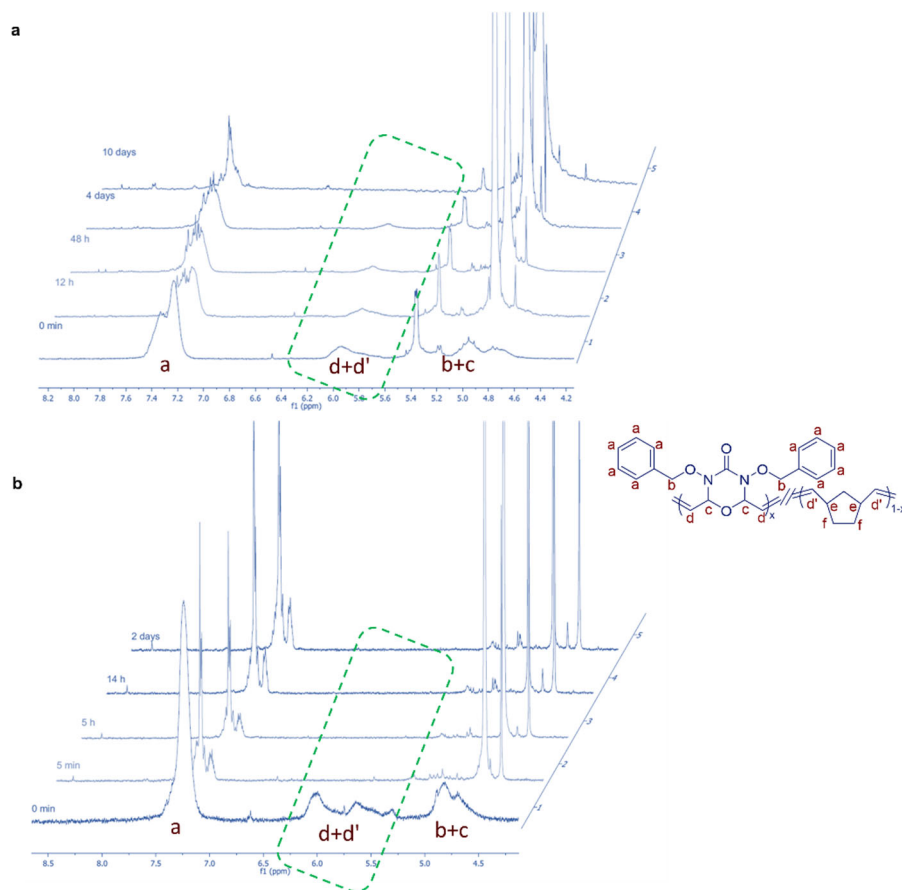


Figure 3.19 Degradation of copolymer **12a(36)-co-14f(64)**, monitored by ^1H -NMR ($\text{Acetone-}d_6$). a) pH = 1; b) pH = 13.5.

For more direct comparison, a homopolymer of **3.14a** (Figure 3.18) was also prepared and its pH sensitivity was investigated. As expected, *polymer 3.15* was quite stable at a wide range of pH and no decomposition was observed even after several days. This study directly proved the hypothesis that incorporation of polyoxadiazinone into the backbone, assists the disintegration of poly(oxa)norbornene system. Likewise, the copolymer **12a(36)-co-14f(64)** exhibited similar acid and base sensitivity whereas no decomposition was observed for the parent polynorbornene. The polymer **12a(36)-co-14f(64)** was exposed to pH 1 and pH 13.5 and complete backbone decomposition was observed after 72 and 2 hours, respectively (Figure 3.19).

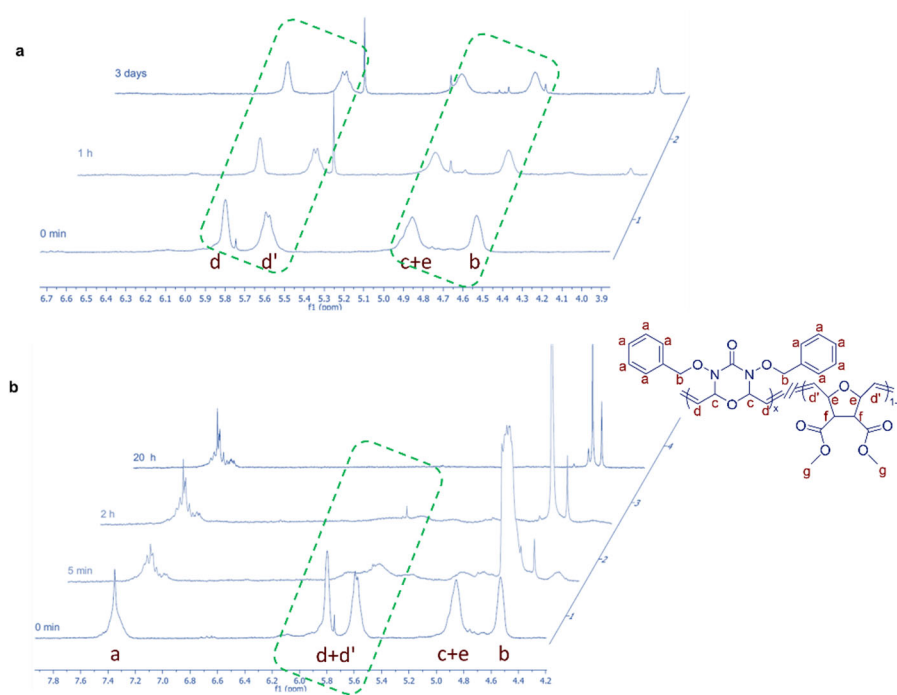


Figure 3.20 Degradation of copolymer **12a(9)-co-14g(91)**, monitored by ^1H -NMR (Acetone- d_6). a) pH = 1; b) pH = 13.5.

To estimate the minimum oxazinone content for vulnerable copolymer backbone, all the copolymers in Table 3.2 were treated with acidic and basic solutions. For the polymer **12a(27)-co-14g(73)**, only 27% incorporation of polyoxadiazinone to the poly(oxa)norbornene (Table 3.2, entry 16) is enough for the backbone to degrade at pH 1 and pH 13.5. In contrast, with only 10% or less amount of polyoxadiazinone in the poly(oxa)norbornene backbone (Table 3.2, entry 3 and 17), the polymers **12a(10)-co-14b(90)** and **12a(9)-co-14g(91)** did not show significant decomposition at pH 1 even after several days. Interestingly, both copolymers could degrade in basic condition of pH 13.5 although the rate is relatively slower, probably because of the relatively low molecular weight (Figure 3.20).

Therefore, less than 10% of polyoxadiazinone content was insufficient to make the entire backbone vulnerable although the copolymers bearing very low content of oxadiazinone was still degradable in basic condition (Figure 3.20b).

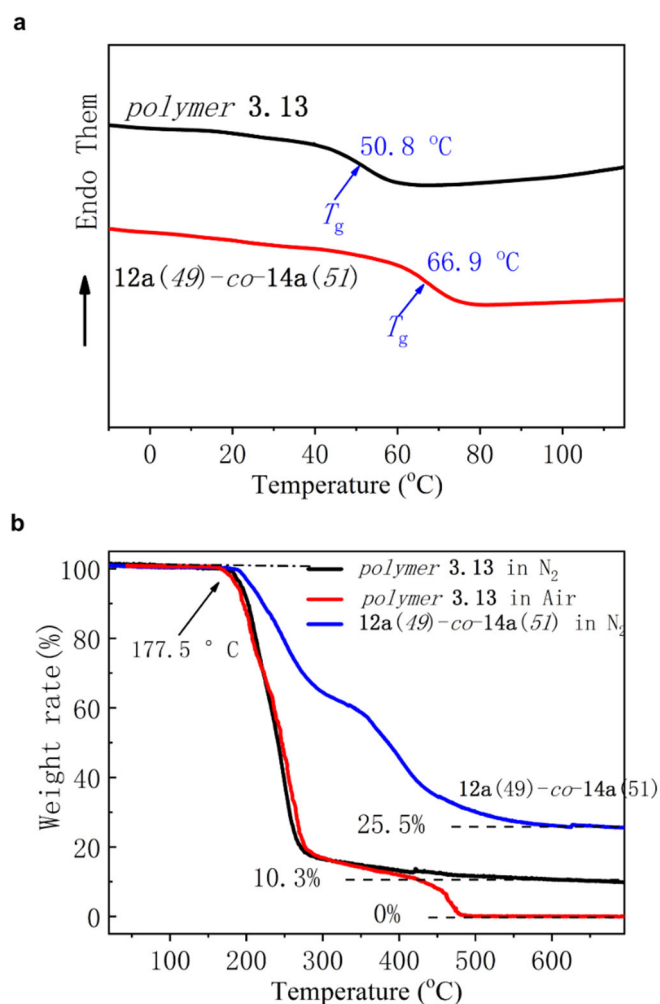
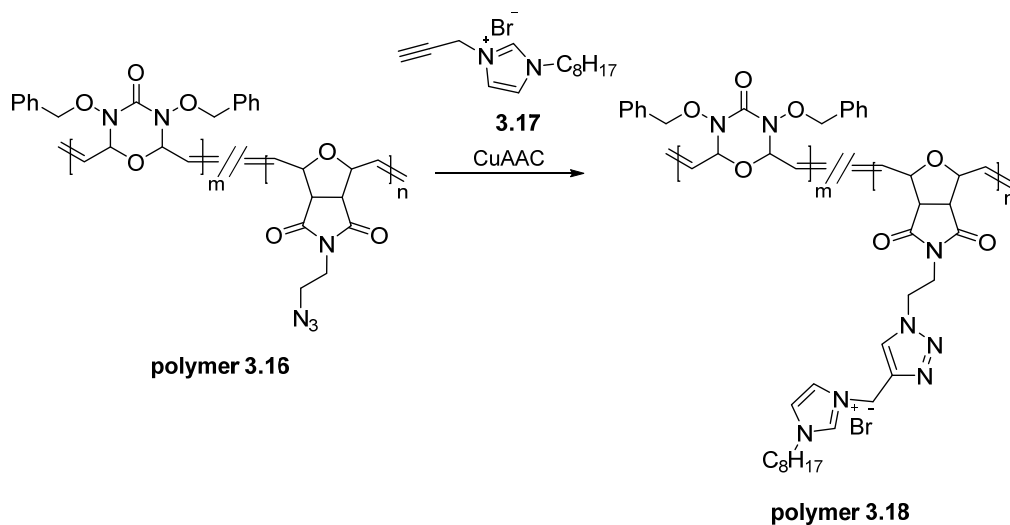


Figure 3.21 a) The second heating curve based on DSC of the *polymer 3.13a* and *12a(49)-co-14a(51)*. b) TGA results of the *polymer 3.13a* and *12a(49)-co-14a(51)*. Heating rate: 10 °C/min for both DSC and TGA.

In addition, physical properties of the polymers were also studied by DSC and TGA using *polymer 3.13a* and *12a(49)-co-14a(51)* as model compounds (Figure 3.21). Briefly, *polymer 3.13a* and *12a(49)-co-14a(51)* have glass transition temperatures of 50.8 °C and

66.9 °C, respectively. Meanwhile, both samples started thermal decomposition at 177.5 °C. The results suggested that the polymers are stable in ambient environment but fragile in acidic and basic media.

In line with our strong interest in developing antibacterial polymers, the pendant bromo groups in copolymer **12a**(47)-*co*-**14c**(53) were converted into azido groups by reacting with tetrabutylammonium azide, adding more versatility to the polymer. Subsequently, the azido groups were extended further by conjugating with positively charged small molecule **3.17** through copper mediated click reaction (Scheme 3.2). The appearance of peak at 8.36 and 8.22 ppm in the ¹H-NMR from triazole ring confirmed the successfully conjugation (Figure 3.22).



Scheme 3.2 Incorporation of cationic group into copolymer through click reaction.

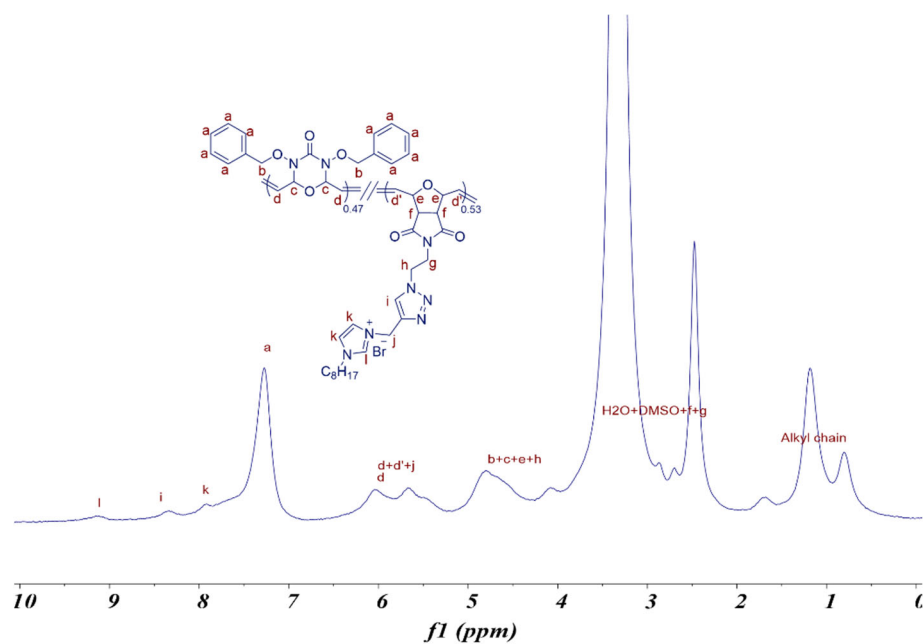


Figure 3.22 ^1H -NMR of polymer 3.18 with imidazolium salt in DMSO-d_6 .

Indeed, polyoxadiazinone can serve as a versatile content in designing new degradable polymers and the copolymers for antibacterial application is ongoing in our laboratory.

3.3 Conclusion

The oxadiazabicyclooctenone olefin was utilized as a versatile monomer for the construction of new pH-sensitive polymers by ring opening metathesis polymerization (ROMP). The resulting polymer degrades when exposed to acidic or basic media. The degradability can also be introduced into poly(oxa)norbornenes backbone by copolymerization with oxadiazinone monomer. The rate and thoroughness of degradation can be controlled by varying pH and the proportion of polyoxadiazinone in the backbone. In terms of functional copolymers, cationic small molecule was successfully conjugated, offering an opportunity for further modification. Preliminary results suggest that the scaffold is possible to be applied in developing antimicrobial polymers although some remained issues need to be addressed.

3.4 Experimental Section

3.4.1 Methods and materials

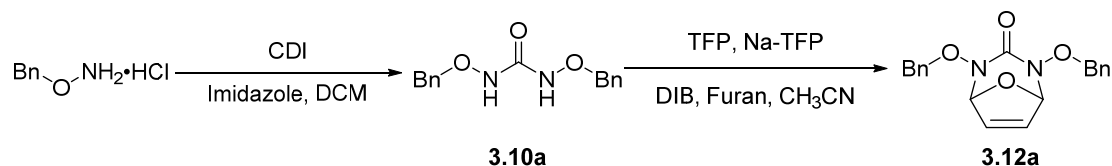
All reactions were carried out in oven-dried glassware under nitrogen or argon atmosphere unless otherwise noted. Dialysis was used for purification in some cases. Chemicals and solvents are purchased from Alfa-Aesar, Sigma-Aldrich and VWR and used without further purification unless otherwise noted. Anhydrous toluene (over sodium/benzophenone), tetrahydrofuran (THF, over sodium/benzophenone), dichloromethane (DCM, over calcium hydride) and triethylamine (Et₃N, over calcium hydride) were freshly distilled under nitrogen atmosphere before use. All the other anhydrous solvents were purchased from Sigma-Aldrich and used as received. TFP-Na salt was prepared following the reported procedure.⁹ Deuterated solvents are obtained from Cambridge Isotope Laboratories and used as received. Thin layer chromatography (TLC) with Merck TLC silica gel 60 F254 plate was used to monitor reaction. UV, potassium permanganate, ceric ammonium molybdate and iodine staining were used to visualize compounds on TLC plates. Flash column chromatography with silica gel 60 (0.010-0.063 mm) was applied for the purification of organic compounds. Regenerated cellulose dialysis tubing (MWCO 3500 Da or 12000 Da) was purchased from Fisher Scientific. Deionized water was obtained from a Merck Millipore Integral 3 water purification system.

3.4.2 Instrumentation

^1H and ^{13}C and 2D NMR spectra were recorded on Bruker Avance 300, Bruker Avance 400, Bruker AVIII 400 and JEOL JNM-ECA 400 spectrometers using deuterated solvents as reference. Mass spectra were obtained using an Agilent 6230 TOF LC/MS with an electrospray (ESI) source with purine and HP-0921 as an internal calibrates. HRMS spectra were recorded on a Waters Q-Tof premierTM mass spectrometer. IR spectra were recorded using FTIR Restige-21 (Shimadzu) either on solid KBr Platte or neat. Slow addition of reagents was performed with syringe pump (model: NE-300) from New Era Pump Systems Inc. KUBOTA centrifuge machine (model: 2420) was used to separate the solid polymers from the solution. Gel permeation chromatography (GPC) was carried out on a Shimadzu liquid chromatography system equipped with a Shimadzu refractive index detector (RID-10A) and two Agilent Polargel columns operating at 40 °C using DMF (with 1 wt % LiBr) or THF as the eluent at a flow rate of 1 mL/min using polystyrene kit as standard. Glass translation temperature (T_g) of polymers were determined by differential scanning calorimetry (DSC) using a TA Instruments DSC-Q10 operating at heating rate of 10 °C/min from 0 °C to 130 °C under nitrogen atmosphere. Thermal stability of polymers was determined by thermo gravimetric analysis (TGA) using Perkin Elmer *Diamond* TG/DTA running at heating rate of 10 °C/min from room temperature to 700 °C under nitrogen atmosphere.

3.4.3 Synthesis of monomer and polymers

Synthesis of monomer 3.12a

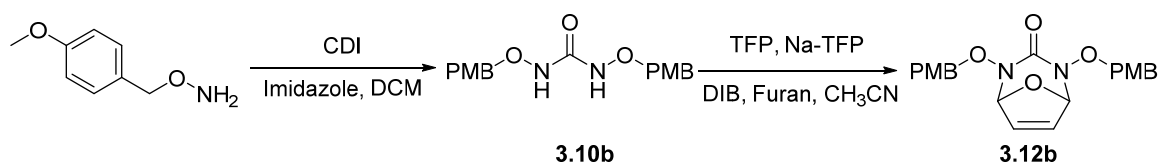


The O-benzylhydroxylamine hydrochloride (5.0 g, 31.45 mmol) was dissolved in 75 mL dry DCM and then cooled to 0 °C followed by addition of imidazole (3.20 g, 47.17 mmol) to make the corresponding free amine. The coupling reagent 1,1'-carbonyldiimidazole (CDI) (2.54 g, 15.72 mmol) was dissolved in 20 mL DCM and added to the mixture at 0 °C for 10 min, and the mixture was stirred at room temperature overnight. The reaction was quenched by adding 50 mL water and the organic layer was separated and washed with water (50 mL \times 3) and brine, dried over Na_2SO_4 , filtered and concentrated to give crude product. The crude product was recrystallized from DCM/hexane giving white solid **3.10a** (6.9 g, 80% Yield). $^1\text{H-NMR}$ (300 MHz, CDCl_3): δ 7.66 (s, 1H), 7.38-7.32 (m, 5H), 4.78 (s, 2H); $^{13}\text{C-NMR}$ (75 MHz, CDCl_3): 159.6, 135.0, 129.2, 128.8, 128.7, 78.7; IR ($\bar{\nu}_{\text{max}}$): 3236, 2924, 2866, 2360, 2345, 1662, 1489, 1307 cm^{-1} ; HRMS (ESI): m/z $[\text{M}+\text{H}]^+$ calcd for $\text{C}_{16}\text{H}_{17}\text{N}_2\text{O}_3$ 273.1241, found 273.1241.

To a 250 mL round-bottom flask (Flask-A), 40 mL of dried CH_3CN was added and cooled to 0 °C, Na-salt of 2,2,3,3-tetrafluoro-1-propanol (1.132 g, 7.350 mmol) and 1 mL of 2,2,3,3-tetrafluoro-1-propanol were added. Subsequently, (diacetoxyiodo)benzene (DIB) (2.360 g, 7.350 mmol) was added to the solution and the mixture was stirred vigorously at 0 °C. A solution of furan (1.34 mL, 18.350 mol) and compound **3.10a** (1.0 g, 3.670 mol) in 20 mL of dried CH_3CN were prepared in another flask (Flask-B) and was added to Flask-A through syringe pump over 60 min. After finishing the addition, the mixture was stirred for

another 15 min. After consumption of the starting material (compound **3.10a**), the reaction was quenched by adding 20 mL of cold water and 100 mL ethyl acetate was added. The organic layer was separated and washed twice with water, brine and dried over Na_2SO_4 , filtered and concentrated to give crude product. The crude product was purified by column chromatography giving the product **3.12a** (1.03 g, Yield: 83%). $^1\text{H-NMR}$ (500 MHz, CDCl_3): δ 7.46-7.45 (m, 2H), 7.38-7.37 (m, 8H), 6.34 (s, 2H), 5.25 (s, 2H), 5.03 (d, $J = 11.0$ Hz, 2H), 4.94 (d, $J = 11.0$ Hz, 2H); $^{13}\text{C-NMR}$ (75 MHz, CDCl_3): 160.2, 135.7, 133.6, 129.6, 128.7, 128.5, 92.5, 78.8; IR ($\bar{\nu}_{\text{max}}$): 2939, 2866, 2364, 1728, 1454, 1342, 1195, 1080 cm^{-1} ; HRMS (ESI): m/z $[\text{M}+\text{H}]^+$ calcd for $\text{C}_{19}\text{H}_{19}\text{N}_2\text{O}_4$ 339.1345, found 339.1352.

Synthesis of monomer **3.12b**

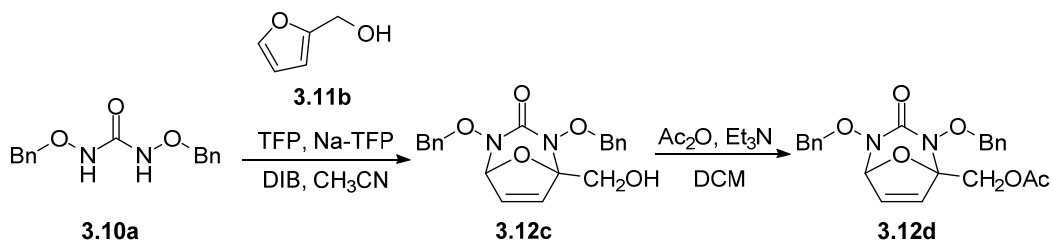


The O-(4-methoxybenzyl)hydroxylamine (3.0 g, 19.60 mmol) was dissolved in 50 mL dry DCM and cooled to 0 °C. Imidazole (1.620 g, 23.53 mol) was added to the mixture followed by addition of coupling reagent 1,1'-carbonyldiimidazole (CDI) (1.587 g, 9.80 mmol in 20 mL DCM) at 0 °C for 10 min, and the mixture was stirred at room temperature overnight. The reaction was quenched by adding 50 mL water and the organic layer was separated and washed with water (50 mL \times 3) and brine, dried over Na_2SO_4 , filtered and concentrated to give crude product. The crude product was recrystallized from DCM/hexane giving **3.10b** (2.45 g, 74% Yield). $^1\text{H-NMR}$ (300 MHz, CDCl_3): δ 7.50 (s, 1H),

7.24 (d, $J = 8.6$, 2H), 6.87 (d, $J = 8.6$, 2H), 4.71 (s, 2H), 3.81 (s, 3H); ^{13}C -NMR (75 MHz, CDCl_3): 160.1, 159.5, 130.9, 127.1, 114.0, 78.3, 55.3; IR ($\bar{\nu}_{\text{max}}$): 3228, 2924, 2835, 2360, 1670, 1512, 1473, 1033 cm^{-1} ; HRMS (ESI): m/z $[\text{M}+\text{H}]^+$ calcd for $\text{C}_{17}\text{H}_{21}\text{N}_2\text{O}_5$ 333.1450, found 333.1454.

To a 250 mL round-bottom flask (Flask-A), 40 mL of dried CH_3CN was added and cooled to 0 °C, Na-salt of 2,2,3,3-tetrafluoro-1-propanol (0.700 g, 4.64 mmol) and 0.85 mL of 2,2,3,3-tetrafluoro-1-propanol were added. Subsequently, (diacetoxyiodo)benzene (DIB) (1.840 g, 5.80 mmol) was added to the solution and the mixture was stirred vigorously at 0 °C. A solution of furan (1.00 mL, 14.450 mol) and compound **3.10b** (0.960 g, 2.90 mol) in 20 mL of dried CH_3CN were taken in another flask (Flask-B). After that, the solution from Flask-B, was added to Flask-A through syringe pump over 60 min. After finishing the addition, the mixture was stirred for another 15 min. After consumption of the starting material (compound **3.10b**), the reaction was quenched by adding 20 mL of cold water and 100 mL ethyl acetate was added. The organic layer was separated and washed twice with water, brine and dried over Na_2SO_4 , filtered and concentrated to give crude product. The crude product was purified by column chromatography giving the product **3.12b** (1.15 g, Yield: 79%). ^1H -NMR (500 MHz, CDCl_3): δ 7.37 (d, $J = 8.5$ Hz, 4H), 6.89 (d, $J = 8.5$ Hz, 4H), 6.34 (s, 2H), 5.20 (s, 2H), 4.95 (d, $J = 11.0$ Hz, 2H), 4.86 (d, $J = 11.0$ Hz, 2H), 3.81 (s, 6H); ^{13}C -NMR (75 MHz, CDCl_3): 160.0, 133.6, 131.2, 127.9, 113.9, 92.5, 78.4, 55.2; IR ($\bar{\nu}_{\text{max}}$): 2935, 2860, 2360, 1724, 1612, 1512, 1249 cm^{-1} ; HRMS (ESI): m/z $[\text{M}+\text{H}]^+$ calcd for $\text{C}_{21}\text{H}_{23}\text{N}_2\text{O}_6$ 399.1556, found 399.1553.

Synthesis of monomer **3.12c** and **3.12d**

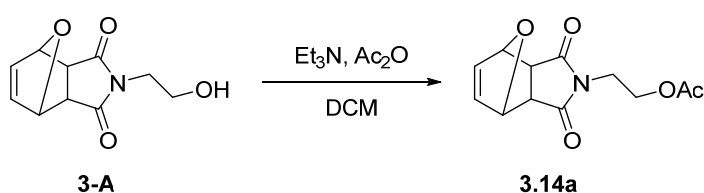


To a 250 mL round-bottom flask (Flask-A), 40 mL of dried CH_3CN was added and cooled to 0°C , Na-salt of 2,2,3,3-tetrafluoro-1-propanol (0.670 g, 4.41 mmol) and 0.81 mL of 2,2,3,3-tetrafluoro-1-propanol were added. Then (diacetoxyiodo)benzene (DIB) (1.420 g, 4.41 mmol) was added to the solution and the mixture was stirred vigorously at 0°C . A solution of Furan (0.80 mL, 11.0 mol) and the compound **3.10a** (0.600 g, 2.20 mol) in 15 mL of dried CH_3CN were prepared in another flask (Flask-B) and was added to Flask-A through syringe pump over 60 min. After finishing the addition, the mixture was stirred for another 15 min. After consumption of the starting material (compound **3.10a**), the reaction was quenched by adding 20 mL of cold water and 100 mL ethyl acetate was added. The organic layer was separated and washed twice with water, brine and dried over Na_2SO_4 , filtered and concentrated under reduced pressure to give crude product. The crude product was purified by column chromatography giving the product **3.12c** (0.598 g, Yield: 73%). $^1\text{H-NMR}$ (400 MHz, CDCl_3): δ 7.50-7.48 (m, 4H), 7.42-7.40 (m, 6H), 6.48 (d, J = 6.0 Hz, 1H), 6.43 (d, J = 5.8 Hz, 1H), 5.32 (d, J = 5.2 Hz, 1H), 5.17 (d, J = 10.0 Hz, 1H), 5.09 (d, J = 11.2 Hz, 1H), 4.97 (d, J = 10.4, 11.6 Hz, 1H), 3.96 (dd, J = 12.8, 7.6 Hz, 1H), 3.89 (dd, J = 12.8, 7.6 Hz, 1H), 1.69-1.66 (m, 1H); $^{13}\text{C-NMR}$ (75 MHz, CDCl_3): δ 161.9, 135.6, 135.0, 134.8, 134.3, 129.9, 129.6, 128.8, 128.6, 101.9, 92.4, 79.6, 78.7, 60.8; IR ($\tilde{\nu}_{\text{max}}$): 3437, 2934, 2360, 1708,

1454, 1276, 1068 cm^{-1} ; HRMS (ESI): m/z $[\text{M}+\text{H}]^+$ calcd for $\text{C}_{20}\text{H}_{21}\text{N}_2\text{O}_5$ 369.1450, found 369.1454.

Compound **3.12c** (200 mg, 0.545 mmol) was dissolved in 10 mL DCM and acetylated with Et_3N (148 μL , 1.1 mmol) and Ac_2O (62 μL , 0.6 mmol) to get the crude product. The final product **3.12d** was obtained via column chromatography (208 mg, Yield: 94 %). ^1H -NMR (300 MHz, CDCl_3): δ 7.41-7.33 (m, 4H), 7.32-7.30 (m, 6H), 6.41 (dd, $J = 5.7, 0.9$ Hz, 1H), 6.35 (d, $J = 5.7$ Hz, 1H), 5.27 (d, $J = 1.2$ Hz, 1H), 5.11 (d, $J = 9.9$ Hz, 1H), 5.00 (d, $J = 9.9$ Hz, 1H), 4.46 (d, $J = 11.1$ Hz, 1H), 4.80 (d, $J = 10.0$ Hz, 1H), 4.51 (d, $J = 12.6$ Hz, 1H), 4.30 (d, $J = 12.6$ Hz, 1H), 2.03 (s, 3H); ^{13}C -NMR (75 MHz, CDCl_3): δ 170.2, 161.6, 135.6, 134.8, 134.5, 134.4, 129.8, 129.5, 128.9, 128.8, 128.6, 128.5, 100.2, 92.3, 79.7, 78.7, 60.9, 20.6; IR ($\tilde{\nu}_{\text{max}}$): 2860, 2360, 1739, 1369, 1226, 1022 cm^{-1} ; HRMS (ESI): m/z $[\text{M}+\text{H}]^+$ calcd for $\text{C}_{22}\text{H}_{23}\text{N}_2\text{O}_6$ 411.1556, found 411.1551.

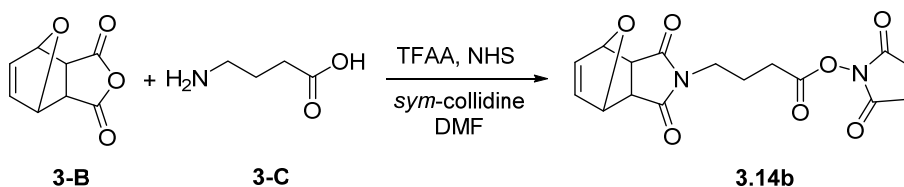
Synthesis of monomer 3.14a



The compound **3-A** was prepared by following reported procedure.¹⁵ To a solution of **3-A** (350 mg, 1.675 mmol) in 5 mL DCM was added Et_3N (0.45 mL, 3.350 mmol) and Ac_2O (0.20 mL 0.6 mmol). The reaction mixture was stirred at room temperature for 6 h and quenched by adding 20 mL water. The organic layer was separated and washed with water (50 mL \times 3) and brine, dried over Na_2SO_4 , filtered and concentrated to give crude

product. The crude product was purified by column chromatography giving the product **3.14a** (381 mg, Yield: 90%). $^1\text{H-NMR}$ (400 MHz, CDCl_3): δ 6.48 (s, 2H), 5.23 (s, 2H), 4.21-4.17 (m, 2H), 3.74-3.71 (m, 2H), 2.83 (s, 2H), 1.97 (s, 3H); $^{13}\text{C-NMR}$ (100 MHz, CDCl_3): δ 176.0, 170.8, 136.5, 80.9, 60.5, 47.4, 37.8, 20.7; IR ($\tilde{\nu}_{\text{max}}$): 3008, 2958, 1739, 1693, 1431, 1234, 1029 cm^{-1} ; HRMS (ESI): m/z $[\text{M}+\text{H}]^+$ calcd for $\text{C}_{12}\text{H}_{14}\text{NO}_5$ 252.0872, found 252.0876.

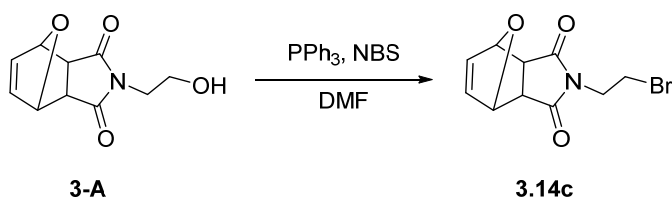
Synthesis of monomer **3.14b**



The starting material **3-B** (3.0 g, 18.0 mmol) was dissolved in 90 mL of dry DMF followed by addition of 4-aminobutanoic acid (**3-C**, 1.86 g, 18.0 mmol) at 0 °C and stirred at room temperature for 6 h. The resulting solution was cooled to 0 °C and *sym*-collidine (4.98 mL, 37.8 mmol) was added dropwise to the reaction flask (Flask A). In a separate flask (Flask B), a solution of *N*-hydroxysuccinimide (NHS, 8.280 g, 72.0 mmol) in 90 mL DMF, was stirred at 0 °C followed by addition of trifluoroacetic anhydride (TFAA, 10.1 mL, 72.0 mmol) dropwise. The reaction mixture was stirred for 10 min followed by addition of *sym*-collidine (9.5 mL, 72 mmol) dropwise. After stirred for 10 min, the solution in Flask B was added by positive-pressure cannula to Flask A over a period of 1 h. Both flasks were kept at 0 °C during the addition. After addition was complete, the reaction mixture was warmed to room temperature and stirred overnight. After completion of the reaction (monitored by TLC), the reaction mixture was diluted with DCM (300 mL) and 1 M HCl

(250 mL). The organic layer was separated and washed with 1 M HCl (2 × 250 mL) and dried over Na₂SO₄, filtered and concentrated to give crude product. The crude product was purified by column chromatography giving the product **3.14b** (4.65 g, Yield: 74%). ¹H-NMR (300 MHz, CDCl₃): δ 6.53 (s, 2H), 5.28 (s, 2H), 3.63 (t, *J*=6.9 Hz, 2H), 2.89-2.84 (m, 6H), 2.65 (t, *J*=7.6 Hz, 2H) 2.08-2.03 (m, 2H); ¹³C-NMR (75 MHz, CDCl₃): δ 176.2, 168.9, 167.8, 136.5, 80.9, 47.4, 37.6, 28.2, 25.5, 22.5; IR (ν_{max}): 3014, 2964, 1736, 1698, 1643, 1400, 1231, 1024 cm⁻¹; HRMS (ESI): *m/z* [M+H]⁺ calcd for C₁₆H₁₇N₂O₇ 349.1036, found 349.1038.

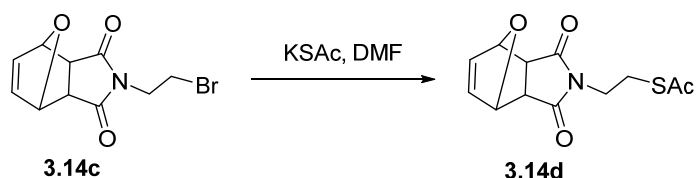
Synthesis of monomer **3.14c**



The compound **3-A** (2.80 g, 13.4 mmol) was dissolved in 15 ml of dry DMF followed by addition of triphenylphosphine (7.00 g, 26.7 mmol) and the mixture was cooled to 0 °C. NBS (3.92 g, 22.0 mmol) was added to the mixture and allowed to warm up to room temperature and stirred for 12 h. Then 50 mL ice cold water was added and extracted with 50 mL of ethyl acetate. The organic layer was combined and washed with water (25 mL × 2), dried over Na₂SO₄, filtered and concentrated to give crude product. The crude product was purified by column chromatography giving the product **3.14c** (2.07 g, Yield: 57 %). ¹H-NMR (300 MHz, CDCl₃): δ 6.54 (s, 2H); 5.31-5.30 (m, 2H); 3.92 (t, *J* = 6.9 Hz, 2H); 3.50 (t, *J* = 6.9 Hz, 2H); 2.91 (s, 2H). ¹³C-NMR (125 MHz, CDCl₃): δ 175.7, 136.3, 80.9, 47.4, 40.1, 26.9.

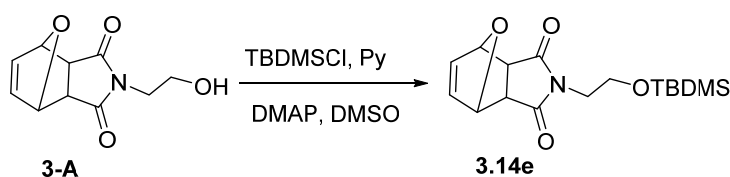
IR: 2931, 2854, 2341, 1701, 1396, 1334, 1253, 1192, 1110, 1026 cm^{-1} ; HRMS (ESI): m/z $[\text{M}+\text{H}]^+$ calcd for $\text{C}_{10}\text{H}_{10}\text{BrNNaO}_3$ 293.9742, found 293.9746.

Synthesis of monomer 3.14d



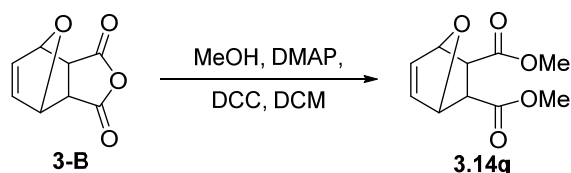
To a solution of bromo compound **3.14c** (485 mg, 1.78 mmol) in 3 mL of dry DMF, Potassium thioacetate (1.01 g, 8.87 mmol) was added and the mixture was heated at 60 °C for 3h and thereafter stirred at room temperature overnight. The mixture was diluted with 20 mL of water. The organic layer was separated and washed with water (25 mL \times 2) and brine, dried over Na_2SO_4 , filtered and concentrated to give crude product. The crude product was purified by column chromatography giving the product **3.14d** (421 mg, Yield: 88 %). ^1H -NMR (300 MHz, CDCl_3): δ 6.50 (s, 2H); 5.25 (s, 2H); 3.69 (t, J = 6.6 Hz, 2H); 3.10 (t, J = 6.6 Hz, 2H); 2.83 (s, 2H), 2.30 (s, 3H). ^{13}C -NMR (75 MHz, CDCl_3): δ 194.9, 175.9, 136.5, 80.8, 47.4, 38.0, 30.5, 26.6; IR: 2931, 1743, 1701, 1431, 1392, 1165, 1134, 1010 cm^{-1} ; HRMS (ESI): m/z $[\text{M}+\text{H}]^+$ calcd for $\text{C}_{12}\text{H}_{14}\text{NO}_7\text{S}$ 268.0644, found 268.0647.

Synthesis of monomer 3.14e



The compound **3-A** (365 mg, 1.75 mmol) was dissolved in 2 mL of dry DMSO and pyridine (0.20 mL, 2.63 mmol) was added to the solution at 0 °C. TBDMSCl (315 mg, 2.10 mmol) and DMAP (21 mg, 0.17 mmol) were added to the reaction mixture. The mixture was stirred at room temperature overnight. The mixture was diluted with 20 mL of water and 20 mL ethyl acetate was added. The organic layers were combined and washed with water (25 mL \times 2), dried over Na₂SO₄, filtered and concentrated to give crude product. The crude product was purified by column chromatography giving the product **3.14e** (334 mg, Yield: 88 %). ¹H-NMR (300 MHz, CDCl₃): δ 6.50 (s, 2H); 5.20 (s, 2H); 3.74-3.3.70 (m, 2H); 3.64-3.60 (m, 2H); 2.86 (s, 2H), 0.85 (s, 9H); 0.01 (s, 6H). ¹³C-NMR (75 MHz, CDCl₃): δ 176.1, 136.5, 80.8, 59.1, 47.4, 41.0, 25.7, 18.1, -5.54; IR: 3055, 2931, 2322, 1705, 1435, 1396, 1184, 1118, 1024 cm⁻¹; HRMS (ESI): m/z [M+H]⁺ calcd for C₁₆H₂₆NO₄Si 324.1631, found 324.1641.

Synthesis of monomer **3.14g**



The starting material **3-B** (3.0 g, 18.0 mmol) was dissolved in 150 mL of dry DCM followed by addition dry MeOH (2 mL, 50 mmol) at 0 °C, and catalytic amount of DMAP (220 mg, 1.80 mmol) was added. The mixture was stirred at room temperature for 6 h, thereafter, the mixture was cooled to 0 °C and DCC (3.8 g, 18.5 mmol) was added portion wise and the mixture was warmed up to room temperature and stirred overnight and quenched by adding 100 mL water. The organic layer was separated and washed with

water (50 mL \times 3) and brine, dried over Na₂SO₄, filtered and concentrated to give crude product. The crude product was purified by column chromatography giving the product **3.14g** (2.65 g, Yield: 69%). ¹H-NMR (300 MHz, CDCl₃): δ 6.45 (s, 2H), 5.26 (s, 2H), 3.70 (s, 6H), 2.891 (s, 2H); ¹³C-NMR (75 MHz, CDCl₃): δ 171.9, 136.6, 80.4, 52.2, 46.9; IR ($\tilde{\nu}_{\max}$): 2944, 1746, 1430, 1367, 1360, 1249, 1151, 1004 cm⁻¹; HRMS (ESI): m/z [M+H]⁺ calcd for C₁₀H₁₃O₅ 213.073, found 213.079.

3.4.4 Synthesis of polymers

General procedure for homopolymerization

The monomer (0.15 mmol) was dissolved in degassed THF and stirred at room temperature for 5 min. Also, corresponding amount of Grubbs catalyst was dissolved in calculated amount of solvent and added to the reaction mixture under inert condition. The mixture was stirred for 2 h at room temperature. The reaction was quenched with ethyl vinyl ether (100 μ L) and the solution was stirred overnight at room temperature. The resulted polymer was precipitated out by adding Et₂O/hexane or MeOH (30 mL) and isolated via centrifugation, purified by dissolving-precipitation cycles and dried under vacuum for 6 h to remove all the solvent.

Procedure for determining reaction kinetics

The progress of the reaction was monitored by ¹H-NMR spectroscopy by performing the polymerization in NMR tube under inert condition. The monomer **3.12a** (20 mg) was dissolved in 0.5 mL CDCl₃ and degassed by freeze-thaw technique. At this point, ¹H-NMR

was recorded and the monomer peak at 6.36 ppm for olefinic proton will serve as standard at time = t_0 . Thereafter, 1 mg of Grubbs 1st generation catalyst was dissolved in another vial in 100 μ L DCM- d_2 (degassed) and added to the NMR tube. The ^1H -NMR was recorded by different time intervals. The increase of peak area at 5.80 ppm is corresponding to newly formed polymer. Finally, the plot of $\ln[A_0/A_t]$ against time was fitted to give a straight line which suggested that the polymerization reaction follows the pseudo first-order reaction kinetics.

General procedure for copolymerization

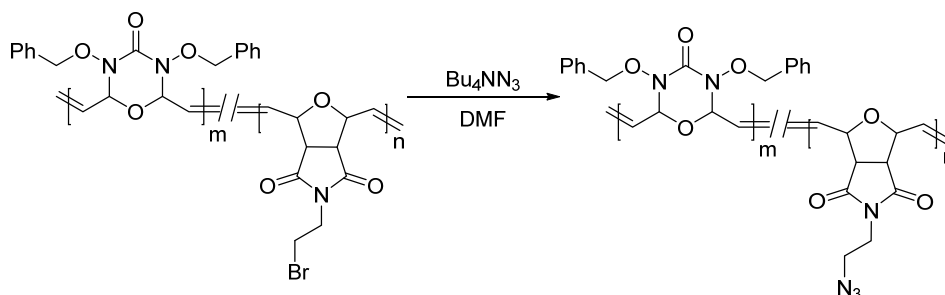
Both monomers with appropriate molar ratio were taken in a vial and dissolved completely in the respective solvent. Thereafter, Grubbs catalyst was dissolved in calculated amount of solvent and added to the reaction mixture. The mixture was stirred at room temperature for 6 h. The reaction was quenched with ethyl vinyl ether (100 μ L) and the solution was stirred overnight at room temperature. The reaction mixture was triturated using Et₂O or MeOH (30 mL) and the resulting solid was isolated via centrifugation purified by dissolving-precipitation cycles and dried under vacuum for 6 h to remove trace solvent. The observed ratio of the respective monomer in the polymer was calculated from the ^1H -NMR spectra.

Synthesis of block copolymer 12a-block-14a

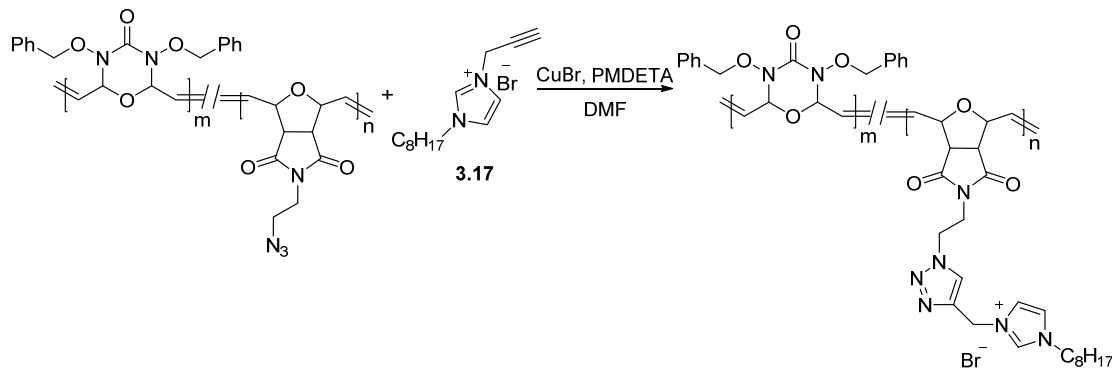
The monomer **3.14a** (37.2 mg, 0.148 mmol) was dissolved in 250 μ L degassed THF and Grubbs 1st generation catalyst (4.8 mg, 0.006 mmol, in 50 μ L of THF) was added to the mixture. The mixture stirred at room temperature for 6 h, after consumption of the

monomer **3.14a**, monomer **3.12a** (50 mg, 0.148 mmol) was added to the mixture in inert atmosphere. The reaction mixture was stirred for another 6 h. The final polymer was obtained followed the general procedure for copolymerization.

3.4.5 Post-modification of copolymers



The bromo polymer **12a**(47)-*co*-**14d**(53) (65 mg) was dissolved in 2 mL DMF followed by addition tetrabutylammonium azide (250 mg) at room temperature. The mixture was stirred at room temperature for 36 h. After that, the polymer was precipitated out by adding excess MeOH purified by dissolving-precipitation cycles and dried under reduced pressure. $^1\text{H-NMR}$ (300 MHz, CD_2Cl_2): δ 7.25-7.24 (m), 6.00-5.74 (m), 5.13-4.26 (m), 3.60 (brs), 3.43 (brs), 3.31 (brs); IR: 2947, 2881, 2110, 1708, 1396, 1330, 1226, 1176, 1037 cm^{-1} . The strong absorption at 2110 cm^{-1} in IR spectra confirmed formation of the product.



The azido polymer (14 mg) and corresponding imidazolium salt **3.17** were dissolved in 1 mL DMF in vial followed by addition of CuBr (9 mg) and PMDETA (10 μ L) at room temperature. The mixture was degassed by freeze-thaw technique and stirred at room temperature overnight under N₂ atmosphere. After that, the polymer was precipitated out by adding excess MeOH and the unreacted reagents and CuBr were removed by dialysis against DI water and lyophilized to afford final polymer as pale-brown solid. ¹H-NMR (500 MHz, DMSO-d₆): δ 9.13 (brs), 8.33-7.91 (m), 7.26 (brs), 6.05-5.68 (m), 4.74-4.10 (m), 2.87-2.67 (m), 1.69-0.84 (m); IR: 2934, 2855, 2098, 1708, 1654, 1438, 1373, 1210, 1182, 1037 cm⁻¹.

3.4.6 Degradation behavior of polymers

Degradation studies in acidic media

A stock solution of HCl in methanol-d₄ (3.20 M) was prepared and diluted with suitable deuterated (acetone-d₆, THF-d₈ or DMSO-d₆, depending on the solubility of the polymers) solvents to obtain different pH solutions (pH 1.0, pH 2.0, pH 3.0, pH 4.0). 5 mg of the respective polymer was dissolved in 1 mL of the different pH solution and monitored by ¹H-NMR spectroscopy and GPC.

Degradation studies in basic media

Preparation of NaOMe-d₃: 200 mg of sodium metal was added to 5 mL of MeOH-d₄ at 0 °C under nitrogen atmosphere and allowed to stir at room temperature for 2 h. After consumption of all the sodium, the excess solvent was evaporated at 50 °C under reduced

pressure. The round bottom flask containing NaOMe-d₃ product was flushed with nitrogen before removing the flask from rotary evaporator. The NaOMe-d₃ product was stored under nitrogen in the refrigerator until further use.

The different basic solutions were prepared by dissolving NaOMe-d₃ in suitable deuterated solvents depending on the solubility of the polymers. 25 mg of the NaOMe-d₃ was dissolved in MeOH-d₄ to get a stock solution of 0.4 M of NaOMe-d₃, and the stock solution was diluted with DMSO-d₆ to get different pH solutions (pH 10.5, pH 11.5, pH 12.5, pH 13.5). 5 mg of the respective polymer was dissolved in 1 mL of respective pH solution and monitored by ¹H-NMR spectroscopy and GPC.

3.5 References

- [1] A. Mallick, Y. Xu, Y. Lin, J. He, M. B. Chan-Park, X.-W. Liu, *Polym. Chem.* **2018**, *9*, 372.
- [2] a) M. M. Caruso, D. A. Davis, Q. Shen, S. A. Odom, N. R. Sottos, S. R. White, J. S. Moore, *Chem. Rev.* **2009**, *109*, 5755; b) A. S. Jones, J. D. Rule, J. S. Moore, N. R. Sottos, S. R. White, *J. R. Soc. Interface* **2007**, *4*, 395; c) C. W. Bielawski, R. H. Grubbs, *Prog. Polym. Sci.* **2007**, *32*, 1; d) E. M. Kolonko, J. K. Pontrello, S. L. Mangold, L. L. Kiessling, *J. Am. Chem. Soc.* **2009**, *131*, 7327.
- [3] a) L. L. Kiessling, J. C. Grim, *Chem. Soc. Rev.* **2013**, *42*, 4476; b) L. L. Kiessling, J. E. Gestwicki, L. E. Strong, *Angew. Chem. Int. Ed.* **2006**, *45*, 2348; c) K. H. Mortell, R. V. Weatherman, L. L. Kiessling, *J. Am. Chem. Soc.* **1996**, *118*, 2297; d) A. H. Courtney, E. B. Puffer, J. K. Pontrello, Z.-Q. Yang, L. L. Kiessling, *Proc. Natl. Acad. Sci.* **2009**, *106*, 2500.
- [4] a) K. Lienkamp, G. N. Tew, *Chem. Eur. J.* **2009**, *15*, 11784; b) F. Sgolastra, B. M. deRonde, J. M. Sarapas, A. Som, G. N. Tew, *Acc. Chem. Res.* **2013**, *46*, 2977; c) A. Som, A. Reuter, G. N. Tew, *Angew. Chem. Int. Ed.* **2012**, *51*, 980; d) A. Ö. Tezgel, G. Gonzalez-Perez, J. C. Telfer, B. A. Osborne, L. M. Minter, G. N. Tew, *Mol. Ther.* **2013**, *21*, 201.
- [5] a) C.-C. Chang, T. Emrick, *Macromolecules* **2014**, *47*, 1344; b) S. Hilf, A. F. M. Kilbinger, *Macromolecules* **2009**, *42*, 4127; c) S. Hilf, E. Berger-Nicoletti, R. H. Grubbs, A. F. M. Kilbinger, *Angew. Chem. Int. Ed.* **2006**, *45*, 8045.
- [6] I. Czelusniak, E. Khosravi, A. M. Kenwright, C. W. G. Ansell, *Macromolecules* **2007**, *40*, 1444.
- [7] a) M. Xie, J. Dang, H. Han, W. Wang, J. Liu, X. He, Y. Zhang, *Macromolecules* **2008**, *41*, 9004; b) J. Wang, H. Lu, Y. Ren, Y. Zhang, M. Morton, J. Cheng, Y. Lin, *Macromolecules* **2011**, *44*, 8699.

- [8] a) H. Ying, J. Cheng, *J. Am. Chem. Soc.* **2014**, 136, 16974; b) H. Ying, Y. Zhang, J. Cheng, *Nat. Commun.* **2014**, 5, 3218.
- [9] D. Anumandla, R. Littlefield, C. S. Jeffrey, *Org. Lett.* **2014**, 16, 5112.
- [10] a) D. J. Walsh, S. H. Lau, M. G. Hyatt, D. Guironnet, *J. Am. Chem. Soc.* **2017**, 139, 13644; b) J. A. Love, J. P. Morgan, T. M. Trnka, R. H. Grubbs, *Angew. Chem. Int. Ed.* **2002**, 41, 4035.
- [11] a) B. R. Maughon, R. H. Grubbs, *Macromolecules* **1997**, 30, 3459; b) W. D. Mulhearn, R. A. Register, *ACS Macro Lett.* **2017**, 6, 112.
- [12] M. Liu, J. van Hensbergen, R. P. Burford, A. B. Lowe, *Polym. Chem.* **2012**, 3, 1647.
- [13] a) L. Pichavant, H. Carrié, M. N. Nguyen, L. Plawinski, M.-C. Durrieu, V. Héroguez, *Biomacromolecules* **2016**, 17, 1339; b) Y. Zha, M. L. Disabb-Miller, Z. D. Johnson, M. A. Hickner, G. N. Tew, *J. Am. Chem. Soc.* **2012**, 134, 4493; c) B. M. deRonde, J. A. Torres, L. M. Minter, G. N. Tew, *Biomacromolecules* **2015**, 16, 3172; d) P. W. Lee, S. A. Isarov, J. D. Wallat, S. K. Molugu, S. Shukla, J. E. P. Sun, J. Zhang, Y. Zheng, M. Lucius Dougherty, D. Konkolewicz, P. L. Stewart, N. F. Steinmetz, M. J. A. Hore, J. K. Pokorski, *J. Am. Chem. Soc.* **2017**, 139, 3312.
- [14] M. Fineman, S. D. Ross, *J. Polym. Sci.* **1950**, 5, 259.
- [15] R. Klein, F. Übel, H. Frey, *Macromol. Rapid Commun.* **2015**, 36, 1822.

Chapter 4

Design and Synthesis of Peptidoglycan-Based Antibody-Recruiting Molecules

4.1 Introduction

Although the development of antimicrobial polymers mimicking antimicrobial peptides has circumvented some issues caused by bacterial resistance. The polydispersity of polymers as well as their biocompatibility are becoming the bottleneck to be approved for marketing. On the other hand, various antimicrobial peptides found in immune system eradicate pathogens through initiating immune responses.¹ Moreover, immunotherapy has been extensively applied in practical cancer treatment, implying their great potential in combatting pathogens.² In addition, biomolecules without biocidal groups will fundamentally avoid exerting pressure on bacteria, slowing down the rapid development of drug resistance. In fact, microorganisms including pathogens are ubiquitous in life systems, and human immune system is maintaining a balance until breaking by pathogens escaped from detection, causing severe infectious diseases.^{2e,3} Therefore, developing new agents to regulate the immune system for combatting pathogens will be a beneficial complement to traditional therapeutic strategies.

Despite the difference in cellular structures and physiochemical environments, immunotherapeutic strategies in curing cancers are possible to be translated to fight bacterial pathogens as vaccination does. The great achievement of vaccination therapy has demonstrated the feasibility of immunoregulation in practical applications. Indeed, monoclonal antibodies (mAbs) have been dominating the immunotherapeutic market since Milstein et al. developed an efficient process in production.⁴ Besides, various conjugates of mAbs with drugs have been developed and applied widely as therapeutics.⁵

However, similar as antimicrobial peptides, antibody-based agents are also costly to produce and unstable to store, limiting their broader applications.⁶

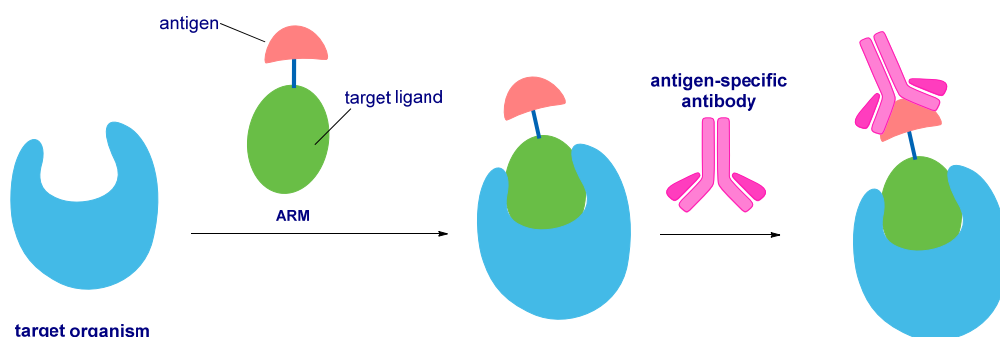


Figure 4.1 Bifunctional molecules with antigen and target ligand termini.

Interestingly, it is the bispecific antibodies that inspired the design of synthetic bifunctional compounds, ushering a new field.^{5a,7} Such bifunctional molecules are consisting of two termini, one is for targeting receptors on cancer or microbial cells while the other could bind with antibodies (Figure 4.1).^{7b,7c} Specifically, bifunctional molecules consisting of partial IgG and CD4 was demonstrated to bind gp120 of HIV and promote immune response on HIV-infected cells.

Moreover, this strategy attracted considerable attentions although the molecule reported was an antibody derivative. For instance, Wang et al. reported a bifunctional compound bearing fused peptide and trisaccharide (α -Gal), and great binding affinity of the molecule with anti-Gal antibodies was observed, showing anti-HIV activity (Figure 4.2a).⁸ Besides, Spiegel and coworkers designed a non-peptidic compound for anti-HIV application, and they gave such compounds a simplified name, ARMs (antibody-

recruiting molecules), demonstrating the great potential of DNP (dinitrophenyl) group in antibody recruitment (Figure 4.2b).⁹

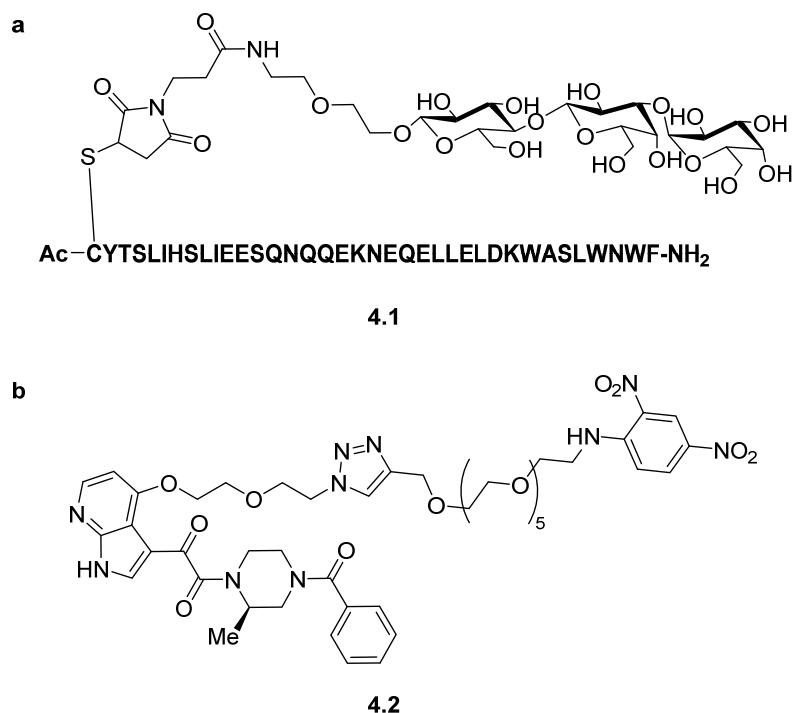


Figure 4.2 Antibody-recruiting molecules (ARMs) for anti-HIV application. a) Peptidic; b) Non-peptidic.

Aside from the anti-HIV application, ARMs have been widely employed in cancer immunotherapy. For example, the Spiegel group also utilized ARMs bearing DNP moiety to bind prostate cancer cell and successfully activated immune system to destruct the cells (Figure 4.3a).¹⁰

Moreover, as a frequently used imaging molecule, fluorescein was also applied to build ARMs, which displayed great efficiency in stimulating immune responses, and provide visualization of the tumor site simultaneously (Figure 4.3b).¹¹ It is noteworthy that

antibodies recruited in this system are not from human serum although it can be generated by immunization in vivo and obtained from exogenous source smoothly.¹²

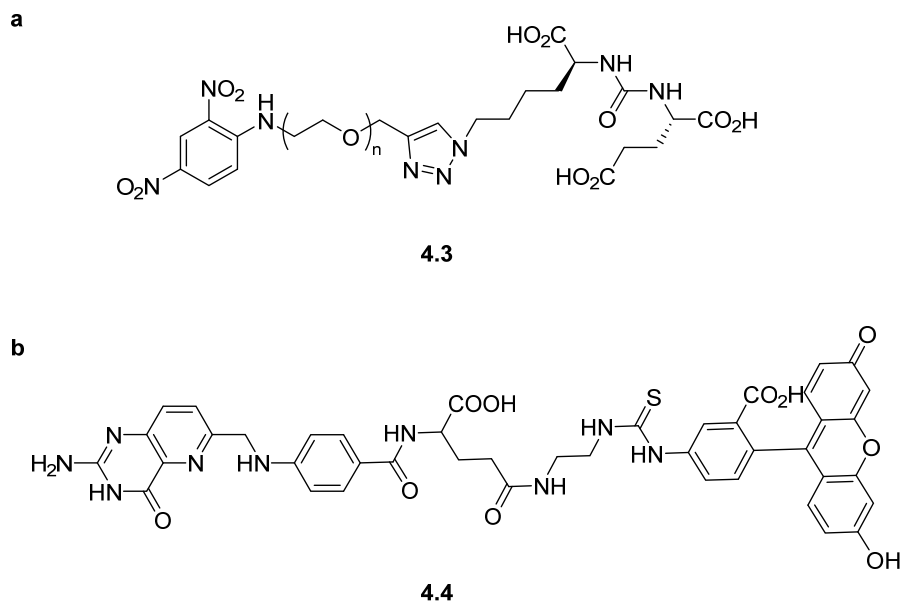


Figure 4.3 ARMs for cancer immunotherapy. a) Peptidic; b) Non-peptidic.

Furthermore, Whitesides and coworkers incorporated the dye molecule into a bifunctional polymer, which could successfully opsonize the surface of Gram-positive bacteria, leading to final clearance by macrophages (Figure 4.4a).¹³ In the system, the authors employed vancomycin as the ligand to bind bacterial cells which is a well-known antibiotic inhibiting the synthesis of cell wall. Likewise, a combination of mannose and α -Gal in polyacrylamide was prepared as examined towards Gram-negative *E. coli* and humoral antibodies. It is noteworthy that the authors also prepared a small molecule bearing the two subunits, the results revealed the advantage of multivalent interactions in binding which was exerted by polymers (Figure 4.4b).¹⁴ Such multivalency from polymers have been extensively studied by Kiessling and coworkers in glycopolymers-based ARMs,

which is particularly important in promoting the interactions between weak pairs of antigen and immune effector.¹⁵

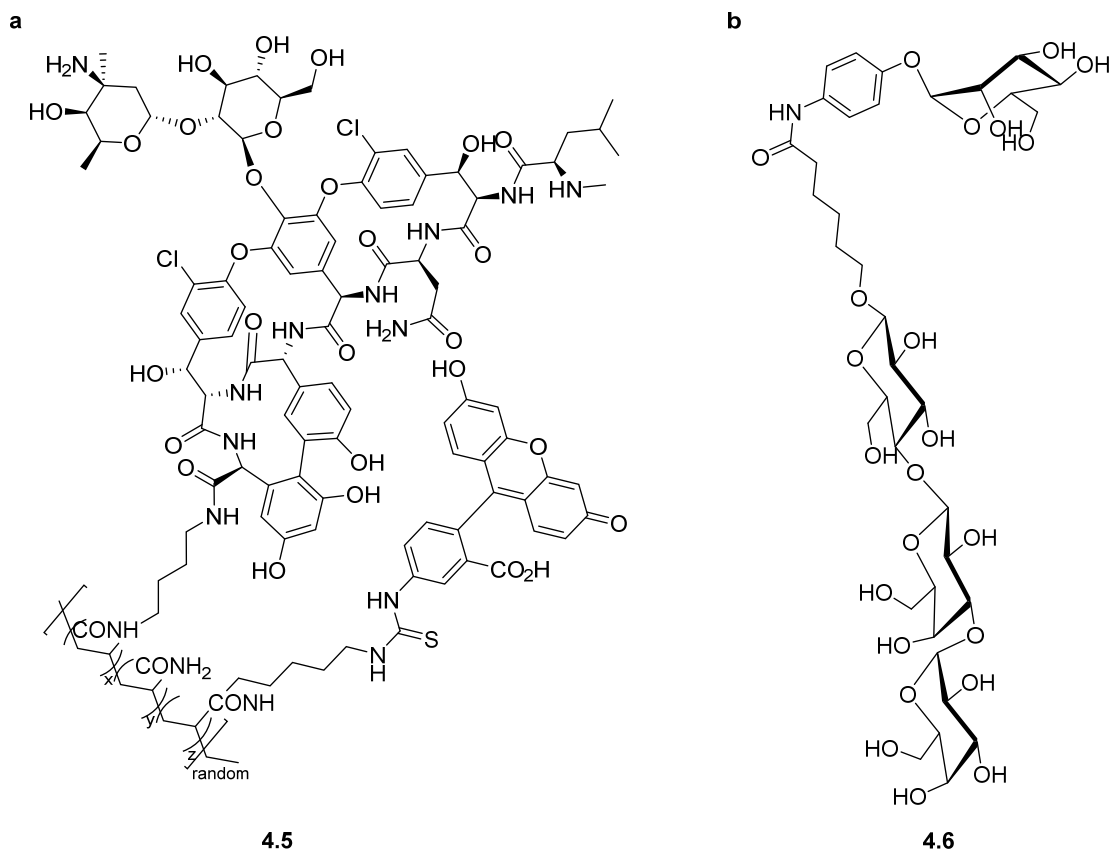


Figure 4.4 Bifunctional molecules for bacterial targeting and clearance. a) Polymer; b) Small molecule.

With regard to antibodies, both exogenous and endogenous sources exhibited good potency towards cancer cells or bacterial cells. However, the absence of exogenous antibodies in human body would require additionally induced immunization with those foreign molecules, putting the hosts on risk. Alternatively, extra feeding of exogenous antibodies will be a choice, still, it is risky to digest foreign molecules rather than make the

utmost of pre-existed antibody pool. Therefore, it is ideal to develop ARMs with haptens that would hire the antibodies in human bloodstream.

Although polymeric scaffold employed could significantly enhance the binding efficiency with the multivalent interactions, the non-covalent binding or less efficient receptor-based recognition will significantly increase the risk of off-target. To this end, inspired by the bacterial surface tagging strategy, the Pires group developed a new approach to remodel bacterial surfaces by ARMs.¹⁶ Interestingly, the authors successfully labelled Gram-positive bacteria through metabolic incorporation of DNP-modified D-amino acids and dipeptides (Figure 4.5).¹⁷

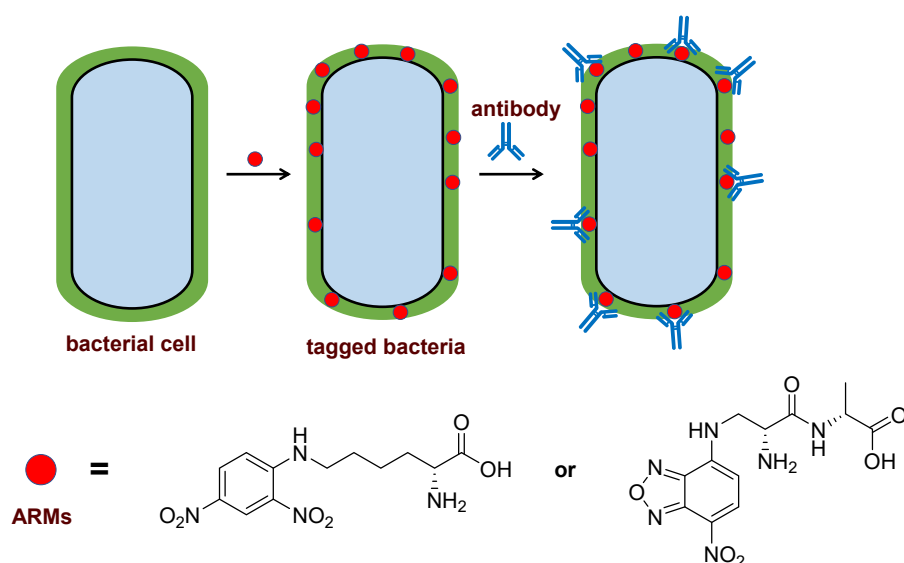


Figure 4.5 ARMs tagging bacterial surface through metabolic incorporation.

Compared to previous recognition process, this approach hijacked the essential biosynthetic process of bacteria, significantly reduced the risk of off-target. Moreover, the decorated bacteria showed drastically reduced cell viability when incubated with anti-DNP antibodies. These results revealed that targeting the critical bioprocess in the

bacterial growth and division is a very promising direction to design new ARMs for combatting bacterial infections. Besides, they also developed ARMs based on vancomycin through metabolic labelling.¹⁸

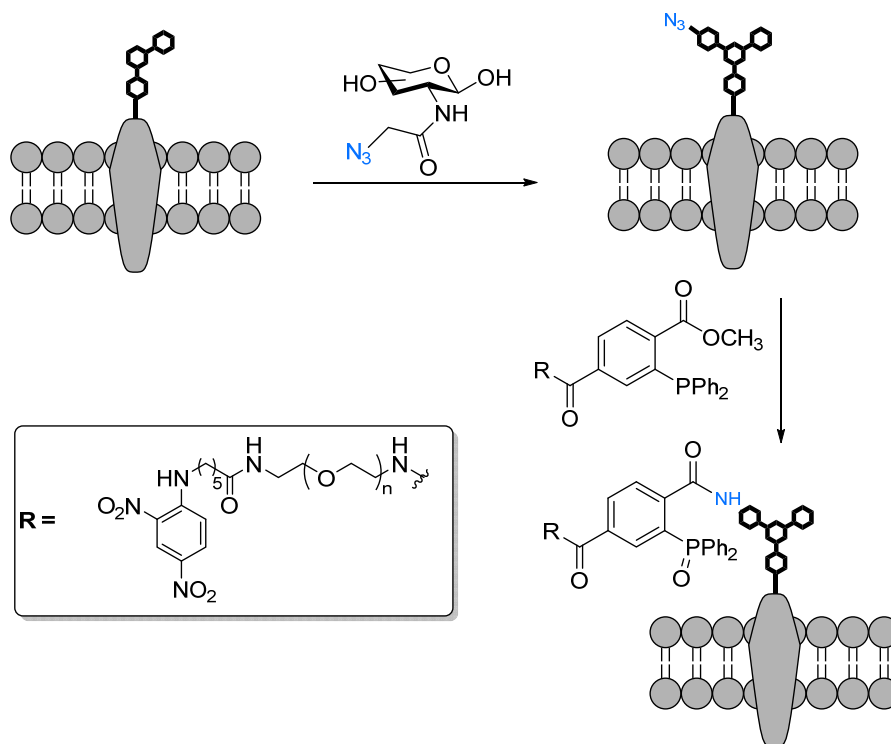


Figure 4.6 ARMs inserted into glycan of Gram-negative strain.

Although the ARMs designed through metabolic incorporation exhibits great advantages over previous approaches, they are only effective towards Gram-positive strains. Bacterial surface labelling by incorporation of unnatural sugars into bacterial glycan has been extensively explored by the Bertozzi group, which inspired the development of ARMs for decorating Gram-negative strains.¹⁹ Dube and coworkers successfully inserted azido-sugars into glycans of Gram-negative bacteria, which was further converted into ARMs by Staudinger reaction with phosphine bearing DNP motif

(Figure 4.6).²⁰ However, this approach requires two-step procedure especially the ligation *in vivo*, which requires all the reagents essentially as demonstrated by the authors.

Given that targeting cell wall by metabolic process has significant advantage over other extant methods in designing ARMs, the challenge is the structural difference between two types of strains. Regardless of the side groups of peptide chain, both Gram-positive and Gram-negative strains share the basic chemical structure in cell wall, namely peptidoglycan.²¹ More specifically, the cell wall is predominantly composed of meshwork of cross-linked peptidoglycans which are β -(1,4)-linked oligomeric glucosamine derivatives with third positions substituted partially.²²

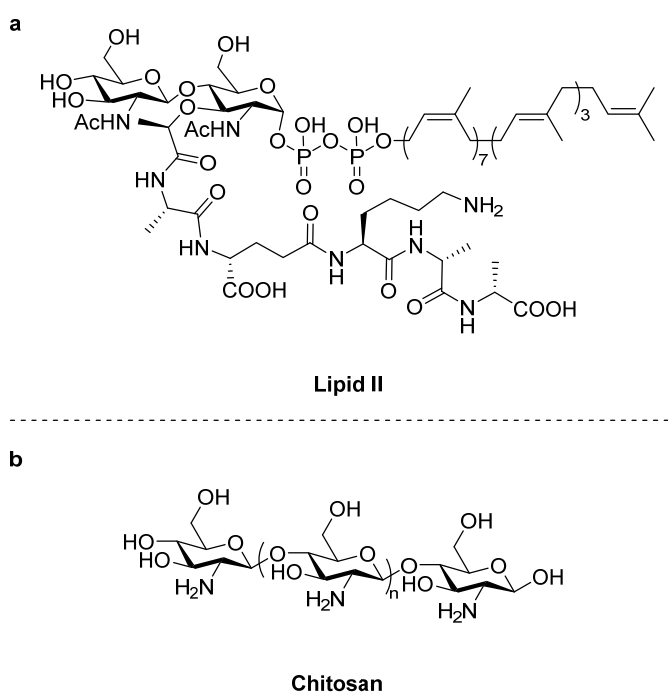


Figure 4.7 Structures of a) lipid II and b) chitosan.

In fact, numerous antibiotics currently used in clinics inhibit bacterial growth or kill by interrupting the cell wall synthesis, for example, vancomycin.²³ In particular, lipid II,

which is a disaccharide unit bearing peptide and phospholipid, plays a vital role in the biosynthetic process of peptidoglycan (Figure 4.7).^{23a,24}

Thus, remarkable efforts have been paid on synthesis of lipid II, lipid IV and their analogs by many excellent scientists.²⁵ However, the highly complicated and tedious chemical synthetic pathway or costly reagents have significantly hindered the development of new therapeutics requiring upscale amounts. As an abundant natural product, chitosan is a linear polymeric glucosamine with β -(1,4)-linkage, and can be readily obtained from deacetylation of chitin which is primary component of shrimp shells.²⁶ Moreover, longer lipid IV analogues have been demonstrated to promote the elongation of peptidoglycan, even in the absence of lipid II although lipid II was considered to be an essential substrate for the peptidoglycan growth.^{25d,25f,27}

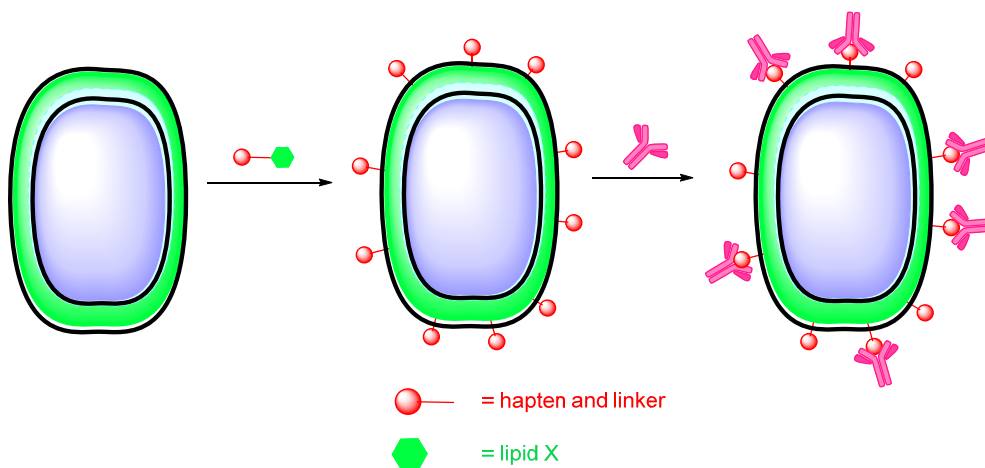


Figure 4.8 Proposed ARMs targeting both Gram-positive and Gram-negative cell wall (No outer membrane in Gram-positive bacteria).

Based on this valuable information, we envisioned that lipid II analogues, lipid X with more sugar units, could be easily produced in large scale from chitosan and benefit our

ARMs design. Besides, inspired by the results that D-Lac-L-Ala is the shortest sequence necessary for transglycosylases to construct peptidoglycans,²⁸ we propose to synthesize ARMs targeting both Gram-positive and Gram-negative cell walls, providing ARMs with broad spectrum activity although it is predictably challenging for Gram-negative strains (Figure 4.8).

4.2 Results and Discussion

Briefly, we have developed an efficient and convenient approach to synthesize a lipid II analogue, peptidoglycan oligomer (PGO), starting from a renewable material, chitosan. Also, metabolic labelling of various bacterial cells with the PGO has been conducted, showing successful incorporation into the cell walls of both Gram-positive and Gram-negative bacteria strains. Specifically, by synthetically conjugating fluorescent rhodamine dye with our PGO, the incorporation of PGO-rhodamine into the cell walls of multiple wild-type bacteria could be visualized by fluorescent microscopy. Encouraged by these exciting results, several haptens have been prepared and conjugated with the PGO to construct antibody-recruiting molecules.

4.2.1 Synthesis of peptidoglycan oligomer (PGO).

Obviously, lipid II is consisting of several fragments, including disaccharide, pyrophosphate with long lipid tail and pentapeptide (Figure 4.9). Based on this, lipid II analogue can be synthesized by a convergent strategy which was also applied in previous reports although chitosan would be the saccharide scaffold in our proposed molecule.^{25a,25f,29} Furthermore, the fragments can be further divided into substructures which are readily to be synthesized separately.

For the synthesis of PGO, technical disclosure has been filed from our group, and the synthetic details will be released later.

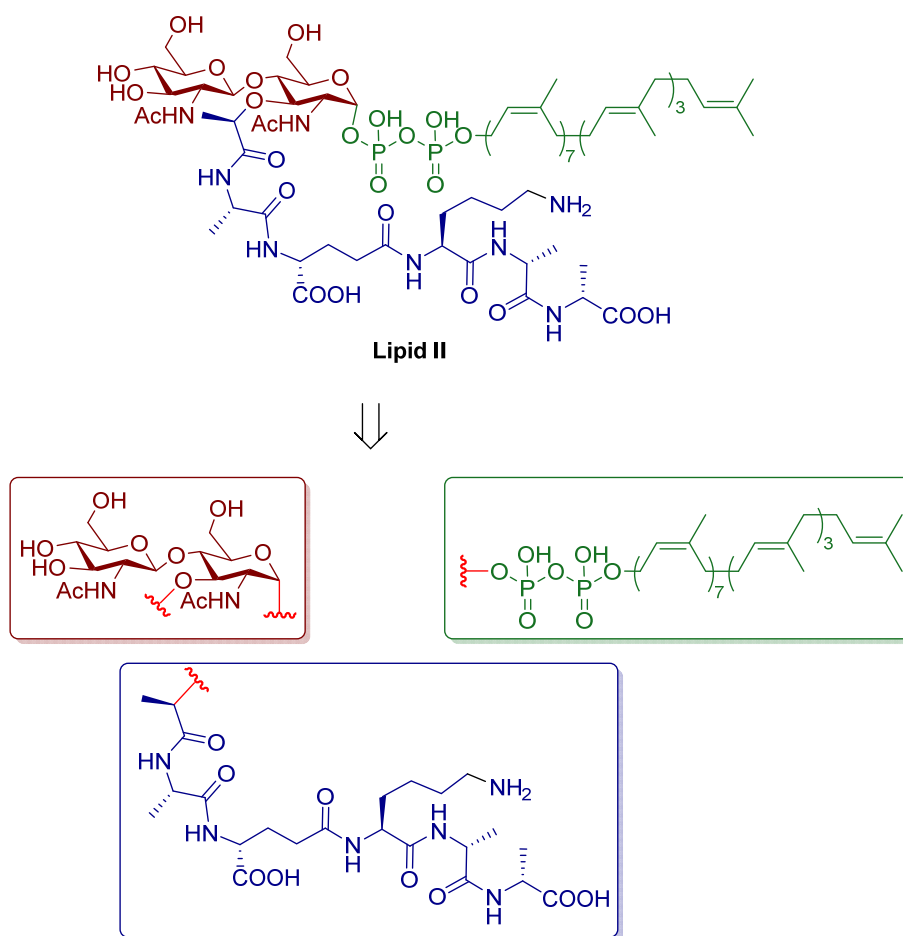


Figure 4.9 Lipid II is composed of three fragments: saccharide, pyrophospholipid and pentapeptide.

4.2.2 Evaluation of the incorporation of PGO into bacterial cell through metabolic process

To evaluate the possibility and efficiency of the synthesized PGO substrate in the labelling bacterial cell walls, rhodamine B, a commonly used dye molecules, was attached to the free amino group from the peptide chain. Specifically, rhodamine B was covalently linked to the free amino group on the side chain of lysine by employing highly reactive sulforhodamine B acid chloride.³⁰ It is noteworthy that modification of the side chain of lysine residue will not affect the biosynthetic process as demonstrated in previous report.²⁸

A variety of bacteria strains, both Gram-positive and Gram-negative, were cultured in the presence of PGO-rhodamine. Meanwhile, the membrane dye FM 1-43fx was used as an indicator dye for bacterial cell surface localization. As can be visualized in microscopic imaging, PGOs-rhodamine was colocalized with FM 1-43fx in all strains tested, indicating the successful incorporation of PGO into bacterial cell walls of both Gram-positive and Gram-negative strains (Figure 4.10a).

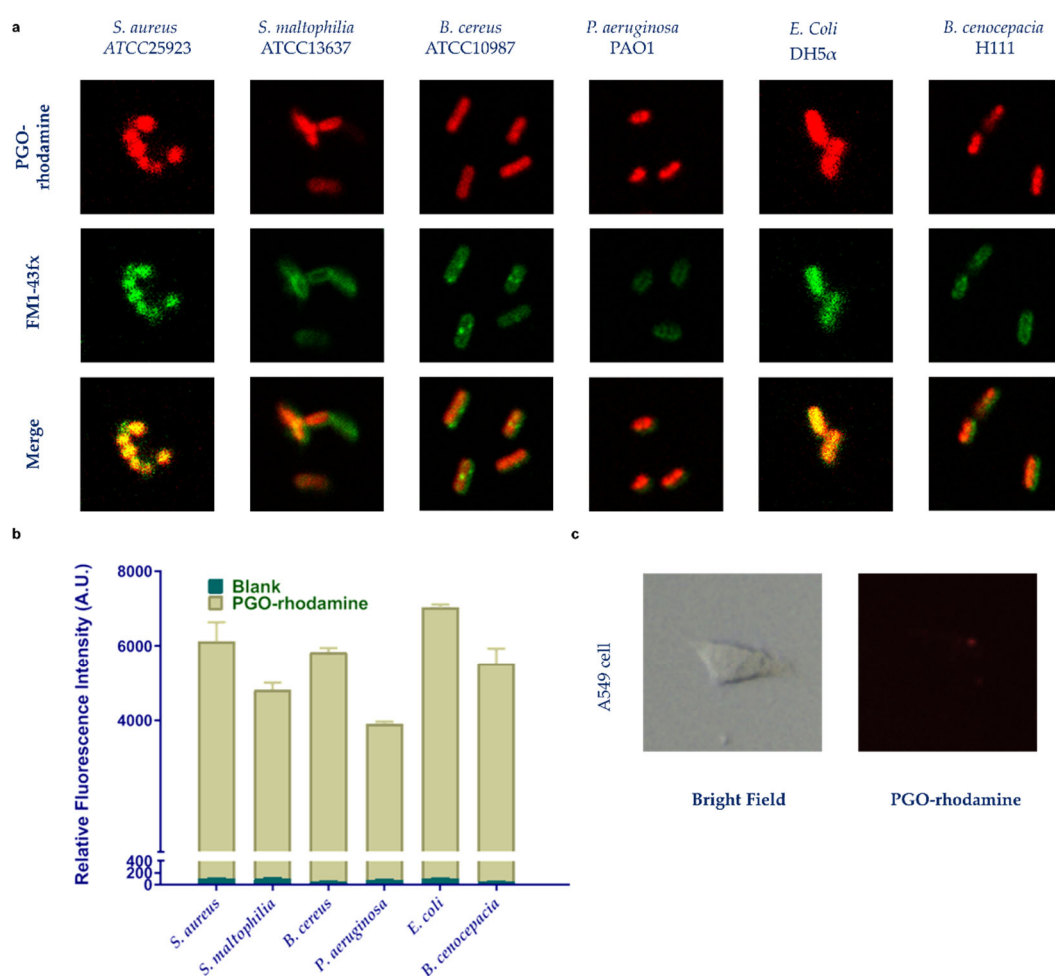


Figure 4.10 Metabolic labeling of bacterial cell walls with PGO-Rhadamine. a) Fluorescence confocal microscopy of incubated bacteria; b) Relative fluorescence intensity by flow cytometry; c) A549 cell (as comparison).

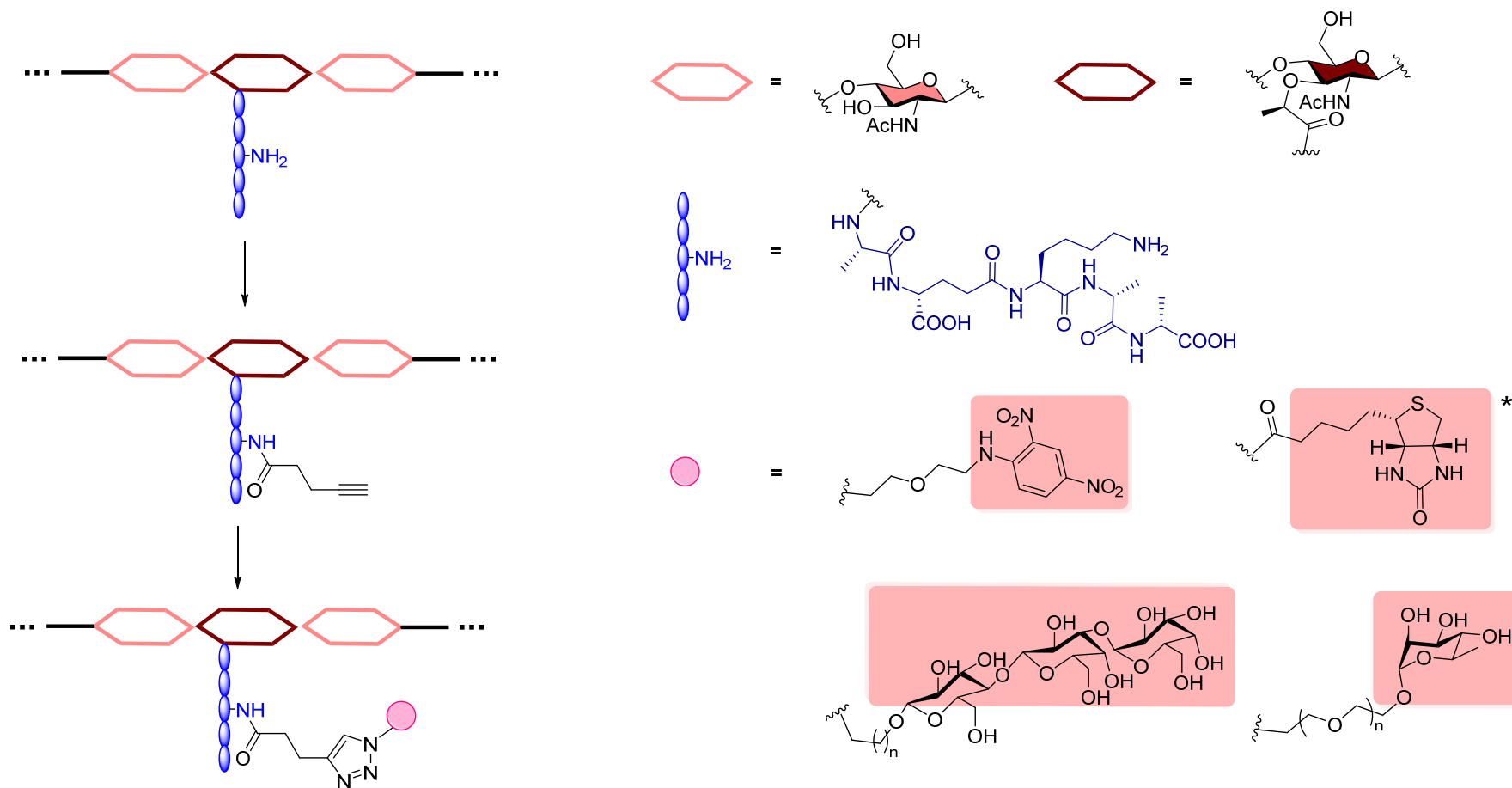


Figure 4.11 Introduction of haptens to the side chain of lysine residue in PGO (*Biotin was attached directly with its NHS ester).

In addition, high fluorescence intensity was observed for these labeled bacterial cells measured by flow cytometry (Figure 4.10b). Amongst them, *Pseudomonas aeruginosa* (*P. aeruginosa*) and *Burkholderia cenocepacia* (*B. cenocepacia*) are highly opportunistic Gram-negative strains which are difficult to treat especially the biofilms formed by them, implying the great possibility in designing new antibody-recruiting molecules based on PGO. In contrast, the human cell could not be labeled by the compound as expected because of the absence of cell wall in human cell.

4.2.3 Construction of antibody-recruiting molecules (ARMs)

As the incorporation of PGO into bacterial cell walls is highly efficiency, and more importantly, both Gram-positive and Gram-negative strains could be hijacked by such compound, we envisioned that bifunctional antibody-recruiting molecules can be readily produced by introducing haptens to the amino group in lysine residue. Therefore, a series of haptens, reported to be active in cancer immunotherapy, were synthesized and conjugated with PGO.^{15a,31} Specifically, PGO compound was modified with highly reactive 4-pentynoic-NHS ester, affording alkyne-functionalized residue in the polymer which is readily clicked with azido-bearing haptens through CuAAC reaction (Figure 4.11).

4.2.4 Biological evaluations of synthesized antibody-recruiting molecules

As an ultimate goal, killing of pathogens or inhibition of their growth by antibacterial agents should not interfere with the host cells. Therefore, for the sake of safety, our synthesized compounds were subjected to cytotoxicity evaluation using A549 cell lines.

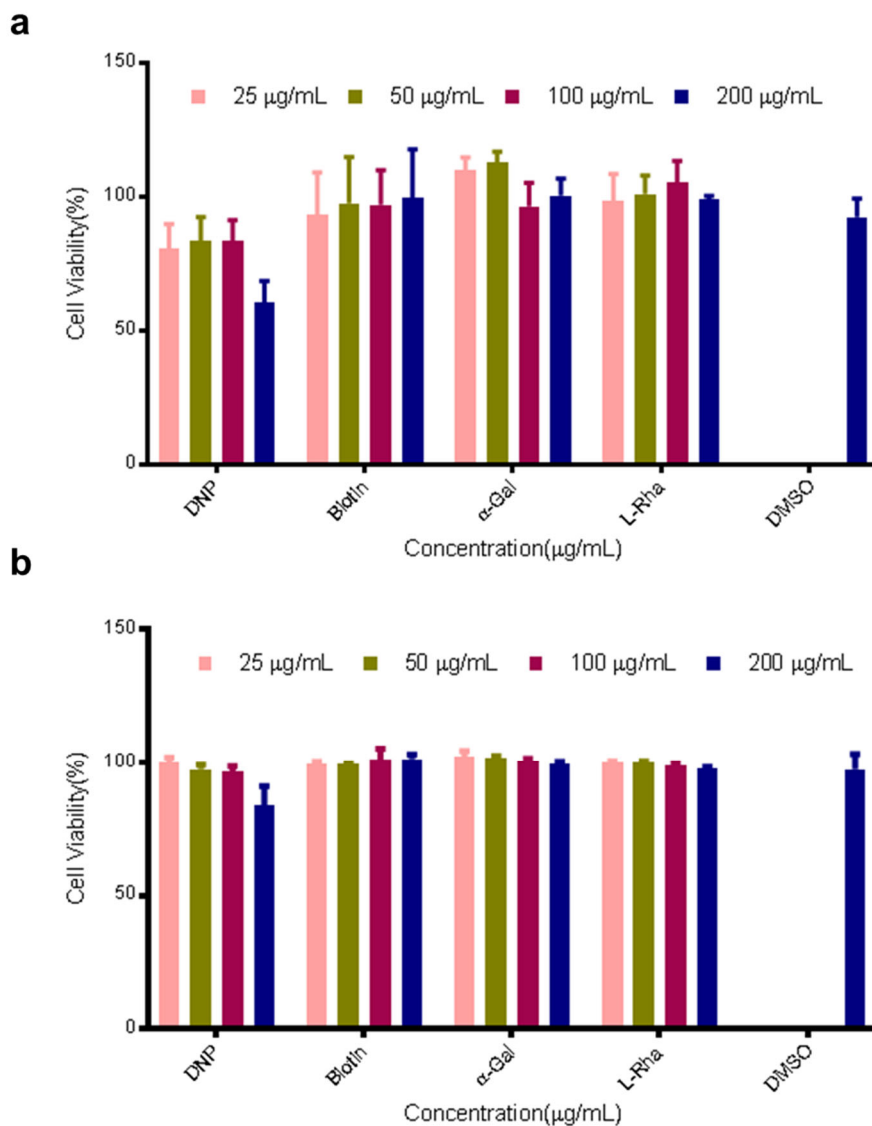


Figure 4.12 Cytotoxicity of synthesized ARMs towards A549 cells. a) 12 h; b) 24 h.

Satisfactorily, all the synthesized compound appeared to be nontoxic towards A549 cells at concentration of 200 $\mu\text{g/mL}$ even after 24 h, although slightly reduced cell viability was observed with DNP-derived ARM (Figure 4.12). Therefore, it should be safe to proceed further evaluations of antibody-recruiting behavior of the compounds. Currently, the materials for antibody-recruiting evaluations are still on the way, especially the customized monoclonal antibodies.

4.3 Conclusion

We have successfully synthesized a lipid II analogue, peptidoglycan oligomer (PGO), with more efficient approach starting from a renewable material, chitosan. By synthetically conjugating fluorescent rhodamine dye with our PGO, the incorporation of PGO-rhodamine into the cell walls of multiple wild-type bacteria could be visualized by fluorescent microscopy. The results demonstrated successful incorporation of PGO into the cell walls of both Gram-positive and Gram-negative bacteria strains through metabolic process. The preliminary results convinced us to employ this compound in developing new antibody-recruiting molecules (ARMs) with broader spectrum of activity. Indeed, several haptens have been prepared and conjugated with our PGO to construct antibody-recruiting molecules. These ARMs showed no toxicity towards A549 cells, rendering them safe materials for further evaluations. Currently, the materials for antibody-recruiting evaluations are still on the way, especially the customized monoclonal antibodies, and more biological evaluations are ongoing in our laboratory.

4.4 Experimental Section

4.4.1 Materials and Methods

The reactions were all performed under nitrogen or argon atmosphere without otherwise noted. Chemicals and solvents are purchased from Alfa-Aesar, Sigma-Aldrich and VWR and used without further purification unless otherwise noted. Anhydrous toluene (over sodium/benzophenone), tetrahydrofuran (THF, over sodium/benzophenone) and dichloromethane (DCM, over calcium hydride) were freshly distilled under nitrogen atmosphere before use. All the other anhydrous solvents were purchased from Sigma-Aldrich and used as received. Polymeric substrates were purified by dialysis using a dialysis tubing cellulose membrane (3.5 kDa MWCO) for 3 days.

Chitosan ($M_w \leq 3000$ Da, degree of deacetylation > 85%) was purchased from Carbosynth Ltd. (Berkshire, UK). Amino acids derivatives and coupling reagents were purchased from GL Biochem Co. (Shanghai, China). Membrane dye FM 1-43fx was purchased from Thermo Fisher Scientific Inc. (Waltham, USA). Haptens based on alpha-Gal were received as a kind gift from Prof. Cao Hongzhi in Shandong University. Deuterated solvents are obtained from Cambridge Isotope Laboratories and used as received. Thin layer chromatography (TLC) with Merck TLC silica gel 60 F254 plate was used to monitor reaction. UV, potassium permanganate and iodine staining were used to visualize compounds on TLC plates. Flash column chromatography with silica gel 60 (0.010-0.063 mm) was applied for the purification of organic compounds. Deionized water was obtained from a Merck Millipore Integral 3 water purification system. Bacterial strains (*Bacillus cereus* ATCC10987, *Staphylococcus aureus* ATCC25923, *Pseudomonas aeruginosa* PAO1, *Burkholderia cenocepacia* H111, *Escherichia coli* DH5 α and *Stenotrophomonas*

maltophilia ATCC13637) were purchased from the American Type Culture Collection (Manassas, USA) and stored at -80 °C. Mueller-Hinton broth (MHB, Difco), brain heart infusion broth (BHI, Difco) and trypticase soy broth (TSB, Difco) were purchased from Beckton, Dickinson and company (Franklin Lakes, USA). Dialysis tubing was purchased from Spectra/Por (Singapore).

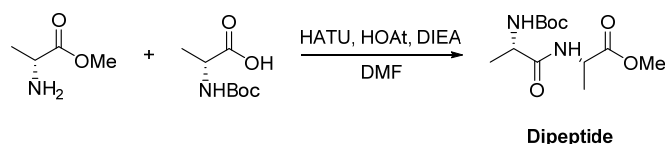
4.4.2 Instruments for characterization

¹H and ¹³C NMR spectra were recorded on Bruker Avance 300, Bruker Avance 400, Bruker AVIII 400 and JEOL JNM-ECA 400 spectrometers using deuterated solvents as reference. Low resolution mass spectra were obtained using an Agilent 6230 TOF LC/MS with an electrospray (ESI) source with purine and HP-0921 as an internal calibrates. HRMS spectra were recorded on a Waters Q-ToF premier™ mass spectrometer. Eppendorf Centrifuge 5430 was used to separate the solid polymers from the solution.

4.4.3 Synthesis of peptides and monophosphate

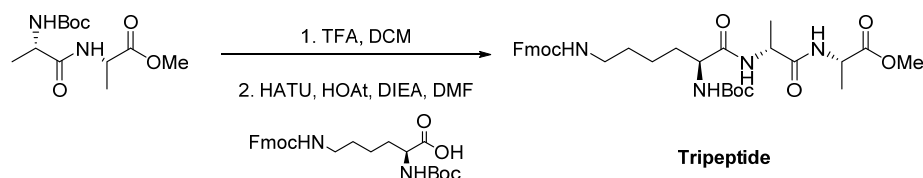
Pentapeptide Synthesis

The peptide synthesis followed the standard procedure for peptide synthesis in solutions with some necessary modifications.³²



To a mixture of Boc-D-Ala-OH (5.2 g, 27.5 mmol), 1-[Bis(dimethylamino)methylene]-1H-1,2,3-triazolo[4,5-b]pyridinium 3-oxid hexafluorophosphate (HATU, 10.5 g, 27.5 mmol) and 1-Hydroxy-7-azabenzotriazole (HOAt, 3.74 g, 27.5 mmol) in anhydrous DMF (15 mL),

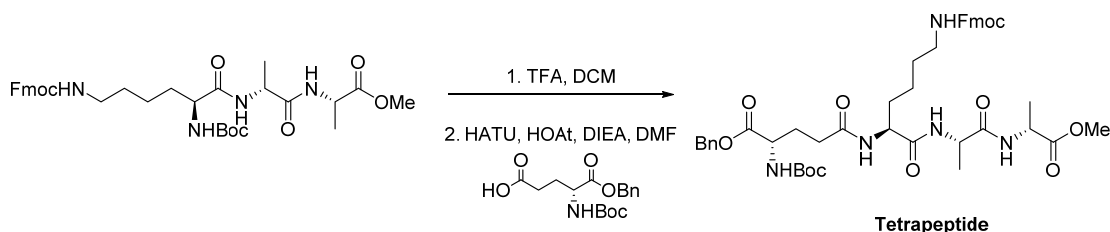
N,N-Diisopropylethylamine (DIEA, 10.3 mL, 62.5 mmol) was added under nitrogen atmosphere and the resulting mixture was stirred for 15-30 min before the addition of H-D-Ala-OMe (2.58 g, 25 mmol). The resulting solution was stirred at room temperature for 24 h before removing the solvent under high vacuum. The residue was dissolved in DCM and washed with water, 0.5 M HCl solution, NaHCO₃ solution and brine successively. The organic layer was collected, dried over Na₂SO₄, filtered and concentrated to give crude product. The crude product was purified with silica-gel column chromatography using acetone-hexane as eluent, affording desired **Dipeptide** as white solid. ¹H NMR (400 MHz, CDCl₃) δ 6.80 (s, 1H), 5.16 (d, *J* = 7.7 Hz, 1H), 4.54 (p, *J* = 7.2 Hz, 1H), 4.18 (s, 1H), 3.71 (s, 3H), 1.42 (s, 9H), 1.37 (d, *J* = 7.2 Hz, 3H), 1.33 (d, *J* = 7.2 Hz, 3H). ¹³C NMR (100 MHz, CDCl₃) δ 173.3, 172.4, 155.6, 80.1, 52.5, 50.0, 48.1, 28.4, 18.4, 18.3. HRMS (ESI): *m/z* [M+Na]⁺ calcd for C₁₂H₂₂N₂NaO₅ 297.1426, found 297.1437.



Dipeptide was dissolved in suitable amount of DCM/TFA (v/v = 1:1), the resulting mixture was stirred at room temperature overnight before removing the solvent under reduced pressure. The residue was neutralized with excess amount of DIEA and concentrated to give crude product for the next step without further purification.

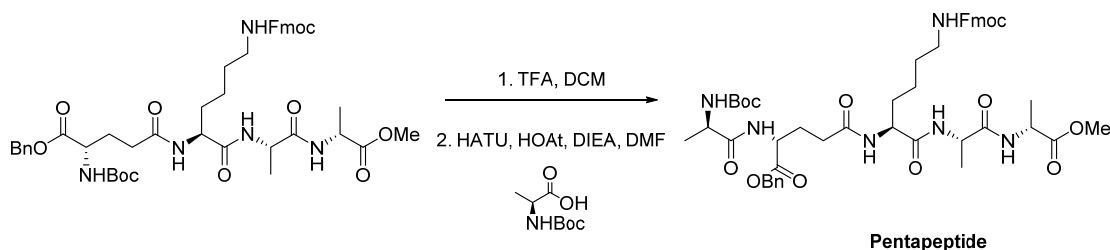
The synthesis of **Tripeptide** followed the same procedure for synthesis of **Dipeptide**. ¹H NMR (400 MHz, DMSO-*d*₆) δ 8.19 (d, *J* = 7.3 Hz, 1H), 8.01 (d, *J* = 8.0 Hz, 1H), 7.85 (dd, *J* = 17.9, 7.4 Hz, 4H), 7.45 – 7.37 (m, 2H), 7.37 – 7.29 (m, 2H), 6.95 (d, *J* = 7.5 Hz, 1H), 6.75 – 6.58 (m, 1H), 4.46 – 3.74 (m, 6H), 3.60 (s, 3H), 2.99 – 2.78 (m, 2H), 1.67 – 1.11 (m, 21H). ¹³C NMR

(100 MHz, DMSO- d_6) δ 172.8, 172.1, 171.9, 157.4, 155.5, 142.6, 139.5, 137.5, 129.0, 127.3, 121.4, 120.1, 109.8, 78.2, 54.6, 51.9, 47.6, 47.5, 38.3, 31.4, 29.3, 28.2, 22.8, 18.2, 16.8. HRMS (ESI): m/z $[M+H]^+$ calcd for $C_{33}H_{45}N_4O_8$ 625.3237, found 625.3238.



The synthesis of **Tetrapeptide** followed the same procedure for synthesis of **Tripeptide**.

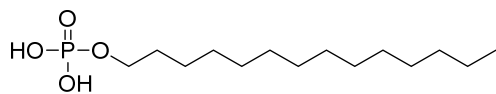
HRMS (ESI): m/z $[M+H]^+$ calcd for $C_{45}H_{58}N_5O_{11}$ 844.4133, found 844.4127.



The synthesis of **Pentapeptide** followed the same procedure for synthesis of **Tripeptide**.

1H NMR (400 MHz, DMSO- d_6) δ 8.27 (d, J = 7.8 Hz, 1H), 8.18 (d, J = 7.5 Hz, 2H), 8.02 (d, J = 7.2 Hz, 1H), 7.88 (d, J = 7.5 Hz, 2H), 7.84 (d, J = 7.5 Hz, 2H), 7.41 (t, J = 7.5 Hz, 2H), 7.38 – 7.24 (m, 8H), 6.86 (d, J = 7.7 Hz, 1H), 6.60 (t, J = 5.9 Hz, 1H), 6.28 (d, J = 1.5 Hz, 2H), 5.11 (s, 2H), 4.27 (dh, 3H), 4.15 (q, J = 7.2 Hz, 1H), 4.02 (p, J = 7.2 Hz, 1H), 3.59 (s, 3H), 2.88 (q, J = 6.6 Hz, 2H), 2.19 (q, J = 7.7 Hz, 2H), 1.97 (h, J = 7.3, 6.6 Hz, 1H), 1.83 (dq, J = 15.0, 8.4, 7.6 Hz, 1H), 1.65 – 0.97 (m, 24H). ^{13}C NMR (100 MHz, DMSO- d_6) δ 173.5, 173.3, 172.5, 172.0, 157.8, 155.4, 143.0, 139.87, 137.88, 136.4, 129.4, 128.8, 128.4, 128.2, 127.7, 121.8, 120.5, 110.2, 78.5, 66.4, 53.5, 52.3, 52.0, 50.1, 48.1, 48.0, 31.9, 31.7, 30.0, 29.8, 28.6, 27.4, 23.1, 18.9, 18.4, 17.2.

HRMS (ESI): m/z $[M+H]^+$ calcd for $C_{48}H_{63}N_6O_{12}$ $[M+H]^+$: 915.4504, found: 915.4493.

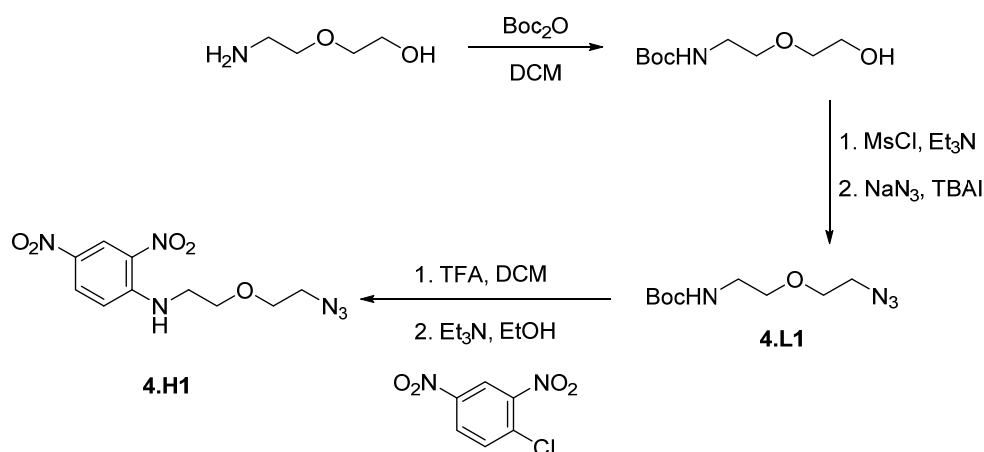
Synthesis of tetradecyl monophosphate³³

The preparation of tetradecyl monophosphate followed the reported procedure.³³ To a solution of phosphorus oxychloride (4.3 g, 28.0 mmol) and triethylamine (6.0 mL, 46.8 mmol) in THF, a solution of 1-tetradecanol (5.0 g, 23.4 mmol) in THF was added dropwise at 0 °C. The resulting mixture was stirred for another 10 min at 0 °C before adding water to hydrolyze the phosphorus oxychloride. The reaction mixture was stirred for extra 1 h at room temperature followed by dilution with ether. The organic solution was washed with water and brine successively before dried over Na₂SO₄. The solution was concentrated in vacuo to give final product with enough purity that can be used directly for the next step without further purification. ¹H NMR (400 MHz, DMSO-*d*₆) δ 3.78 (q, *J* = 6.7 Hz, 2H), 1.63 – 1.45 (m, 2H), 1.44 – 1.01 (m, 26H), 0.94 – 0.78 (m, 3H).

4.4.4 Installation of rhodamine B group

Tagging by sulforhodamine B was done following literature procedures.³⁰ Specifically, 10 mg oligomer **4.8** was dissolved in 2 mL carbonate buffer (0.1 M, pH = 9) and a solution of sulforhodamine B acid chloride in DMF (2 mg/mL, 100 μL) was added. The mixture was left to stir in dark at room temperature for 2 h followed by dialysis against DI water and lyophilization to give PGO-rhodamine conjugate.

4.4.5 Synthesis of haptens and linkers**Dinitrophenyl (DNP) based hapten 4.H1**



The DNP-based hapten **4.H1** and linker were prepared according to reported procedures with necessary modifications.^{9,34}

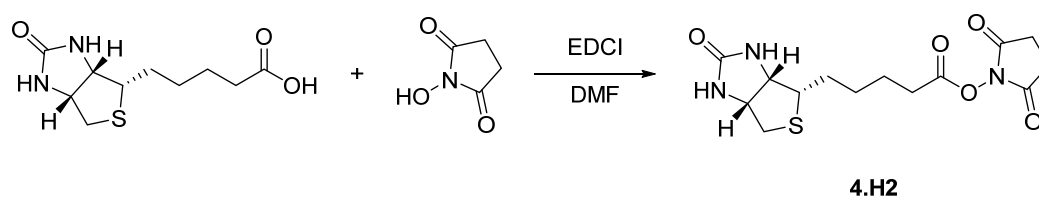
A solution of di-*tert*-butyl decarbonate (6.35 g, 30 mmol) in DCM was added to the solution of 2-(2-aminoethoxy)-ethanol (3.0 mL, 30 mmol) in DCM at 0 °C dropwise. The resulting mixture was stirred for another 30 min at 0 °C before warmed up to room temperature. The mixture was stirred at room temperature overnight before washing with water. The aqueous layer was extracted with DCM and the combined organic layers were washed with brine, dried and concentrated to give intermediate 2-(2-(*tert*-butoxycarbonylamino)ethoxy)ethanol for direct use in the next step without further purification.

To a solution of crude product from previous step (5 g, 24.4 mmol) in toluene was added triethyl amine (6.3 mL, 48.8 mmol) and cooled to ice bath temperature before methane sulfonyl chloride (2.2 mL, 26.9 mmol) was added dropwise at the same temperature. After 10 min of stirring at room temperature, tetrabutylammonium iodide (9.0 g, 24.4 mmol) and a aqueous solution of sodium azide (3.2 g, 48.8 mmol) was added and heated at 70 °C for 4h. After cooling down to room temperature, water was added and extracted twice with ethyl acetate before dried over Na_2SO_4 . The solvent was removed under reduced

pressure and the crude product was purified by silica gel column chromatography to yield compound 1-(2-(*tert*-butoxycarbonylamino)ethoxy)-2-azidoethane **4.L1**. ^1H NMR (500 MHz, CDCl_3) δ 4.94 (s, 1H), 3.62 (t, J = 5.4 Hz, 2H), 3.51 (t, J = 5.2 Hz, 2H), 3.35 (t, J = 5.0 Hz, 2H), 3.32 – 3.27 (m, 2H), 1.41 (s, 9H). ^{13}C NMR (125 MHz, CDCl_3) δ 156.1, 79.4, 70.4, 70.0, 50.7, 40.4, 28.4. MS (ESI) m/z calcd for $\text{C}_9\text{H}_{19}\text{N}_4\text{O}_3$ $[\text{M}+\text{H}]^+$ 231.15, found 231.32.

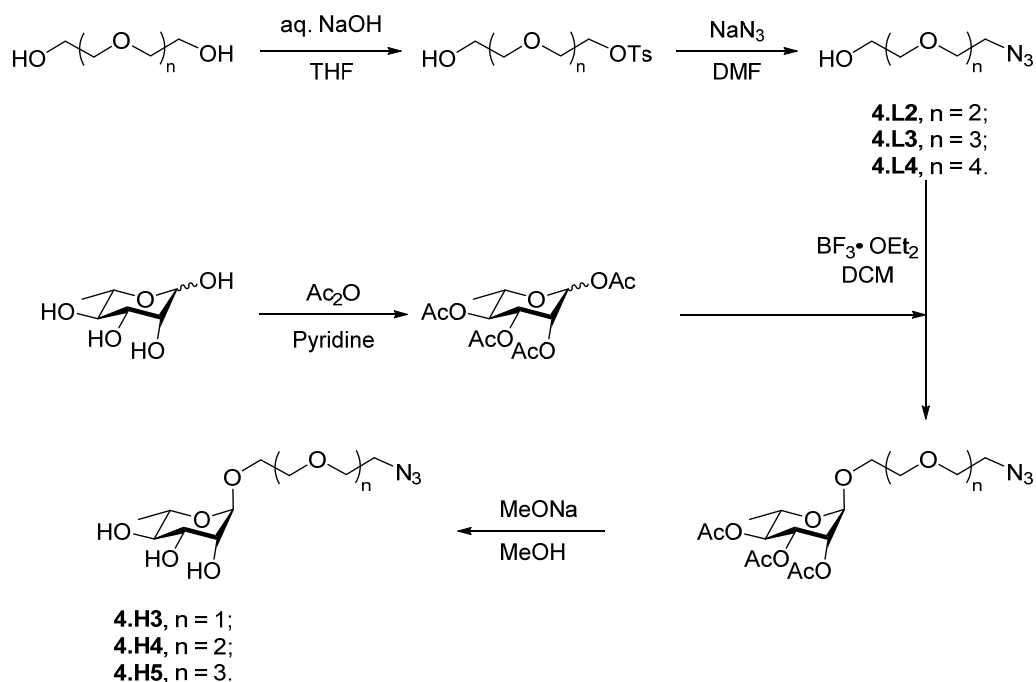
The compound **4.L1** (5.3 g, 23 mmol) was dissolved in TFA/DCM (v/v = 1:1) and stirred at room temperature overnight before removing the solvent. The residue was used directly for the next step without further purification. To a solution of the crude product from previous step in EtOH was added triethylamine (11.9 mL, 46 mmol) and 1-chloro-2,4-dinitrobenzene (4.9 g, 24.2 mmol). The reaction flask was then fitted with a reflux condenser and the mixture was heated to reflux for 2 h, cooled, concentrated and the residue was re-dissolved in water and extracted with DCM. The organic layers were combined, dried over Na_2SO_4 and concentrated to a yellow oil that was further purified by silica-gel flash chromatography to give **4.H1** as yellow oil. ^1H NMR (400 MHz, CDCl_3) δ 9.11 (d, J = 2.4 Hz, 1H), 8.25 (dd, J = 9.5, 2.7 Hz, 1H), 6.98 (d, J = 9.5 Hz, 1H), 3.83 (t, J = 5.1 Hz, 2H), 3.72 (t, J = 4.8 Hz, 2H), 3.64 (q, J = 5.2 Hz, 2H), 3.42 (t, J = 4.9 Hz, 2H). ^{13}C NMR (100 MHz, CDCl_3) δ 148.6, 136.3, 130.7, 130.4, 124.4, 114.2, 70.3, 68.9, 50.8, 43.3. HRMS (ESI): m/z $[\text{M}+\text{H}]^+$ calcd for $\text{C}_{10}\text{H}_{13}\text{N}_6\text{O}_5$ 297.0947, found 297.0940.

Biotin-NHS ester **4.H2**

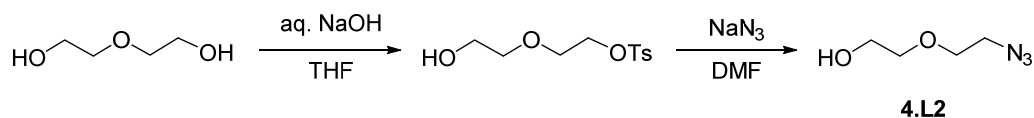


The biotin-NHS ester was prepared by following the reported procedure.³⁵ To a solution of D-biotin (2.44 g, 10 mmol) in DMF, N-hydroxysuccinimide (1.38 g, 12 mmol) and EDCI (3.84 g, 20 mmol) were added and the reaction mixture was stirred at room temperature overnight before removing the solvent under high vacuum. The residue was recrystallized from EtOH/AcOH/H₂O (95:1:4), giving final product **4.H2** as white powder. ¹H NMR (500 MHz, DMSO-*d*₆) δ 6.42 (s, 1H), 6.36 (s, 1H), 4.36 – 4.26 (m, 1H), 4.19 – 4.10 (m, 1H), 3.15 – 3.05 (m, 1H), 2.86 – 2.77 (m, 5H), 2.66 (t, *J* = 7.4 Hz, 2H), 2.57 (d, *J* = 12.4 Hz, 1H), 1.74 – 1.58 (m, 3H), 1.55 – 1.36 (m, 3H). ¹³C NMR (125 MHz, DMSO-*d*₆) δ 170.3, 168.9, 162.7, 61.0, 59.2, 55.2, 39.9, 30.0, 27.8, 27.6, 25.5, 24.3. MS (ESI) *m/z* calcd for C₁₄H₂₀N₃O₅S [M+H]⁺ 342.11, found 342.03.

L-rhamnose based haptens **4.H3-4.H5**



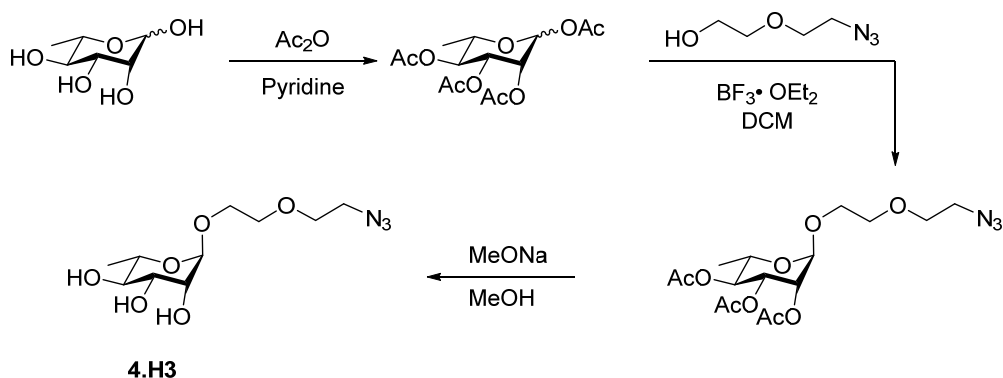
The linkers of azido-PEG were prepared following the reported procedure with necessary modification.³⁶ All the L-rhamnose based haptens were prepared using the same procedures. As an example, the preparation of hapten **4.H3** will be described in detail.



Diethylene glycol (11.9 g, 112 mmol) was dissolved in 20 mL THF, NaOH solution (6.73 g, 168 mmol in 15 mL water). The mixture was cooled down to 0 °C by ice/water bath followed by adding the solution of TsCl (25.67 g, 135 mmol) in THF dropwise to the mixture. The solution was stirred for another 1 h before the solvent was evaporated. The residue was re-dissolved in DCM and successively washed with water and brine before drying over MgSO₄, filtered and concentrated to give crude product which was further purified by silica-gel flash chromatography to give the product as pale yellow oil. ¹H NMR (400 MHz, CDCl₃) δ 7.76 (d, *J* = 8.2 Hz, 2H), 7.32 (d, *J* = 7.9 Hz, 2H), 4.24 – 4.08 (m, 2H), 3.72 – 3.59 (m, 4H), 3.52 – 3.47 (m, 2H), 2.49 (s, 1H), 2.41 (s, 3H). ¹³C NMR (100 MHz, CDCl₃) δ 145.0, 133.0, 129.9, 128.0, 72.5, 69.3, 68.6, 61.6, 21.7. MS (ESI) *m/z* calcd for C₁₁H₁₇O₅S [M+H]⁺ 261.08, found 261.13.

To a solution of compound from previous step (5.5 g, 20 mmol) in DMF, NaN₃ (2.21 g, 34 mmol) was added. The resulting suspension was stirred at 50 °C for 12 h before cooled down to room temperature. The mixture was diluted with water and extracted with DCM. The combined extracts were washed with water and dried over Na₂SO₄. The product **4.L2** was obtained after concentrated, as a light yellow oil. ¹H NMR (400 MHz, CDCl₃) δ 3.76 – 3.68 (m, 2H), 3.68 – 3.62 (m, 2H), 3.60 – 3.53 (m, 2H), 3.37 (t, *J* = 5.0 Hz, 2H), 2.49 (s, 1H). ¹³C

NMR (100 MHz, CDCl₃) δ 72.5, 70.0, 61.7, 50.7. HRMS (ESI): m/z [M+Na]⁺ calcd for C₄H₉N₃NaO₂ 154.0592, found 154.0597.

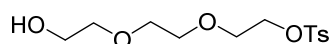


To a solution of L-rhamnose (10.0 g, 60 mmol) in pyridine was added acetic anhydride (35 mL, 377 mmol) followed by addition of DMAP (0.2 g). After stirring overnight before concentrated under reduced pressure. The residue was diluted with ethyl acetate and successively washed with 1M HCl solution, saturated NaHCO₃ and brine. The organic layer was concentrated and dried under vacuum to give crude product peracetate L-rhamnose for direct use in the next step without further purification.

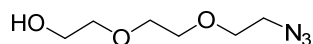
Crude peracetate L-rhamnose from previous step (1.0 g, 3.0 mmol) and azido linker **4.L2** (1.18 g, 4.5 mmol) was dissolved in anhydrous DCM and cooled to 0 °C, followed by addition of boron trifluoride etherate (1.8 mL, 15 mmol) dropwise. The reaction mixture was slowly warmed up to room temperature and stirred overnight before quenched by addition of triethylamine. The mixture was concentrated and diluted with ethyl acetate, washed with. saturated NaHCO₃ and brine, successively. The organic layer was dried over anhydrous Na₂SO₄, filtered, concentrated and subjected to silica-gel column chromatography using EA-hexane as eluent, giving desired product as colorless oil. ¹H NMR (400 MHz, CDCl₃) δ 5.30 – 5.21 (m, 2H), 5.02 (t, J = 9.9 Hz, 1H), 4.75 (d, J = 1.7 Hz,

1H), 4.00 – 3.85 (m, 1H), 3.84 – 3.72 (m, 1H), 3.69 – 3.55 (m, 5H), 3.36 (t, $J = 5.0$ Hz, 2H), 2.11 (s, 3H), 2.01 (s, 3H), 1.95 (s, 3H), 1.18 (d, $J = 6.3$ Hz, 3H). ^{13}C NMR (100 MHz, CDCl_3) δ 170.2, 170.09, 170.06, 97.7, 71.2, 70.3, 70.2, 69.9, 69.2, 67.2, 66.4, 50.8, 20.9, 20.84, 20.77, 17.5. HRMS (ESI): m/z $[\text{M}+\text{Na}]^+$ calcd for $\text{C}_{16}\text{H}_{25}\text{N}_3\text{NaO}_9$ 426.1488, found 426.1486.

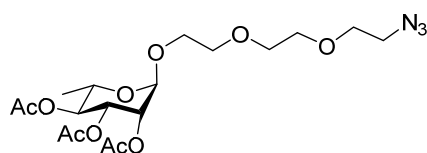
To the solution of triacetyl azido compound from previous step (0.25 g, 0.56 mmol) in anhydrous MeOH was added sodium methoxide (0.2 mL, 0.5 M in MeOH). The reaction mixture was stirred at room temperature overnight before neutralized with acidic resin. The resulting mixture was filtered, and filtrate was concentrated to give product **4.H3** as pale-yellow oil. ^1H NMR (400 MHz, Methanol- d_4) δ 4.71 (d, $J = 1.7$ Hz, 1H), 3.86 – 3.75 (m, 2H), 3.73 – 3.55 (m, 7H), 3.44 – 3.33 (m, 3H), 1.26 (d, $J = 6.2$ Hz, 3H). ^{13}C NMR (100 MHz, Methanol- d_4) δ 101.8, 73.9, 72.3, 72.1, 71.22, 71.18, 69.8, 67.8, 51.7, 18.0. HRMS (ESI): m/z $[\text{M}+\text{Na}]^+$ calcd for $\text{C}_{10}\text{H}_{19}\text{N}_3\text{NaO}_6$ 300.1172, found 300.1172.



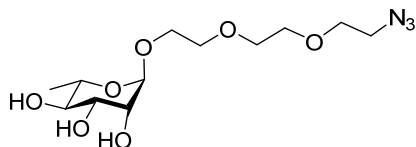
^1H NMR (400 MHz, CDCl_3) δ 7.76 (d, $J = 8.2$ Hz, 2H), 7.31 (d, $J = 8.2$ Hz, 2H), 4.18 – 4.09 (m, 2H), 3.73 – 3.63 (m, 4H), 3.61 – 3.49 (m, 6H), 2.53 (s, 1H), 2.41 (s, 3H). ^{13}C NMR (100 MHz, CDCl_3) δ 144.9, 132.9, 129.9, 128.0, 72.5, 70.8, 70.3, 69.2, 68.7, 61.7, 21.7. MS (ESI) m/z calcd for $\text{C}_{13}\text{H}_{21}\text{O}_6\text{S}$ $[\text{M}+\text{H}]^+$ 305.11, found 304.97.



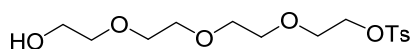
^1H NMR (500 MHz, CDCl_3) δ 3.73 (t, $J = 5.2$ Hz, 2H), 3.70 – 3.64 (m, 6H), 3.64 – 3.56 (m, 2H), 3.40 (t, $J = 5.0$ Hz, 2H), 2.76 (s, 1H). ^{13}C NMR (125 MHz, CDCl_3) δ 72.6, 70.6, 70.3, 70.0, 61.7, 50.6. MS (ESI) m/z calcd for $\text{C}_6\text{H}_{14}\text{N}_3\text{O}_3$ $[\text{M}+\text{H}]^+$ 176.10, found 176.38.



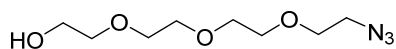
^1H NMR (400 MHz, CDCl_3) δ 5.33 – 5.20 (m, 2H), 5.09 – 4.97 (m, 1H), 4.75 (s, 1H), 3.96 – 3.85 (m, 1H), 3.84 – 3.73 (m, 1H), 3.71 – 3.57 (m, 9H), 3.38 (t, J = 5.1 Hz, 2H), 2.12 (s, 3H), 2.02 (s, 3H), 1.96 (s, 3H), 1.19 (d, J = 6.0 Hz, 3H). ^{13}C NMR (100 MHz, CDCl_3) δ 170.2, 170.11, 170.08, 97.7, 71.2, 70.9, 70.8, 70.21, 70.17, 70.0, 69.2, 67.2, 66.4, 50.8, 21.0, 20.9, 20.8, 17.5. MS (ESI) m/z calcd for $\text{C}_{18}\text{H}_{30}\text{N}_3\text{O}_{10}$ $[\text{M}+\text{H}]^+$ 448.19, found 447.75.



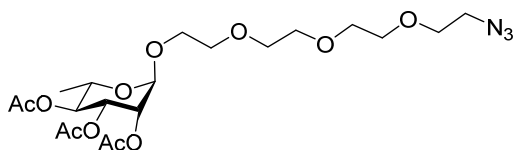
^1H NMR (400 MHz, Methanol- d_4) δ 4.73 (d, J = 1.8 Hz, 1H), 3.87 – 3.77 (m, 2H), 3.74 – 3.58 (m, 11H), 3.42 – 3.36 (m, 3H), 1.28 (d, J = 6.3 Hz, 3H). ^{13}C NMR (100 MHz, Methanol- d_4) δ 101.8, 73.9, 72.3, 72.2, 71.7, 71.5, 71.4, 71.2, 69.7, 67.7, 51.7, 18.0. MS (ESI) m/z calcd for $\text{C}_{12}\text{H}_{24}\text{N}_3\text{O}_7$ $[\text{M}+\text{H}]^+$ 322.16, found 321.91.



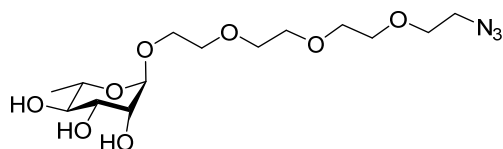
^1H NMR (400 MHz, CDCl_3) δ 7.76 (d, J = 8.2 Hz, 2H), 7.31 (d, J = 8.0 Hz, 2H), 4.13 (t, J = 4.7 Hz, 2H), 3.72 – 3.51 (m, 14H), 2.50 (s, 1H), 2.41 (s, 3H). ^{13}C NMR (100 MHz, CDCl_3) δ 144.9, 133.0, 129.9, 128.1, 72.6, 70.8, 70.7, 70.5, 70.4, 69.3, 68.8, 61.8, 21.7. MS (ESI) m/z calcd for $\text{C}_{15}\text{H}_{25}\text{O}_7\text{S}$ $[\text{M}+\text{H}]^+$ 349.13, found 349.02.



^1H NMR (400 MHz, CDCl_3) δ 3.73 – 3.67 (m, 2H), 3.67 – 3.60 (m, 10H), 3.61 – 3.54 (m, 2H), 3.37 (t, J = 5.1 Hz, 2H), 2.69 (s, 1H). ^{13}C NMR (100 MHz, CDCl_3) δ 72.5, 70.7, 70.7, 70.6, 70.3, 70.0, 61.7, 50.7. MS (ESI) m/z calcd for $\text{C}_8\text{H}_{18}\text{N}_3\text{O}_4$ $[\text{M}+\text{H}]^+$ 220.13, found 219.93.



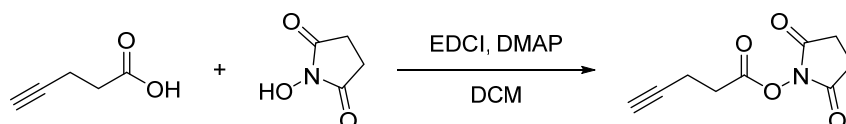
^1H NMR (500 MHz, CDCl_3) δ 5.34 – 5.22 (m, 2H), 5.04 (t, J = 9.9 Hz, 1H), 4.76 (s, 1H), 3.98 – 3.85 (m, 1H), 3.83 – 3.72 (m, 1H), 3.72 – 3.57 (m, 13H), 17H), 3.38 (t, J = 5.0 Hz, 2H), 2.13 (s, 3H), 2.03 (s, 3H), 1.96 (s, 3H), 1.20 (d, J = 6.2 Hz, 3H). ^{13}C NMR (125 MHz, CDCl_3) δ 170.0, 169.9, 169.8, 97.5, 71.0, 70.7, 70.6, 70.0, 69.9, 69.7, 69.0, 67.0, 66.2, 50.6, 20.8, 20.7, 20.6, 17.3. HRMS (ESI): m/z $[\text{M}+\text{NH}_4]^+$ calcd for $\text{C}_{20}\text{H}_{37}\text{N}_4\text{O}_{11}$ 509.2459, found 509.2456.



^1H NMR (400 MHz, Methanol- d_4) δ 4.76 (d, J = 1.7 Hz, 1H), 3.89 – 3.79 (m, 2H), 3.74 – 3.59 (m, 15H), 3.45 – 3.37 (m, 3H), 1.30 (d, J = 6.1 Hz, 3H). ^{13}C NMR (100 MHz, Methanol- d_4) δ 101.8, 74.0, 72.3, 72.2, 71.6, 71.5, 71.4, 71.1, 69.7, 67.7, 51.7, 18.0. HRMS (ESI): m/z $[\text{M}+\text{Na}]^+$ calcd for $\text{C}_{14}\text{H}_{27}\text{N}_3\text{NaO}_8$ 388.1696, found 388.1698.

4.4.6 Construction of antibody-recruiting molecules

4-pentynoic-NHS ester



The pentynoic-NHS ester was prepared according to reported procedure.³⁷ To a solution of 4-pentynoic acid (1.0 g, 10 mmol) in DCM, N-hydroxysuccinimide (1.34 g, 11.5 mmol) and EDCI (3.91 g, 20 mmol) were added and the resulting solution was stirred for 2 h before washed with 2.5% NaHSO_4 solution. The solution was dried and concentrated to give final product as white solid in high purity without further purification. ^1H NMR (400 MHz, CDCl_3) δ 3.00 – 2.76 (m, 6H), 2.69 – 2.53 (m, 2H), 2.05 (t, J = 2.8 Hz, 1H). ^{13}C NMR

(100 MHz, CDCl₃) δ 169.1, 167.2, 81.0, 70.1, 30.4, 25.7, 14.2. HRMS (ESI): m/z [M+H]⁺ calcd for C₉H₁₀NO₄ 196.0610, found 196.0615.

Conjugation of NHS ester with amino group on lysine residue

The conjugation of NHS esters with the primary amine on the lysine followed the reported procedure for other compounds bearing amino groups.³⁸ As an example, a solution of 4-pentynoic-NHS ester in DMSO/H₂O (v/v = 2:1, saturated with NaHCO₃) was added into the solution of PGO in DMSO/H₂O (v/v = 2:1, saturated with NaHCO₃), the resulting mixture was stirred at room temperature overnight before transferring to dialysis tubing. The mixture was dialyzed against DI for 3 days and lyophilized to give fluffy solid. The conjugation of biotin-NHS followed the same procedure.

Conjugation of haptens with alkynylated PGO

To the solution of alkynylated solution in DMSO/H₂O (v/v = 4:1), hapten was added with excess amount (with respect to the estimated alkynyl groups), followed by the addition of CuSO₄ (catalytic amount) and sodium ascorbate (excess amount). The resulting mixture was stirred at room temperature for 24 h before transferred into dialysis tubing. The reaction mixture was dialyzed against 0.05 M EDTA in water for 2 d and DI water for another 2 d. Lyophilization of the solution in the dialysis tubing afforded the final products as puffy solid.

4.4.7 Biological assays

Determination of the efficiency of labelling bacterial cell walls

Bacillus cereus ATCC10987, *Staphylococcus aureus* ATCC25923, *Pseudomonas aeruginosa* PAO1, *Burkholderia cenocepacia* H111 and *Escherichia coli* DH5 α at 37 °C and *Stenotrophomonas maltophilia* ATCC13637 at 30 °C were incubated in LB medium with shaking overnight. 100-fold diluted bacterial solution were incubated in LB medium at 37 °C with shaking for 4 h, supplemented with 100 μ g/mL testing compounds and protected from light. After centrifugation, supernatant was removed, and the residual cells were washed with phosphate-buffered saline (PBS) three times. A formaldehyde fixation solution (4%) was prepared in PBS and applied to fixate the cells prior to performing flow cytometry analysis (BD Accuri C6 Flow Cytometer, BD, USA) and fluorescence microscopy (LSCM 7 DUO, ZEISS, Germany).

Cytotoxicity assays.

Cell viability was quantitatively analyzed using CellTiter 96 Aqueous One Solution Cell Proliferation Assay (MTS, Promega, USA) according to the manufacture's instruction. Briefly, the A549 cells were routinely grown in DMEM medium supplemented with 10% FBS in a 96-well tissue culture plate with 1.5×10^4 cells/well and incubated at 37 °C with 5% CO₂ overnight. After removal of cell media, A549 cells were washed with PBS and incubated with DMEM containing 10% FBS and certain concentration of testing compounds. After culturing for 7 h, 11 h and 24 h, 20 μ L MTS were transferred into each well of the 96-well assay plate containing samples in 100 μ l of medium followed by incubated at 37 °C with 5% CO₂ in dark for 1 h. The absorbance was measured at 490 nm using a microplate reader (Infinite M200, Tecan, USA). The cell viability results were expressed as percentages relative to the absorbance obtained in the control experiment.

4.5 References

- [1] a) N. Mookherjee, R. E. Hancock, *Cell Mol. Life Sci.* **2007**, *64*, 922; b) M. G. Scott, E. Dullaghan, N. Mookherjee, N. Glavas, M. Waldbrook, A. Thompson, A. Wang, K. Lee, S. Doria, P. Hamill, J. J. Yu, Y. Li, O. Donini, M. M. Guarna, B. B. Finlay, J. R. North, R. E. W. Hancock, *Nat. Biotechnol.* **2007**, *25*, 465; c) E. F. Haney, R. E. W. Hancock, *Pept. Sci.* **2013**, *100*, 572.
- [2] a) R. Zhang, M. M. Billingsley, M. J. Mitchell, *J. Controlled Release* **2018**, *292*, 256; b) S. Burugu, A. R. Dancsok, T. O. Nielsen, *Semin. Cancer Biol.* **2018**, *52*, 39; c) H. Dianat-Moghadam, M. Rokni, F. Marofi, Y. Panahi, M. Yousefi, *J. Cell Physiol.* **2019**, *234*, 259; d) E. C. Ko, D. Raben, S. C. Formenti, *Clin. Cancer Res.* **2018**, *24*, 5792; e) S. K. Mazmanian, J. L. Round, D. L. Kasper, *Nature* **2008**, *453*, 620.
- [3] a) S. K. Mazmanian, C. H. Liu, A. O. Tzianabos, D. L. Kasper, *Cell* **2005**, *122*, 107; b) L. V. Hooper, A. J. Macpherson, *Nat. Rev. Immunol.* **2010**, *10*, 159.
- [4] a) G. Köhler, C. Milstein, *Nature* **1975**, *256*, 495; b) D. M. Ecker, S. D. Jones, H. L. Levine, *mAbs* **2015**, *7*, 9.
- [5] a) C. Spiess, Q. Zhai, P. J. Carter, *Mol. Immunol.* **2015**, *67*, 95; b) A. Beck, L. Goetsch, C. Dumontet, N. Corvaia, *Nat. Rev. Drug Discov.* **2017**, *16*, 315; c) N. Diamantis, U. Banerji, *Brit. J. Cancer* **2016**, *114*, 362.
- [6] K. Imai, A. Takaoka, *Nat. Rev. Cancer* **2006**, *6*, 714.
- [7] a) P. Chames, D. Baty, *Curr. Opin. Drug Discovery Dev.* **2009**, *12*, 276; b) K. M. Shokat, P. G. Schultz, *J. Am. Chem. Soc.* **1991**, *113*, 1861; c) A. Traunecker, J. Schneider, H. Kiefer, K. Karjalainen, *Nature* **1989**, *339*, 68.
- [8] K. P. Naicker, H. Li, A. Heredia, H. Song, L.-X. Wang, *Org. Biomol. Chem.* **2004**, *2*, 660.
- [9] C. G. Parker, R. A. Domaoal, K. S. Anderson, D. A. Spiegel, *J. Am. Chem. Soc.* **2009**, *131*, 16392.
- [10] a) R. P. Murelli, A. X. Zhang, J. Michel, W. L. Jorgensen, D. A. Spiegel, *J. Am. Chem.*

- Soc.* **2009**, *131*, 17090; b) C. E. Jakobsche, P. J. McEnaney, A. X. Zhang, D. A. Spiegel, *ACS Chem. Biol.* **2012**, *7*, 316.
- [11] a) Y. Lu, P. S. Low, *Cancer Immunol. Immunother.* **2002**, *51*, 153; b) Y. Lu, E. Segal, P. S. Low, *Int. J. Cancer* **2005**, *116*, 710.
- [12] M. Popkov, B. Gonzalez, S. C. Sinha, C. F. Barbas, *Proc. Natl. Acad. Sci.* **2009**, *106*, 4378.
- [13] a) V. M. Krishnamurthy, L. J. Quinton, L. A. Estroff, S. J. Metallo, J. M. Isaacs, J. P. Mizgerd, G. M. Whitesides, *Biomaterials* **2006**, *27*, 3663; b) S. J. Metallo, R. S. Kane, R. E. Holmlin, G. M. Whitesides, *J. Am. Chem. Soc.* **2003**, *125*, 4534.
- [14] J. Li, S. Zacharek, X. Chen, J. Wang, W. Zhang, A. Janczuk, P. G. Wang, *Bioorg. Med. Chem.* **1999**, *7*, 1549.
- [15] a) R. M. Owen, C. B. Carlson, J. Xu, P. Mowery, E. Fasella, L. L. Kiessling, *ChemBioChem* **2007**, *8*, 68; b) C. B. Carlson, P. Mowery, R. M. Owen, E. C. Dykhuizen, L. L. Kiessling, *ACS Chem. Biol.* **2007**, *2*, 119; c) N. R. Bennett, D. B. Zwick, A. H. Courtney, L. L. Kiessling, *ACS Chem. Biol.* **2015**, *10*, 1817.
- [16] S. E. Pidgeon, J. M. Fura, W. Leon, M. Birabaharan, D. Vezenov, M. M. Pires, *Angew. Chem. Int. Ed.* **2015**, *54*, 6158.
- [17] a) J. M. Fura, M. J. Sabulski, M. M. Pires, *ACS Chem. Biol.* **2014**, *9*, 1480; b) J. M. Fura, M. M. Pires, *Pept. Sci.* **2015**, *104*, 351; c) J. M. Fura, S. E. Pidgeon, M. Birabaharan, M. M. Pires, *ACS Infect. Dis.* **2016**, *2*, 302.
- [18] a) S. E. Pidgeon, M. M. Pires, *Angew. Chem. Int. Ed.* **2017**, *56*, 8839; b) M. J. Sabulski, S. E. Pidgeon, Marcos M. Pires, *Chem. Sci.* **2017**, *8*, 6804.
- [19] a) J. A. Prescher, D. H. Dube, C. R. Bertozzi, *Nature* **2004**, *430*, 873; b) K. K. Palaniappan, C. R. Bertozzi, *Chem. Rev.* **2016**, *116*, 14277.
- [20] P. Kaewsapsak, O. Esonu, D. H. Dube, *ChemBioChem* **2013**, *14*, 721.
- [21] a) A. Typas, M. Banzhaf, C. A. Gross, W. Vollmer, *Nat. Rev. Microbiol.* **2011**, *10*, 123; b) J.-V. Hölzle, *Microbiol. Mol. Biol. Rev.* **1998**, *62*, 181.
- [22] a) B. de Kruijff, V. van Dam, E. Breukink, *Prostaglandins Leukot. Essent. Fatty Acids*

- 2008, 79, 117; b) W. Vollmer, D. Blanot, M. A. De Pedro, *FEMS Microbiol. Rev.* **2008**, 32, 149.
- [23] a) T. Schneider, T. Kruse, R. Wimmer, I. Wiedemann, V. Sass, U. Pag, A. Jansen, A. K. Nielsen, P. H. Mygind, D. S. Raventós, S. Neve, B. Ravn, A. M. J. J. Bonvin, L. De Maria, A. S. Andersen, L. K. Gammelgaard, H.-G. Sahl, H.-H. Kristensen, *Science* **2010**, 328, 1168; b) I. G. Boneca, G. Chiosis, *Expert Opin. Ther. Targets* **2003**, 7, 311; c) R. Hakenbeck, R. Brückner, D. Denapate, P. Maurer, *Future Microbiol.* **2012**, 7, 395.
- [24] a) D. Münch, H.-G. Sahl, *Biochim. Biophys. Acta* **2015**, 1848, 3062; b) S. F. Oppedijk, N. I. Martin, E. Breukink, *Biochim. Biophys. Acta* **2016**, 1858, 947; c) D. L. Perlstein, Y. Zhang, T.-S. Wang, D. E. Kahne, S. Walker, *J. Am. Chem. Soc.* **2007**, 129, 12674.
- [25] a) M. D. Lebar, T. J. Lupoli, H. Tsukamoto, J. M. May, S. Walker, D. Kahne, *J. Am. Chem. Soc.* **2013**, 135, 4632; b) M. S. VanNieuwenhze, S. C. Mauldin, M. Zia-Ebrahimi, B. E. Winger, W. J. Hornback, S. L. Saha, J. A. Aikins, L. C. Blaszcak, *J. Am. Chem. Soc.* **2002**, 124, 3656; c) B. Schwartz, J. A. Markwalder, Y. Wang, *J. Am. Chem. Soc.* **2001**, 123, 11638; d) H.-W. Shih, K.-T. Chen, T.-J. R. Cheng, C.-H. Wong, W.-C. Cheng, *Org. Lett.* **2011**, 13, 4600; e) L.-Y. Huang, S.-H. Huang, Y.-C. Chang, W.-C. Cheng, T.-J. R. Cheng, C.-H. Wong, *Angew. Chem. Int. Ed.* **2014**, 53, 8060; f) Y. Zhang, E. J. Fechter, T.-S. A. Wang, D. Barrett, S. Walker, D. E. Kahne, *J. Am. Chem. Soc.* **2007**, 129, 3080.
- [26] a) M. N. V. Ravi Kumar, *React. Funct. Polym.* **2000**, 46, 1; b) M. Rinaudo, *Prog. Polym. Sci.* **2006**, 31, 603; c) C. K. S. Pillai, W. Paul, C. P. Sharma, *Prog. Polym. Sci.* **2009**, 34, 641.
- [27] a) T.-S. A. Wang, T. J. Lupoli, Y. Sumida, H. Tsukamoto, Y. Wu, Y. Rebets, D. E. Kahne, S. Walker, *J. Am. Chem. Soc.* **2011**, 133, 8528; b) D. Barrett, T.-S. A. Wang, Y. Yuan, Y. Zhang, D. Kahne, S. Walker, *J. Biol. Chem.* **2007**, 282, 31964.
- [28] H.-W. Shih, Y.-F. Chang, W.-J. Li, F.-C. Meng, C.-Y. Huang, C. Ma, T.-J. R. Cheng, C.-H. Wong, W.-C. Cheng, *Angew. Chem. Int. Ed.* **2012**, 51, 10123.

- [29] N. Wang, H. Hasegawa, C.-y. Huang, K. Fukase, Y. Fujimoto, *Chem. Asian J.* **2017**, 12, 27.
- [30] G. T. Hermanson, in *Bioconjugate Techniques (Third edition)*, Academic Press, Boston, **2013**, pp. 395.
- [31] a) A. F. Rullo, K. J. Fitzgerald, V. Muthusamy, M. Liu, C. Yuan, M. Huang, M. Kim, A. E. Cho, D. A. Spiegel, *Angew. Chem. Int. Ed.* **2016**, 55, 3642; b) C. R. Bertozzi, M. D. Bednarski, *J. Am. Chem. Soc.* **1992**, 114, 5543; c) X. Li, X. Rao, L. Cai, X. Liu, H. Wang, W. Wu, C. Zhu, M. Chen, P. G. Wang, W. Yi, *ACS Chem. Biol.* **2016**, 11, 1205.
- [32] a) O. Yoshio, *Curr. Org. Chem.* **2001**, 5, 1; b) T. J. Lupoli, H. Tsukamoto, E. H. Doud, T.-S. A. Wang, S. Walker, D. Kahne, *J. Am. Chem. Soc.* **2011**, 133, 10748.
- [33] M. Koufaki, V. Polychroniou, T. Calogeropoulou, A. Tsotinis, M. Drees, H. H. Fiebig, S. LeClerc, H. R. Hendriks, A. Makriyannis, *J. Med. Chem.* **1996**, 39, 2609.
- [34] M. A. Azagarsamy, V. Yesilyurt, S. Thayumanavan, *J. Am. Chem. Soc.* **2010**, 132, 4550.
- [35] J. Wang, M. Uttamchandani, L. P. Sun, S. Q. Yao, *Chem. Commun.* **2006**, 717.
- [36] a) M. A. Abdel-Rahman, A. M. Al-Abd, *Eur. J. Med. Chem.* **2013**, 69, 848; b) X. Wu, L. Gao, J. Sun, X.-Y. Hu, L. Wang, *Chin. Chem. Lett.* **2016**, 27, 1655; c) W. Chen, L. Gu, W. Zhang, E. Motari, L. Cai, T. J. Styslinger, P. G. Wang, *ACS Chem. Biol.* **2011**, 6, 185.
- [37] E. D. Funder, A. B. Jensen, T. Tørring, A. L. B. Kodal, A. R. Azcargorta, K. V. Gothelf, *J. Org. Chem.* **2012**, 77, 3134.
- [38] a) L. Huang, R. J. Kerns, *Bioorg. Med. Chem.* **2006**, 14, 2300; b) K. Fukunaga, T. Watanabe, D. Novitasari, H. Ohashi, R. Abe, T. Hoshaka, *Chem. Commun.* **2018**, 54, 12734.

Chapter 5

Summary and Perspectives

The objective of this thesis is to develop polymeric materials for combatting drug resistance of bacteria. In this research, two strategies for combatting bacterial infections have been successfully exploited. One strategy is developing cationic polymers for antibacterial application. The other is the development of antibody-recruiting molecules for combatting bacterial infections.

Specifically, a series of glycosylated polycaprolactones bearing cationic groups have been developed. The antibacterial activity and toxicity of the polymers were evaluated. The structure-activity relationship has shown that introducing carbohydrates could significantly reduce the toxicity of the antibacterial polymers. Moreover, by studying the effects of different sugars, polymer with optimal biological profile has been identified. The degradability of the polymer has also been studied and the results showed the degradability of the polymer in physiological conditions and faster killing than degradation. Glycosylated polycaprolactones with cationic groups have shown faster killing than vancomycin. This is the first example of biodegradable glycopolymers for antibacterial applications.

Moreover, pH-sensitive ROMP polymers have been developed by employing a versatile monomer, and the degradability has been successfully introduced into functional polymers. Cationic group has been incorporated to the polymer, which will be further developed into antibacterial polymers. Currently, the polymers are degradable only in relatively strong acidic and basic media which will cause problems in biological applications. Anyway, this is first example of functional ROMP polymers with fully degradable backbone although there is still a long way to antibacterial applications.

On the other hand, a facile synthesis of peptidoglycan oligomer (PGO) has been developed. The PGO has shown great efficiency in labeling both Gram-positive and Gram-negative bacterial cell wall via metabolic process. Based on this, a series of antibody-recruiting molecules (ARMs) have been developed and the preliminary biological results have shown that the ARMs are non-toxic and very promising in combatting bacterial infections. Since this strategy is relying on endogenous antibodies which have already been in the defense system, it should not stimulate the development of bacterial resistance. This is the first example of ARMs based on peptidoglycan for antibacterial application.

In short, we have successfully developed polymeric materials with new antibacterial mechanisms. The results have shown that the materials are very promising which will be further studied in our laboratory. Further animal studies will be conducted for the glycosylated polycaprolactones and more biological studies will be carried out for the ROMP polymers as well as the degradability issue. For the antibody-recruiting molecules, more biological studies will be carried out including animal tests. Also, more ARMs based on the component of bacterial cells will be developed, especially the glycans in the cells.